

2.12 Appendices

2.12.1 Certification Tests on CTU-1

2.12.2 Certification Tests on CTU-2

2.12.3 Structural Evaluation for MIT and MURR Fuel

2.12.1 Certification Tests on CTU-1

This report describes the methods and results of a series of tests performed on the Advanced Test Reactor (ATR) Fresh Fuel Shipping Container (FFSC) transportation package shown in Figure 2.12.1-1. The objective of testing was to conduct drop tests in accordance with the requirements of 10 CFR 71, §71.71 Normal Conditions of Transport (NCT), and §71.73 Hypothetical Accident Conditions (HAC). The verification of the loose fuel plate basket structural integrity and the performance of the package insulation are supported by the tests described in Section 2.12.1, *Certification Tests on CTU-2*.

Testing was performed at Sandia National Laboratories (SNL) in Albuquerque, New Mexico between May 21 and May 23, 2007. Data logs were maintained to track the testing that was performed. In addition, color photographs and videos were taken to document relevant events.

2.12.1.1 Overview

There are three primary objectives for the certification test program:

1. To demonstrate that, after a worst-case series of NCT and HAC free drop and puncture events, the package maintains containment of radioactive contents.
2. To demonstrate that, after a worst-case series of NCT and HAC free drop and puncture events, geometry of both the fuel and package are controlled as necessary to maintain subcriticality.
3. To demonstrate that, after the free drop and puncture bar events, the package retains the thermal protection necessary to maintain the fuel below its melting point during the thermal evaluation.

Several orientations were tested to ensure that the worst-case series of free and puncture drop events had been considered. Post-impact examination demonstrated that the package sufficiently met the design objectives. The design objectives include:

- The package closure remained attached to the body and did not become unlocked as evidenced by no rotation of the closure, thus maintaining containment.
- The package dimensions remained essentially the same providing adequate geometry control.
- Punctures and tears in the outer shell were prevented and thermal insulation was retained for protection during the fire event.
- Reconfiguration of the ATR fuel element and/or Fuel Handling Enclosure (FHE) is bounded by the criticality analysis.

2.12.1.2 Pretest Measurements and Inspections

The ATR FFSC packaging, the FHE, and ATR fuel element were received at SNL and identified as the ATR Fuel Element Certification Test Unit (CTU). The components arrived fully constructed, although not assembled, and ready for testing. The fabrication serial

number of the ATR FFSC test unit is CTU3. The serial number for the FHE is FHA 2. The packaging and payload are identified as ATR FFSC Certification Test Unit CTU-1.

The ATR fuel element is an ATR Mark VII high enriched uranium (HEU) fuel element. The ATR fuel element, serial number XA-877R, is a rejected production fuel element based on minor dimensional discrepancies. Prior to assembly of the CTU, some basic dimensions from the fuel element were recorded for post-test comparison. Figure 2.12.1-2 is a photograph of the ATR fuel element prior to testing.

The CTU was dimensionally inspected to the drawings at the fabricator and the fabrication records forwarded to PacTec. A Certificate of Compliance was issued by the fabricator of the CTUs documenting compliance with the fabrication drawings. Minor discrepancies between the drawings and the CTUs were identified and independently evaluated. The evaluations concluded that the discrepancies were minor and would not significantly affect the CTU during testing.

There were four fabrication deviations associated with the serial number CTU3 package fabrication:

- The 3/8-16 UNC index lug screws were obtained without specified ASTM F-879 certifications.
- The #10-24 UNC closure handle screws were obtained without specified ASTM F-879 certifications.
- Chemical over testing of the package body closure plate material identified manganese content 0.02% above the ASTM A479 maximum allowable.
- The handle width is specified to be 7.5 ±.3-inches. When measured in the free state (not secured to the closure), the handle width was undersized by approximately 0.1-inches.

Other deviations relative to the CTU are the absence of the stainless nameplate and the use of temporary rigging attachments. These items are also insignificant relative to the weight of the CTU and their impact upon the drop tests.

2.12.1.2.1 Component Weights

Component weights were measured and recorded as shown in Table 2.12.1-1.

2.12.1.2.2 Drop Test Pad and Puncture Bar Measurement and Description

The drop pad consists of a 10.2 x 28-ft x 4 to 8-in. steel plate firmly anchored to a 300 inch reinforced concrete slab embedded in the ground. The estimated weight of the pad is greater than 2 million lbs. Thus the test pad was qualified as an essentially unyielding surface for the approximately 300 lb CTU. The puncture bar measured 6 in. (150 mm) in diameter and was 36 inches above the drop pad for the puncture drops CP1 and CP2. The puncture bar was securely mounted to the drop pad by welding.

2.12.1.2.3 Equipment and Instruments

Instrumentation used for the component weights and drop tests is given in Table 2.12.1-2. All applicable test and measurement equipment were calibrated in accordance with SNL procedures. The instrumentation used was associated with physical measurements, drop height, angle of the package, and temperature. It is noted that the SNL calibration procedures require National Institute of Standards and Technology (NIST) traceability and that SNL records adequately demonstrated that the calibrations were NIST traceable.

A few different methods were used to confirm the drop height of the package including:

- A plumb bob with a stretch resistant string.
- A tape measure.
- A surveyor theodolite.

SNL project personnel under the supervision of PacTec personnel verified the correct height prior to each drop. The angle of the CTU prior to each drop was measured using a digital level.

Photographic backdrops were fabricated and erected 54 ¼ inches away to the North and 103 ½ inches to the West from the center of the drop pad. The squares on the backdrop are approximately 10.5 inches horizontal and 14.4 inches vertical on the North stadia and 12 inches square on the West stadia.

Two high speed digital video cameras were used to record the drop events. The video views were from the front and side of the drop pad, 90 degrees apart. In addition, color photographs were taken to document the testing.

2.12.1.3 Summary of Tests and Results

2.12.1.3.1 Initial Conditions

The initial conditions for the two HAC drops CD3-1 and CD4-1 were performed at reduced temperature. All other NCT drops, HAC drops, and puncture drops were performed at ambient temperature. Figure 2.12.1-3 shows the chilling unit used to chill the CTU. The chilling unit internal temperature cycled between approximately -25 to -75°F as it circulated cold air. The CTU was in the chiller for 15 hours and 17 minutes. Just prior to removing the CTU from the chiller, the surface temperature was approximately -60°F. The target temperature for the ATR fuel element at the time of drop was -20°F. The surface temperature was recorded before CD3-1 and CD4-1 and varied due to the length of time between removal from the chilling unit to the drop. It is estimated that although the surface temperature raised quickly, the internal temperature of the fuel element was close to the target temperature.

2.12.1.3.2 Summary of Testing

Table 2.12.1-3 identifies the sequential order and testing performed on the ATR FFSC CTU.

2.12.1.4 Certification Tests

2.12.1.4.1 Drop Tests

Only one NCT drop was performed followed by seven HAC drops and three drops onto a puncture bar. The testing conditions are considered conservative due to the large number of HAC drops in various orientations on the single CTU. Relatively minor deformations were recorded due to impact attenuating devices (impact limiters) not being used in the design.

Two 30 ft HAC drops performed on the ATR fuel element CTU were at reduced temperature. These two drops were considered the worst case for the ATR fuel element payload with a targeted temperature of -20°F. The other orientations confirmed the performance of the packaging.

Figure 2.12.1-4 illustrates the orientation markings on the CTU to aid in the descriptions provided throughout this report. The test identification numbering reflects the same drop orientation as performed in CTU-2. For example, CD3-1 is the same orientation as the third HAC drop in CTU-2, test CD3-2. The "-1" identifies this drop as a CTU-1 test.

2.12.1.4.1.1 CN1-1 – CG Over Top Corner NCT Drop

A rigging attachment was welded to the bottom end of the CTU to attain the proper orientation. The drop configuration for CN1-1 was with the CG over the top corner of the closure end.

Figure 2.12.1-5 illustrates the drop orientation. Initial conditions were as follows:

- Ambient temperature: 71°F
- Avg. surface temperature: 71°F
- Time: 11:21 a.m. 5/21/2007
- Drop height: 4 ft

The impact location was at corner number 5 identified in Figure 2.12.1-4. Following impact, the CTU bounced slightly and tipped over onto its side. There was minor visible exterior damage at the impact corner. The maximum deformation at the corner was approximately 1/8 inch. The closure handle was also deformed as a result of the drop. The overall length of the package did not change other than the 1/8 inch at the impact corner and compression of the closure handle of approximately 1/2 inch on one side. There was also a 1/8 inch deformation on the side corner approximately 1 ¼ inch from the impact corner. There was no visible deformation or rotation of the closure, other than the handle. Figure 2.12.1-6 and Figure 2.12.1-7 show the CTU following the NCT drop.

2.12.1.4.1.2 CD1-1 – Flat Side, Pockets Down, HAC Drop

Following CN1-1, the temporary rigging attachments were removed. To rig CD1-1 the index lugs on the CTU were removed and lifting eyes installed in their place. The drop configuration for CD1-1 was with the CTU in the typical lifting orientation, horizontal position, with the alignment pockets facing down. Figure 2.12.1-8 illustrates the drop orientation. Initial conditions were as follows:

- Ambient temperature: 76°F

- Avg. surface temperature: 78°F
- Time: 12:20 p.m. 5/21/2007
- Drop height: 30 ft

Following impact, the CTU bounced and rotated slightly in the air. The high speed video was reviewed and the impact was determined to be sufficiently flat. The justification for the determination was the large number of drops planned for the CTU, and that there were two more similar flat side drops. Also, data gathered during engineering test were consistent with the deformation exhibited from the CD1-1 drop.

There were minor visible exterior scratches resulting from the drop. The areas showing the greatest impact marks are at each end plate and near the three internal stiffening ribs. There was no significant bowing or other visible deformation. There was no visible deformation or rotation of the closure and the locking pins remained in the locked position. Figure 2.12.1-9 shows the CTU following the drop.

Upon inspection of the CTU the closure assembly was fully functional and able to be opened as illustrated in Figure 2.12.1-10. The FHE was removed and visually inspected as illustrated in Figure 2.12.1-11. There were no major deformations or cracked welds noticed. One of the spring plungers on the FHE lid was bent slightly but still functional.

As illustrated in Figure 2.12.1-12, there was no visible damage to the fuel element. The fuel element was not removed from the FHE but both end boxes were clearly visible and fully intact.

With the closure assembly removed from the body of the CTU, the locking pin was noticeably bent approximately 1/32 inch as illustrated in Figure 2.12.1-13. This locking pin was located near position number 8 identified in Figure 2.12.1-4. The other locking pin was not deformed and there was no other visible deformation of the closure assembly. It was noticed that the bent locking pin tended to bind when compressed to the open position.

2.12.1.4.1.3 CD2.A-1 – Flat Side, Index Lugs Down, HAC Drop

Following CD1-1, the FHE was reinserted with the hinged lid facing up towards the index lugs and then temporary rigging attachments were welded to the CTU to orient the package in the horizontal position with the index lugs facing down. The lifting eyes used in CD1-1 were removed and the index lugs re-installed with a 22 ft-lb torque applied to the screws. The drop configuration for CD2-1 was with the CTU in the horizontal position, with the index lugs facing down. Figure 2.12.1-14 illustrates the drop orientation. Initial conditions were as follows:

- Ambient temperature: 80°F
- Avg. surface temperature: 82°F
- Time: 2:59 p.m. 5/21/2007
- Drop height: 30 ft

Following impact, the CTU bounced and spun in the air about its longitudinal axis. After viewing the high speed video it was confirmed that the CTU impacted the drop pad at a slight angle on the longitudinal axis which caused the CTU to spin during the rebound. The index lugs did receive much of the impact but due to the angle it may not have been the worst case impact to the index lugs. There was visible exterior damage resulting from the drop at the index lugs. The index lugs were both pressed inward approximately 1/8 inch. There were no visible signs of broken welds.

The center of the package had an inward bow of about 1/16 inch. There was no other significant visible deformation. There was no visible rotation of the closure. Figure 2.12.1-15 and Figure 2.12.1-16 show the CTU following the drop. Following CD2.A-1 the closure could no longer be opened due to the body opening becoming slightly out-of-round. As illustrated in Figure 2.12.1-17, the body and closure assembly pinched in two locations.

The locking pin on the left side (near #8) of Figure 2.12.1-17 is shown stuck in the open – unlocked position. This happened during the inspection and not as a result of the drop. As the locking pins and closure assembly were inspected functionally by the test engineer, the one locking pin would bind in the open position and require a light tap from a hammer to become unstuck. The photo however, was taken before the locking pin was returned to the locked position.

2.12.1.4.2 CD2.B-1 – Flat Side, Index Lugs Down, HAC Drop

Following CD2.A-1, a second drop in the same orientation, package in the horizontal position with the index lugs facing down, was performed. The purpose of the re-test was to confirm the performance of the package in this orientation. It was felt that due to the slight incline of the package at impact, the maximum load on the index lugs was not experienced. Figure 2.12.1-18 illustrates the drop orientation which was rotated slightly to account for rotation during the drop. Initial conditions were as follows:

- Ambient temperature: 77°F
- Avg. surface temperature: 80°F
- Time: 4:07 p.m. 5/21/2007
- Drop height: 30 ft

During the drop the high speed video showed that the CTU rotated past the horizontal position in the air and impacted at an incline again. Furthermore, the rigging caught a gust of wind and blew to the side and caught the North stadia board. Following impact, the CTU bounced and spun in the air about the longitudinal axis indicating a non-flat impact. The index lugs were both pressed inward approximately 3/16 inch, at the greatest point, from the original surface of the tube. There were no visible signs of broken welds. The handle of the closure assembly broke loose at point #6 shown in Figure 2.12.1-4. The two screws both sheared off and the opposite side remained attached. There was no other significant visible deformation. There was no visible deformation or rotation of the closure and the locking pins remained in the locked position following the drop. During a functional test of the closure assembly the locking pins functioned well (with the locking pin near #8 binding in the open position) and the closure could rotate approximately ¼ inch. Figure 2.12.1-19 and Figure 2.12.1-20 show the CTU following the drop.

2.12.1.4.3 CD3-1 –Flat Side HAC Drop

The CTU was fitted with temporary rigging attachments for both CD3-1 and CD4-1 prior to chilling to minimize warming of the CTU prior to the drops. The CTU was removed from the chilling unit after 15 hours and 17 minutes with the average surface temperature reading -57°F, 14 minutes prior to CD3-1. Figure 2.12.1-21 shows the CTU in the chiller prior to removal. The CTU was oriented for a drop onto the long side with the pockets and index lugs oriented at 90° to the drop pad. The drop configuration was with the CTU's side parallel to the horizontal. Figure 2.12.1-22 illustrates the drop orientation. Initial conditions were as follows:

- Ambient temperature: 67°F
- Avg. surface temperature: +13°F
- Time: 9:31 a.m. 5/22/2007
- Drop height: 30 ft

Following impact, the CTU bounced slightly and came to rest in its standard position with the index lugs facing up. The impact side showed just minor scratches and impact marks from the drop. Figure 2.12.1-23 and Figure 2.12.1-24 show the CTU following the drop. The impact side showed a slight bowing of the ends. Using a straight edge, the maximum gap at each end was approximately 1/8 inch. There was no visible rotation of the closure and the locking pins remained in the locked position following the CD3-1 drop.

As illustrated in Figure 2.12.1-25, the closure assembly was functionally tested and upon close inspection it was found that the locking pin near point #4 (bottom of picture) had sheared off between the closure assembly and body preventing the locking pin from engaging in the body. The locking pin near point #8 was engaged following the drop but continued to bind in the open - unlocked position when depressed by hand. Figure 2.12.1-25 shows this locking pin in the open position following the attempt to open the closure. The closure assembly could partially rotate approximately 1/4 inch but was unable to fully rotate to the open position. The locking pin near point #8 was returned to the locked position following the inspection. The dull gray color seen on the photographs is frost.

2.12.1.4.4 CD4-1 –CG Over Bottom End HAC Drop

Immediately after CD3-1, rigging was attached to the pre-welded lugs near the closure and the CTU prepared for the CD4-1 drop. The time between CD3-1 and CD4-1 was 33 minutes. During that time the CTU was kept elevated above the drop pad. The drop configuration was with the CTU in the vertical position, with the bottom end down (closure end up). Figure 2.12.1-26 illustrates the drop orientation. Initial conditions were as follows:

- Ambient temperature: 64°F
- Avg. surface temperature: 42°F
- Time: 10:04 a.m. 5/22/2007
- Drop height: 30 ft

Following impact the outer shell of the CTU exhibited minor bowing near the impact end with the greatest deformation measuring approximately 1/8 inch on the 90° side per Figure 2.12.1-4. The overall length of the package body was compared with the initial measurements at the eight locations and found to have compressed a maximum of approximately 1/8 inch. There was no visible deformation or rotation of the closure following the drop and the functionality of the closure assembly did not change. Figure 2.12.1-27 and Figure 2.12.1-28 show the CTU following the drop.

2.12.1.4.5 CP3-1 – Oblique, CTU Closure Over Puncture Bar

Following CD4-1 the CTU was positioned for an unscheduled puncture bar drop onto the closure. The purpose for this drop was to attempt to rotate the closure assembly prior to the CD5-1 drop which would severely deform the closure area of the body preventing any chance of

rotation. The temporary rigging attachments from CD3-1 and CD4-1 were removed and new attachments welded for this drop. The puncture bar, 36 inches in height, was welded to the drop pad. For CP3-1, the CTU was hoisted at a 28.3° orientation from horizontal and a 225° twist on the longitudinal axis so the puncture bar would impact one of the ribs in the closure assembly. The closure handle, which had broke off from one side during CD2.B-1, was bend outward to keep from interfering with the targeted impact location. Figure 2.12.1-29 and Figure 2.12.1-30 illustrate the drop orientation. Initial conditions were as follows:

- Ambient temperature: 72°F
- Avg. surface temperature: 73°F
- Time: 11:50 a.m. 5/22/2007
- Drop height: 40 inches

The puncture bar squarely impacted the closure rib and the CTU bounced away from the puncture bar onto the drop pad. Following the drop, the closure assembly rib exhibited minor deformations at the impact point made by the puncture bar. There was no rotation of the closure assembly and the locking pins showed no visible signs of deformation. The locking pin by #8 remained in the locked position. Both locking pins were functioning and able to be moved and compressed against the spring when tested by hand. Note that the locking pin by #4 was previously sheared during the CD3-1 drop. Figure 2.12.1-31 shows the CTU closure following CP3-1.

2.12.1.4.6 CD5-1 – CG Over Top Corner HAC Drop

For CD5-1, the CTU was hoisted in the same orientation as CN1 with the CG over the top corner; point #5 in Figure 2.12.1-4. The closure handle was removed for convenience since it was loose and obstructing the drops. Figure 2.12.1-32 illustrates the drop orientation. Initial conditions were as follows:

- Ambient temperature: 76°F
- Avg. surface temperature: 81°F
- Time: 1:54 p.m. 5/22/2007
- Drop height: 30 ft

Following impact, the CTU bounced slightly and tipped over onto its side. The impact corner was deformed in approximately 5/8 inch. There was modest deformation on the sides of the package near the impact location bulging in approximately 1/2 inch near the index lug pocket and bulged out approximately 5/8 inches on the adjoining side. The impacted corner deformed in approximately 5/8 inch and the opposite corner, #1, had no change in length. Figure 2.12.1-33 through Figure 2.12.1-36 show the CTU following CD5-1.

Following the drop, the closure assembly exhibited deformation with the end of the package and was unable to be rotated more than 1/8 inch in either direction. The locking pins showed no visible signs of deformation and the pin by #8 remained in the locked position. Both locking pins were functioning and able to be moved and compressed against the spring when tested by hand.

2.12.1.4.7 CD2.C-1 – Flat Side, Index Lugs Down, HAC Drop

Following CD5-1 a third drop in the same CD2 orientation, package in the horizontal position with the index lugs facing down, was performed. The purpose of third re-test was to confirm the performance of the package in this orientation. It was felt that due to the incline of the package at impact during the previous drops, the maximum load on the index lugs was not experienced. Both the release mechanism and rigging cables were changed to aid the drop. Figure 2.12.1-37 illustrates the drop orientation. Initial conditions were as follows:

- Ambient temperature: 79°F
- Avg. surface temperature: 79°F
- Time: 2:37 p.m. 5/22/2007
- Drop height: 30 ft

The third try produced a satisfactory drop orientation. Following impact, the CTU bounced and spun just slightly indicating the impact was directly on the index lugs. The index lugs were both pressed inward. The index lug at the closure end was flush with the general surface. The index lug at the bottom end was pushed in to approximately 1/8 inch from the general surface. Figure 2.12.1-38 and Figure 2.12.1-39 show the index lugs following the drop. The index lugs were removed and a cracked weld was revealed under the index lug near the closure end as shown in Figure 2.12.1-40. The length of the cracked weld was approximately 1/2 inch. There was no other significant visible deformation. There was no visible deformation or rotation of the closure as a result of the drop.

2.12.1.4.8 CP2-1 – CG Over Side, 30° Oblique, HAC Puncture Drop

For CP2-1, the CTU was hoisted at a 30° oblique angle with the CG over the edge of the puncture bar. Figure 2.12.1-41 illustrates the drop orientation. Initial conditions were as follows:

- Ambient temperature: 76°F
- Avg. surface temperature: 77°F
- Time: 3:19 p.m. 5/22/2007
- Drop height: 40 inches

As the CTU impacted the puncture bar, there was no tearing or severe deformation. The initial impact caused a deformation of approximately 1/2 inch deep by 5 inches across with a radius the same as the puncture bar. There was no fracture of the outer shell. Figure 2.12.1-42 and Figure 2.12.1-43 show the CTU following the CP2-1 drop.

2.12.1.4.9 CP1-1 – CG Over Center of Closure HAC Puncture Drop

For CP1-1, the CTU was hoisted in the vertical orientation with the closure directly over the puncture bar. Figure 2.12.1-44 illustrates the drop orientation. Initial conditions were as follows:

- Ambient temperature: 79°F
- Avg. surface temperature: 81°F
- Time: 4:06 p.m. 5/22/2007

- Drop height: 40 inches

Following impact, the CTU bounced slightly on the puncture bar, as verified by high speed video, and came to rest in the vertical position on top of the puncture bar as seen in Figure 2.12.1-45. Following the drop, the tamper indicating device (TID) post was deformed into the closure. The closure assembly exhibited minor scratches from the puncture bar. The locking pins showed no visible signs of deformation and the remaining locking pin by #8 remained in the locked position. Both locking pins were functioning and able to be moved and compressed against the spring when tested by hand. Figure 2.12.1-46 shows the CTU in the up-side-down position following CP1-1. Note that both locking pins were binding somewhat following testing and shown in the photographs in the open – unlocked position following the functional tests.

2.12.1.5 Post-test Disassembly and Inspection

The final acceptance criteria for the ATR FFSC package lies with the criticality and thermal evaluations. Any increase in reactivity of the contents resulting from the certification tests must not exceed the allowable as defined in the criticality evaluation. The inspections required to support determination of compliance with the acceptance criteria are identified as follows:

- Inspect the outer shell to verify the thermal performance of the package is unimpaired by the free drop and puncture events. The thermal analysis assumes that the outer shell is intact such that there is no significant communication between the environment and the outer/inner shell annular space during the thermal event.
- Inspect the insulation to verify compliance with the assumptions of the thermal analysis.
- Inspect the overall package to verify that the package geometry remains within the criticality analyses assumptions.
- Inspect the Mark VII fuel element to verify that the fuel geometry remains within the assumptions of the criticality analyses.

Any deviation of the test results from these acceptance criteria must be reconciled with the criticality or thermal evaluations.

2.12.1.5.1 CTU Inspection

Radiological surveys were performed after each drop test and during the disassembly of the package. The radiological survey reports confirm that there was no loss or dispersal of radioactive material from the package or from the ATR fuel element.

The ATR fuel element CTU was disassembled and inspected on May 23, 2007. Prior to disassembly the exterior dimensions were recorded for comparison to the pre-test condition. Table 2.12.1-4 lists the measured dimensions and Figure 2.12.1-4 identifies the location of the identified measurements.

The closure handle was flattened, loosened, and finally removed during testing for convenience. Due to the relatively weak nature of the handle, its presence or absence had no significant effect on any test outcome. The height of the handle changed from 1 3/8 inches to 1/2 inch on one side before being removed. There was very little bowing or change in shape of the package. The maximum

bowing of the package over its length is estimated at approximately $\frac{1}{4}$ inch. During the CD5-1, CG over corner HAC drop, deformation of the outer wall caused the width of the package to increase from 8 inches to approximately $8 \frac{5}{8}$ inches. The same CD5-1 impact caused the outer wall to deform inward approximately $\frac{1}{2}$ inch.

The CTU was disassembled systematically by cutting away the outer layers of the packaging using an abrasive saw. The destructive examination was necessary due to the deformation of the closure and the need to inspect the interior insulation. Figure 2.12.1-47 illustrates the unsuccessful attempt to rotate the closure assembly and open the package with a steel bar and 5 lb hammer. The closure could not be rotated more than approximately $\frac{3}{8}$ inch using the bar and hammer.

The package was cut with an abrasive saw lengthwise along two opposite corners and at the ends to expose the thermal shield. Figure 2.12.1-48 through Figure 2.12.1-50 show the condition of the thermal shields and insulation. The thermal shields were in relatively good shape with dents from both the index lug bosses and pockets on the shields. There was also some minor deformation at each end of the shields by the stiffening rib plates.

The insulation tended to compact towards the closure end except for the bottom end which compacted towards the bottom. The compaction was not uniform but varied around the circumference of the internal pipe. The maximum compaction for all section ranged from $1\text{-}\frac{1}{8}$ inches to $1\text{-}\frac{1}{2}$ inches.

Two thermal shield designs were used; one with a simple overlapping design and the other secured by rivets. There was no appreciable difference between the performance of either design. Both experienced minor deformation at the pockets and index lugs, and at the ends due to impacting the adjoining plates. Furthermore, the compaction of the insulation under each shield was very similar. On the riveted design, there was no failure of any rivet.

The thermal shields and insulation were removed and using an abrasive saw the bottom end plate was removed by cutting the inner tube. Figure 2.12.1-51 illustrates the condition of the bottom end plate. There were no large deformations or punctures of the stainless steel plate. There were no visual indications of broken welds or other damage near the end plate.

As shown in Figure 2.12.1-52 and Figure 2.12.1-53, the inner tube was inspected and the photographs show the areas of greatest deformation. Due to the CG over corner drop deformation, CD5-1, the inner tube bowed out approximately $\frac{1}{4}$ inch. The inner tube also bowed inward approximately $\frac{3}{16}$ inch slightly deforming the FHE aluminum end plate. There were no visible signs of any weld failures associated with the inner tube.

Figure 2.12.1-54 illustrates the relatively unchanged position of the FHE and fuel element within the CTU. Also seen in this figure are pieces of the broken end box at the bottom end and also pieces of neoprene padding from the FHE during removal. The FHE was somewhat difficult to remove and the aluminum end plate had broken off so the ATR fuel element was carefully pulled from the bottom end of the package as illustrated in Figure 2.12.1-55. Both end boxes of the fuel element had shattered into several pieces. These pieces were collected and kept with the fuel element. There were no pieces of the fuel element end boxes found outside the FHE. Once the fuel element was removed, the FHE was pulled from the inner tube. The welds securing each FHE end plate to the body were completely broken and both the end plates were loose. Figure 2.12.1-56 illustrates the area of greatest deformation to the FHE which was at the closure end.

2.12.1.5.2 ATR Fuel Element Inspection

The ATR fuel element was placed on an inspection table and compared against the same pre-test measurements for the fuel plates. Because the fuel element end boxes had shattered and bent the ends of the side plates, some of the fuel plate measurements taken from the side plates could be slightly exaggerated. The measurements included side plate flatness, in plane bending of the side plates, side plate spacing, overall fuel plate spacing, and fuel plate to fuel plate spacing. Table 2.12.1-5 provides the general change in dimensions to the fuel plates. Measurements were generally taken at five locations along the length of the fuel element. The five locations include 1 inch from the end of the fuel plate (neglecting the end boxes), 12 inches from each end of the fuel plate, and at the center of the fuel plate.

Figure 2.12.1-57 through Figure 2.12.1-62 illustrate the condition of the ATR fuel element. As shown in Figure 2.12.1-58 and Figure 2.12.1-59, fragments from the fuel element end boxes deformed and cut into the ends of the fuel plates during testing. At no point did the fuel meat, the embedded uranium within the aluminum cladding, become exposed.

In conclusion, the CTU satisfied the acceptance criteria of preventing loss or dispersal of the contents, the outer shell remained intact, the insulation remained within the assumptions of the thermal analysis, and the package and fuel geometry remained greatly unchanged. The deformations of the package and condition of the ATR fuel element were evaluated against the criticality and thermal evaluations and determined to be within the bounds of the assumptions and conditions used to ensure safety.

Table 2.12.1-1 - Component Weights

Component	Weight (lbs)
Body Assembly	225.0
Closure Assembly	9.0
Fuel Handling Enclosure	14.3
ATR Fuel Element	22.1
Package (fully loaded)	270.4

Table 2.12.1-2 - Instrumentation for Drop Tests

Item Description	Model	Serial Number	Calibration Due Date	Comments
Drop Height Indicators	N/A	N/A	N/A	String plumb bobs made specifically for this testing. The length was established using a metal tape measure.
Tape Measure	Stanley	N/A	N/A	35-ft. steel tape
Digital Level 2'	M-D Building Products	SNL 3665	1/23/09	Used to identify CTU orientation
Digital Level 4'	M-D Building Products	SNL 3666	1/23/09	Used to identify CTU orientation
Scale	NCI	D798311	2/12/08	Used to measure weights of CTU components
Hook Scale	Dively	60418/46180	Aug 2007	Used to measure the weight of the ATR FFSC body
Multilogger Thermometer	Omega Engineering	06000855	10/19/07	Handheld temperature reader for measuring ambient temperature and CTU surface temperature
Temperature Probe	N/A	56194	10/19/07	Probe which attaches to multimeter
Torque Wrench 0-25 ft-lbs	N/A	SNL 1933	2/26/09	Used to apply measured torque to index lug screws

Table 2.12.1.3 - Summary of Testing

Test No.	Test Description	Comments
CN1-1	CG over top corner	CG over top corner drop from 4 ft. Minor deformation at impact corner. Maximum change in length approximately 1/8 inch at impact point only. Closure handle deformed. Closure functions properly.
CD1-1	Flat side drop, pocket side down	Flat side drop from 30 ft. Minor visible scratches and impact marks. Closure functions properly. Package opened and inspected. One locking pin on closure bent slightly but still operable. No visible damage to fuel element.
CD2.A-1	Flat side drop, index lugs facing down	Flat side drop from 30 ft. Impact pushed index lugs into package approximately 1/8 inch. CTU impact was not level on the longitudinal axis causing the package to bounce and spin after impact. A second drop in the same orientation was chosen.
CD2.B-1	Flat side drop, index lugs facing down	Flat side drop from 30 ft. Impact pushed index lugs into package approximately 3/16 inch. CTU impact again was not level due to a gust of wind blowing the rigging straps into the stadia board.
CD3-1	Flat side drop, pockets and index lugs on side, reduced temperature	Flat side drop from 30 ft. Minor visible scratches and impact marks. One locking pin sheared during impact. No rotation of closure. Surface temperature approximately 13°F.
CD4-1	CG over bottom end (vertical), reduced temperature	Flat bottom drop from 30 ft. No appreciable deformation on impact side but minor bowing outward on side near impact end. Maximum change in length approximately 1/8 inch. Surface temperature approximately 41°F.
CP3-1	Closure assembly over puncture bar	Unscheduled drop chosen to ensure performance of closure assembly due to broken locking pin from CD3. Impact caused small deformation to closure assembly rib. There was no rotation of the closure and no other visible damage.
CD5-1	CG over top corner (same orientation as CN1)	CG over top corner drop from 30 ft. Deformation of the corner, including adjoining sides, and minor bending of the closure assembly. Maximum change in length at impact point approximately 5/8 inches.
CD2.C-1	Flat side drop, index lugs facing down	Flat side drop from 30 ft. This third drop on the index lugs was chosen to ensure performance of the outer skin and index lugs in this orientation. The previous two drops did not impact flat on the lugs. Index lug at closure end pushed in flush with general package surface, approximately 1/2 inch. A small crack in the weld between the index lug boss and square tube was recorded.
CP2-1	CG over side, 30° oblique	CG over side puncture drop from 40 in. Minor deformation from impact. Depth of impact approximately 1/2 inch. Width of impact approximately 5" across.

Table 2.12.1.3 - Summary of Testing

Test No.	Test Description	Comments
CP1-1	CG over center of closure (Vertical)	Vertical puncture drop on closure from 40 in.. The tamper indicating device stud pushed into closure assembly. No other visible damage. No rotation of closure assembly.

Table 2.12.1-4 – Package Length Measurements

Test ID	1	2	3	4	5	6	7	8
Pre-Test (in.)	72 ½	72 ½	72 ½	72 ½	72 ½	72 ½	72 ½	72 ½
Post-Test (in.)	72 5/16*	72 ½	72 7/16	72 ¼	71 11/16*	72 ¼	72 ½	72 7/16

*These locations were modified slightly due to the welding and removal of temporary rigging attachments. The change to position #5 was approximately -1/16 inch. There was approximately no change to position #1.

Table 2.12.1-5 - ATR Fuel Element Measurements

Measurement Area	Pre-Test Range (in)	Post-Test Range (in)
Side Plate Flatness	±0.010	±0.075
In-Plane Bending of Side Plates	±0.011	±0.025
Side Plate Spacing - Top	4.113 – 4.130	4.015 – 4.131
Side Plate Spacing - Bottom	1.840 – 1.845	1.837 – 1.845
Height of Top Fuel Plate from Table (top side up)	2.675 – 2.691	2.655 – 2.785
Height of Bottom Fuel Plate from Table (bottom side up)	2.500 – 2.540	2.415 – 2.508
Fuel Plate to Fuel Plate Spacing	0.075 to 0.080	0.023 to 0.098*

* The minimum and maximum fuel plate spacing were in localized areas near the side vents and not representative of the general spacing.

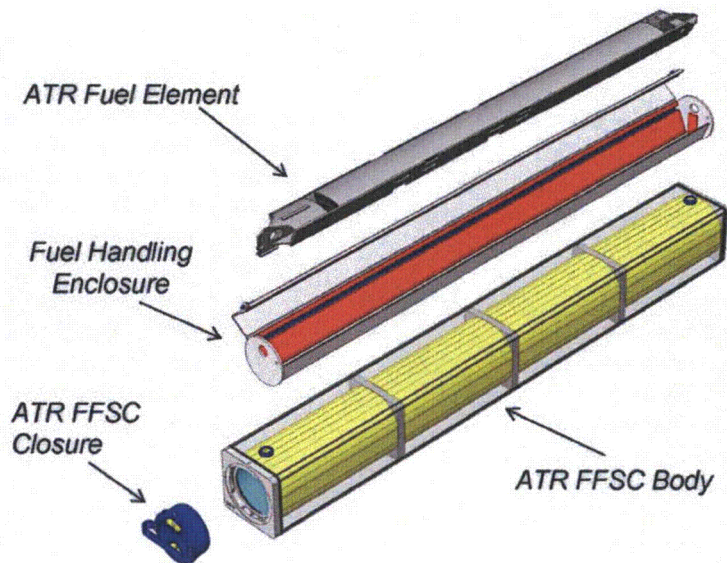


Figure 2.12.1-1 - ATR FFSC



Figure 2.12.1-2 – ATR Fuel Element



Figure 2.12.1-3 – Chilling Unit

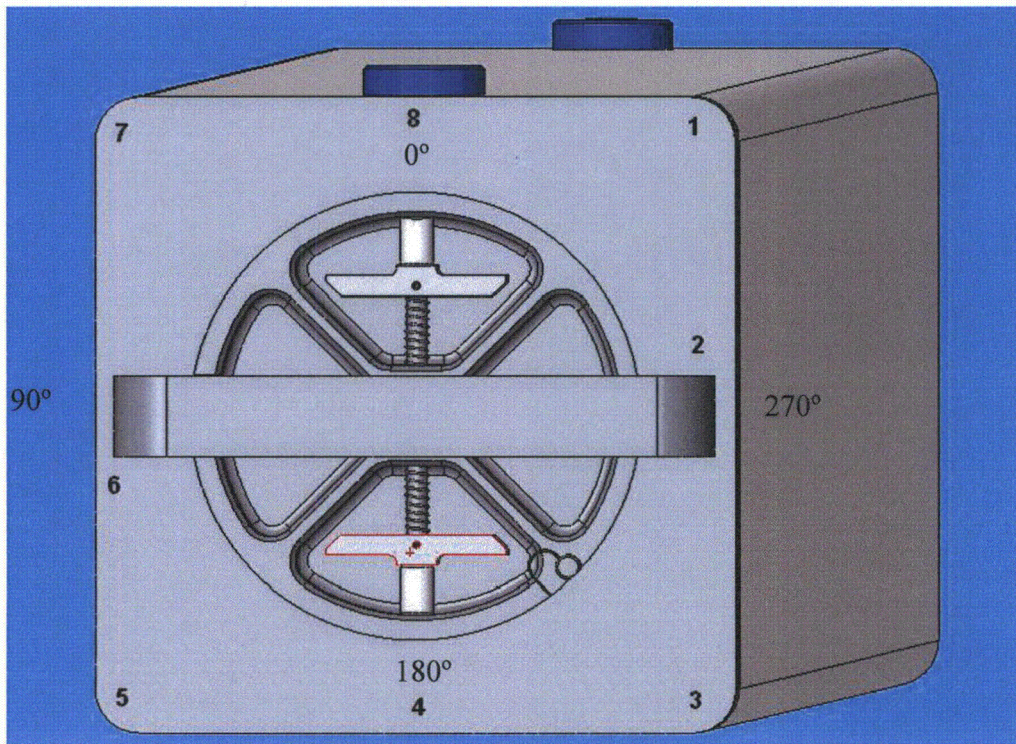


Figure 2.12.1-4 – ATR Package Orientation Markings

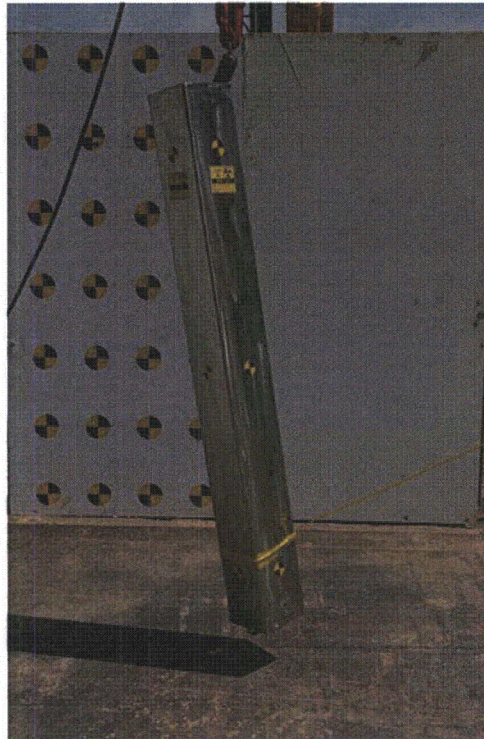


Figure 2.12.1-5 - CN1-1 Drop Orientation

Impact
corner



Figure 2.12.1-6 - CN1-1 Impact Damage



Figure 2.12.1-7 - CN1-1 Impact on Closure Handle

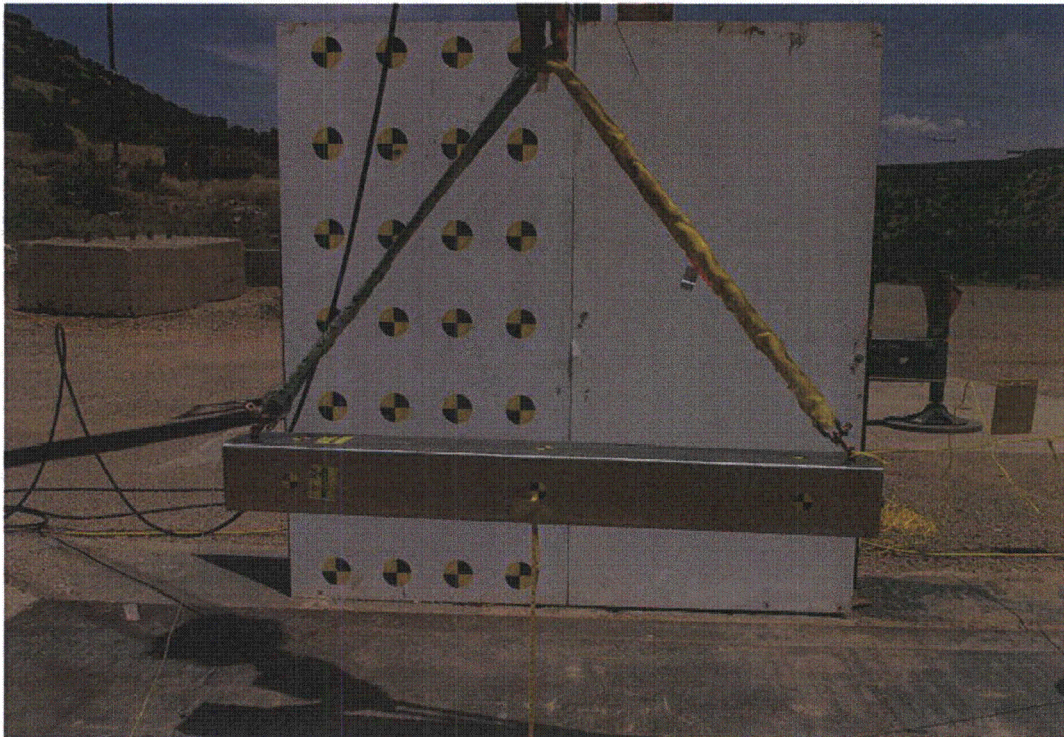


Figure 2.12.1-8 – CD1-1 Drop Orientation

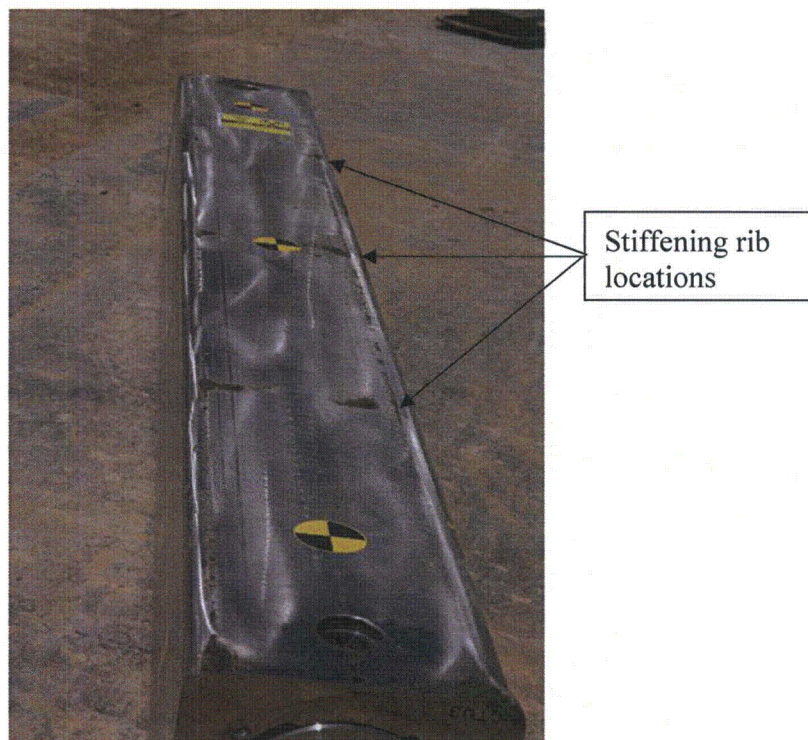


Figure 2.12.1-9 – CD1-1 Impact Side

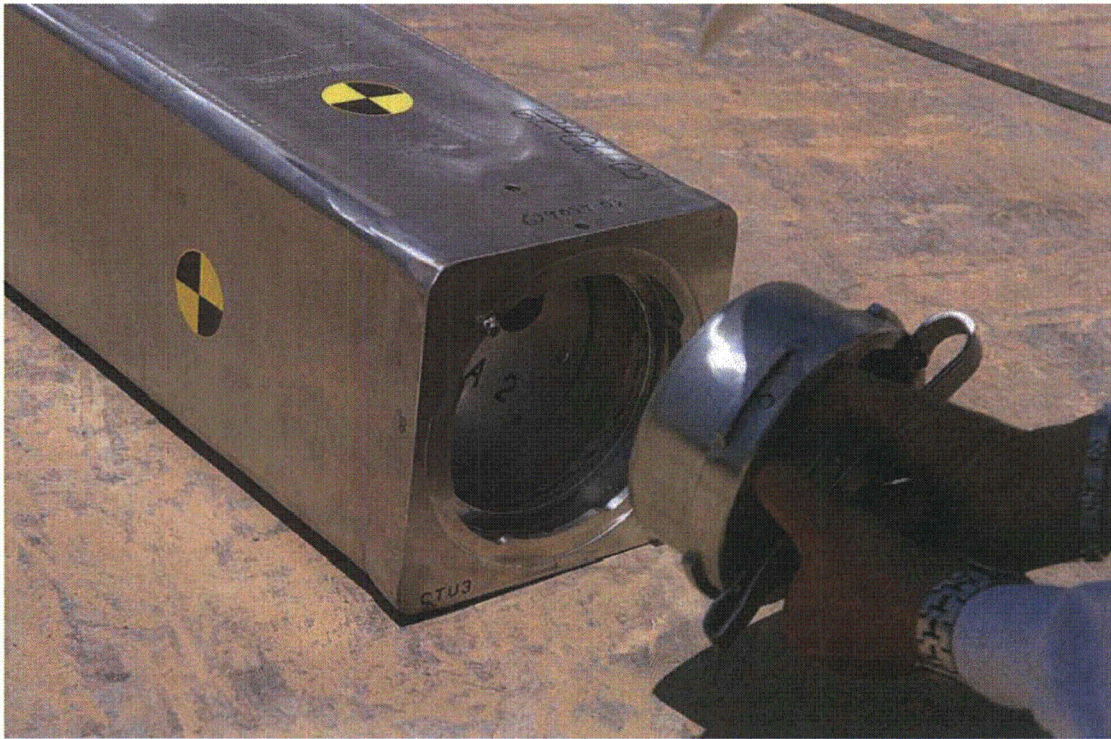


Figure 2.12.1-10 - Opening of CTU Following CD1-1

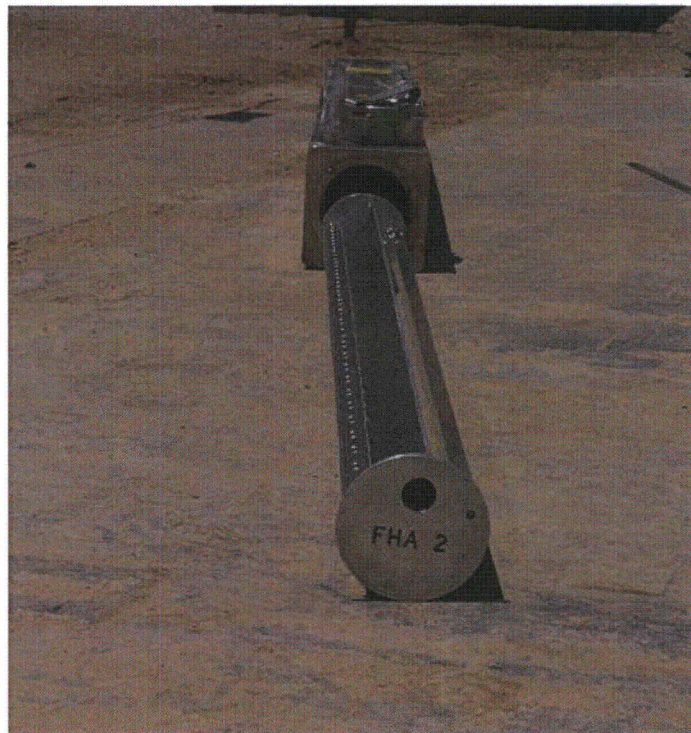


Figure 2.12.1-11 - Inspection of Payload Following CD1-1

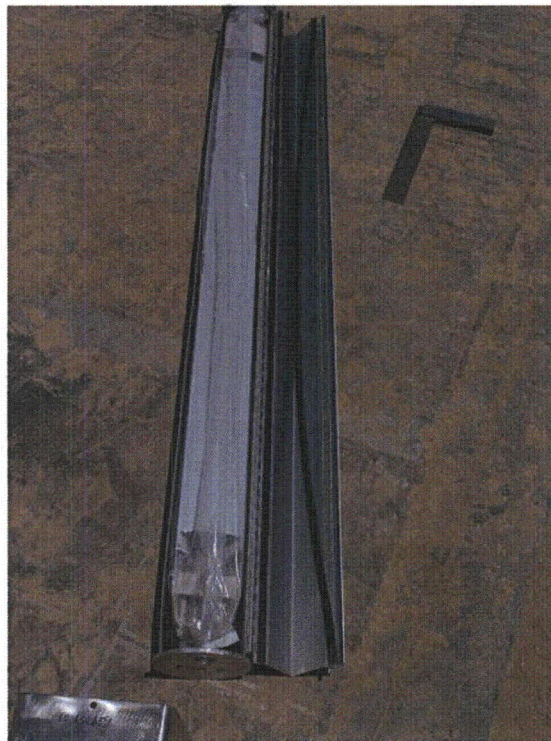


Figure 2.12.1-12 - Inspection of Fuel Element Following CD1-1

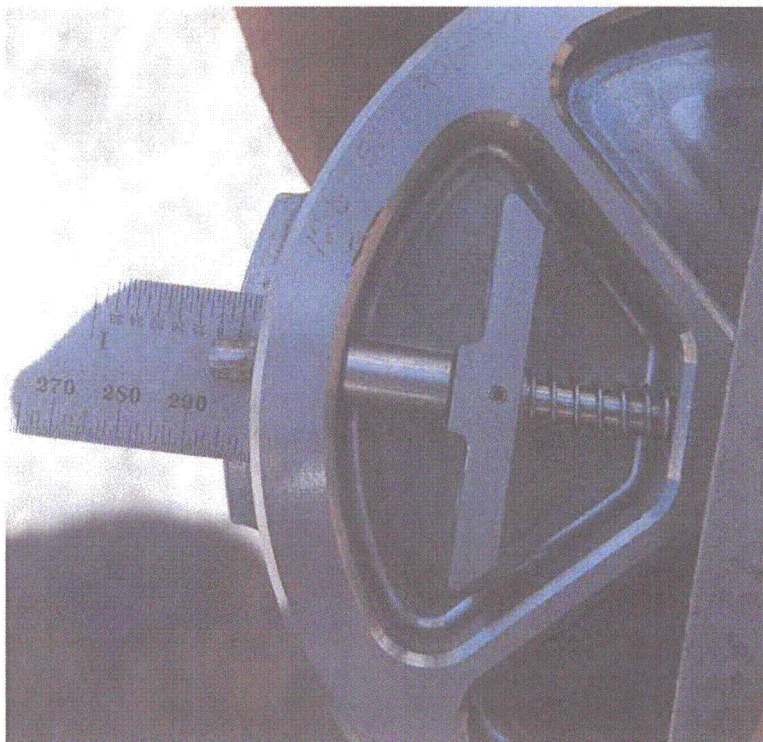


Figure 2.12.1-13 - Inspection of Closure Assembly Following CD1-1

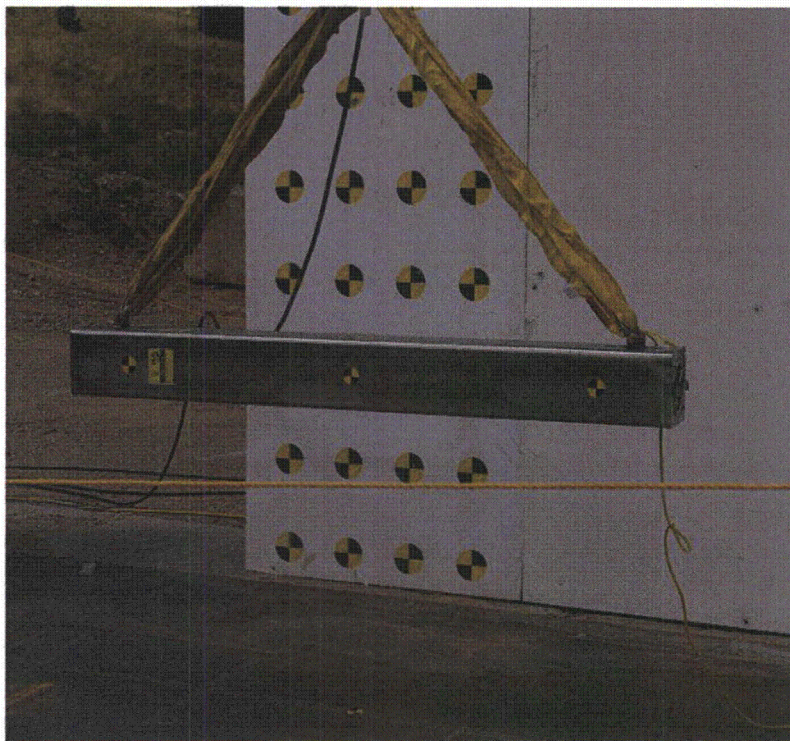


Figure 2.12.1-14 – CD2.A-1

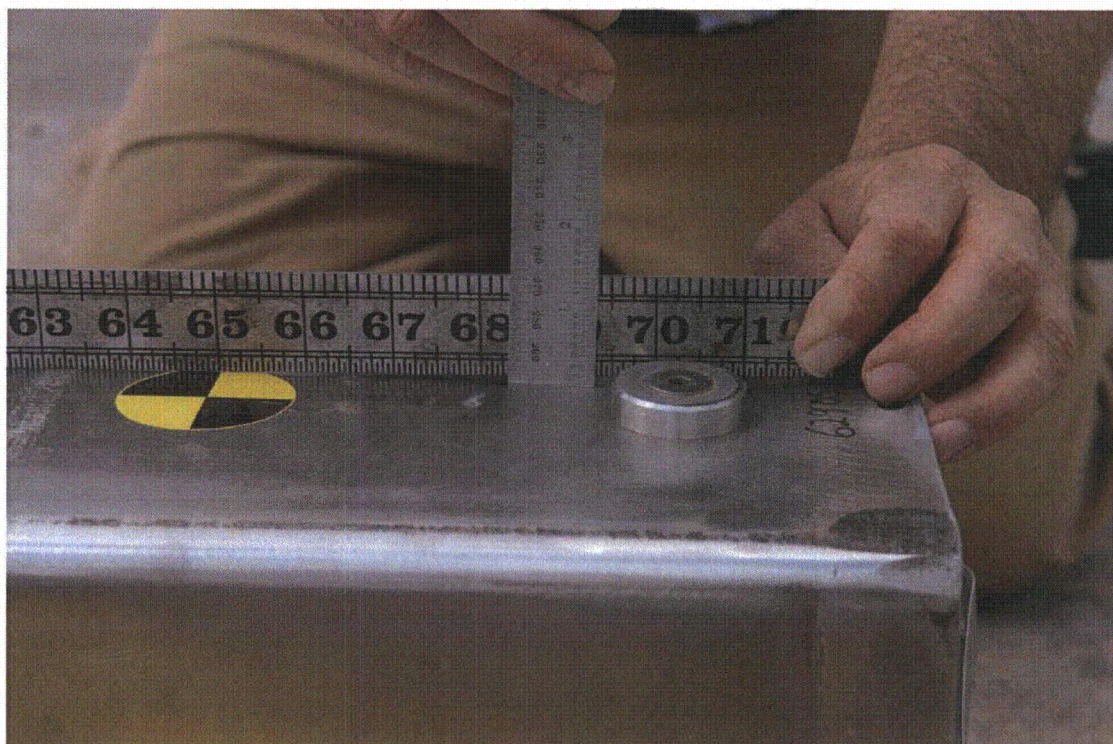


Figure 2.12.1-15 - Index Lug Near Closure End, CD2.A-1

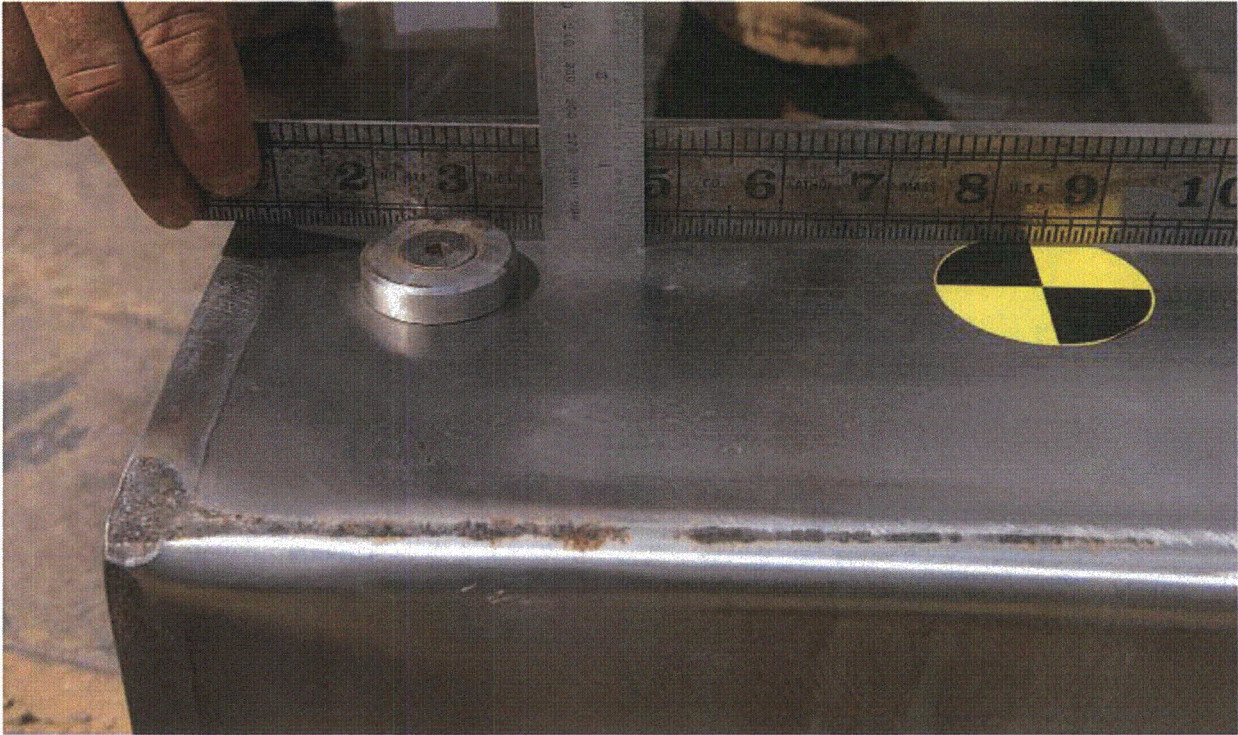


Figure 2.12.1-16 - Index Lug Near Bottom End, CD2.A-1

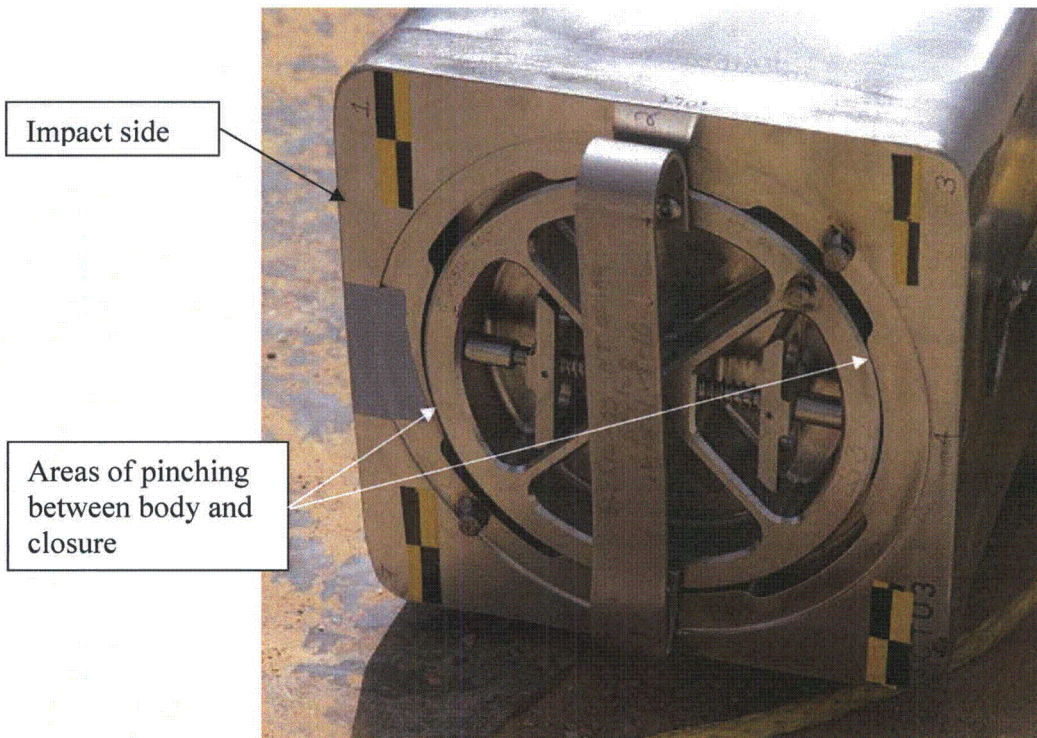


Figure 2.12.1-17 - View of Closure Following CD2.A-1



Figure 2.12.1-18 - CD2.B-1 Drop Orientation

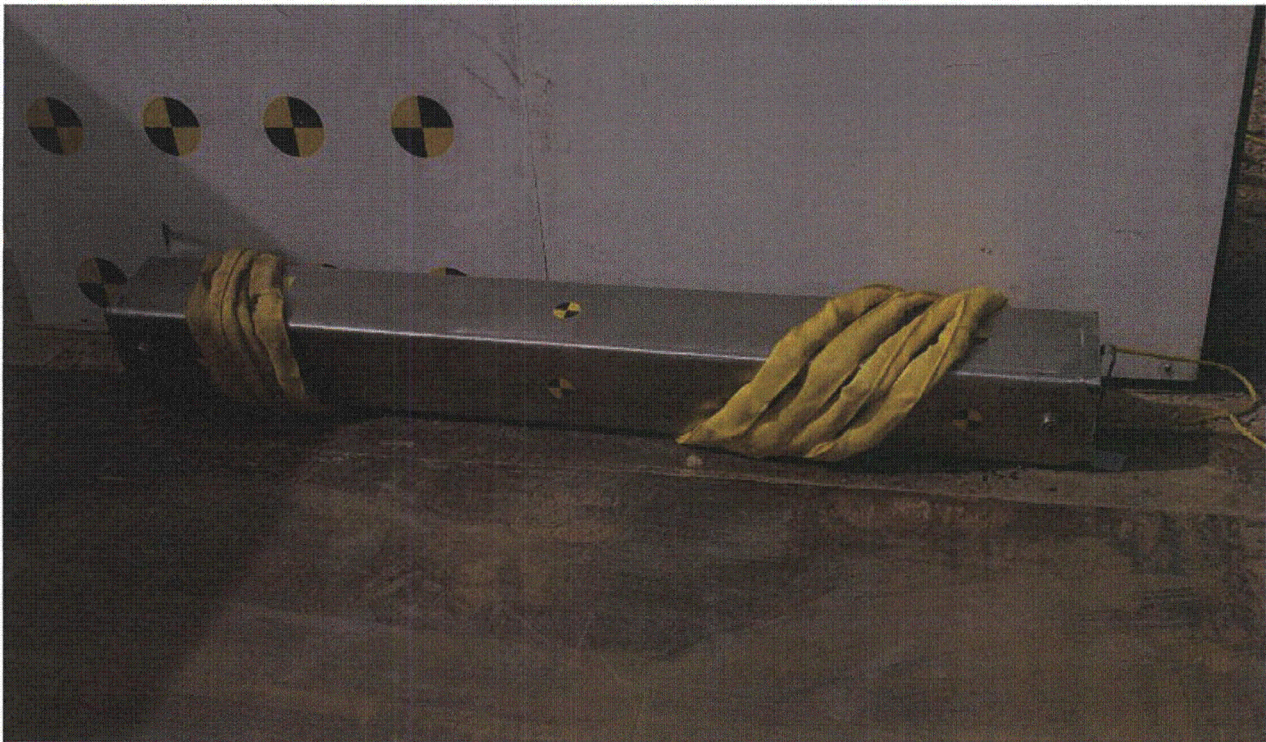


Figure 2.12.1-19 - CTU Position Following CD2.B-1 Drop

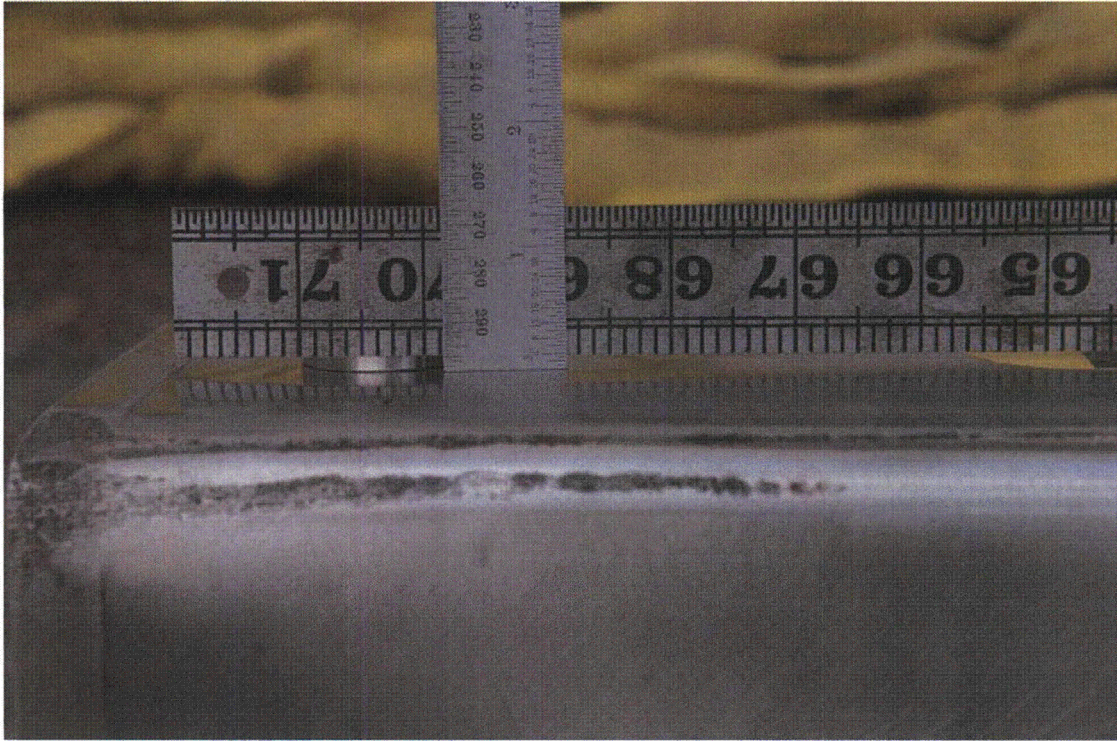


Figure 2.12.1-20 - Index Lug Near Bottom End, CD2.B-1



Figure 2.12.1-21 - CTU in Chiller Unit

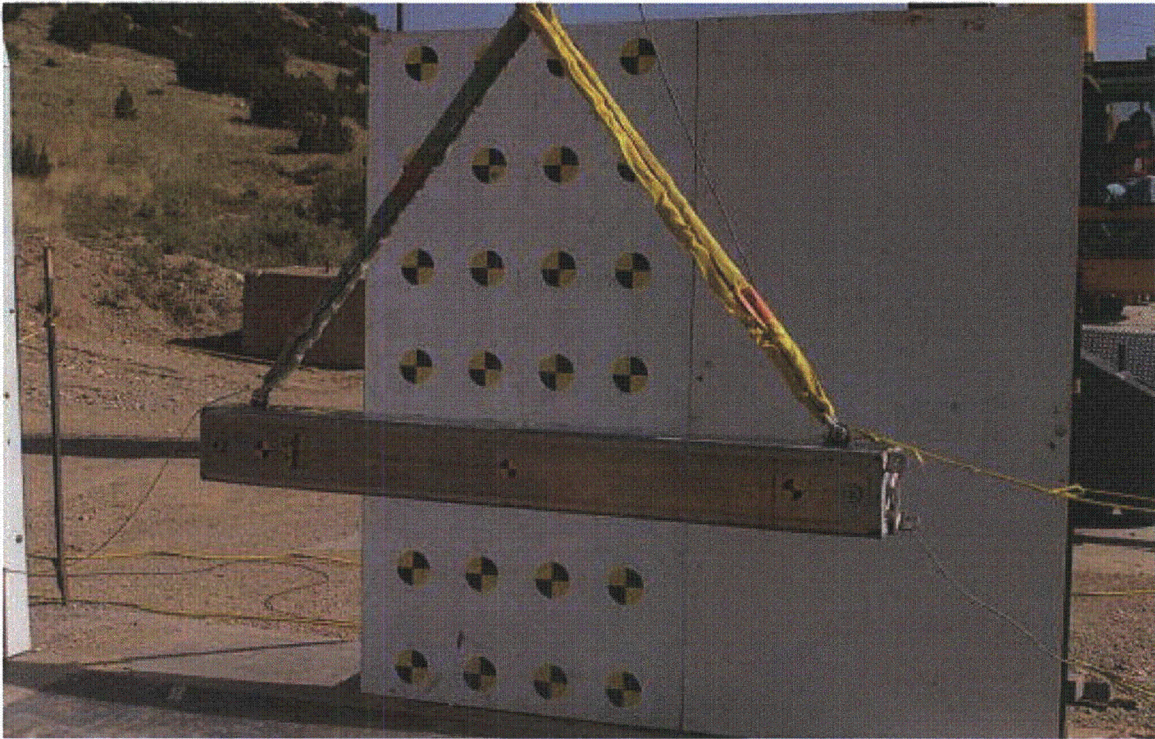


Figure 2.12.1-22 - CD3-1 Drop Orientation



Figure 2.12.1-23 - CTU Following CD3-1 Impact

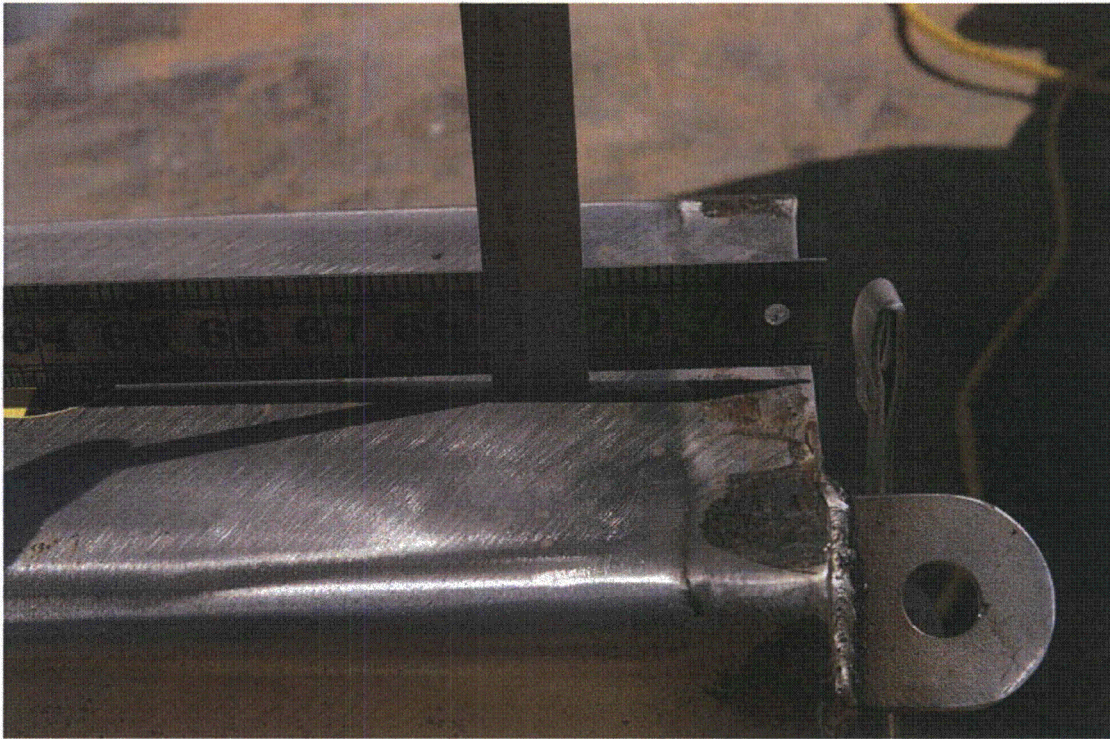


Figure 2.12.1-24 - Deformation Near Closure End Following CD3-1

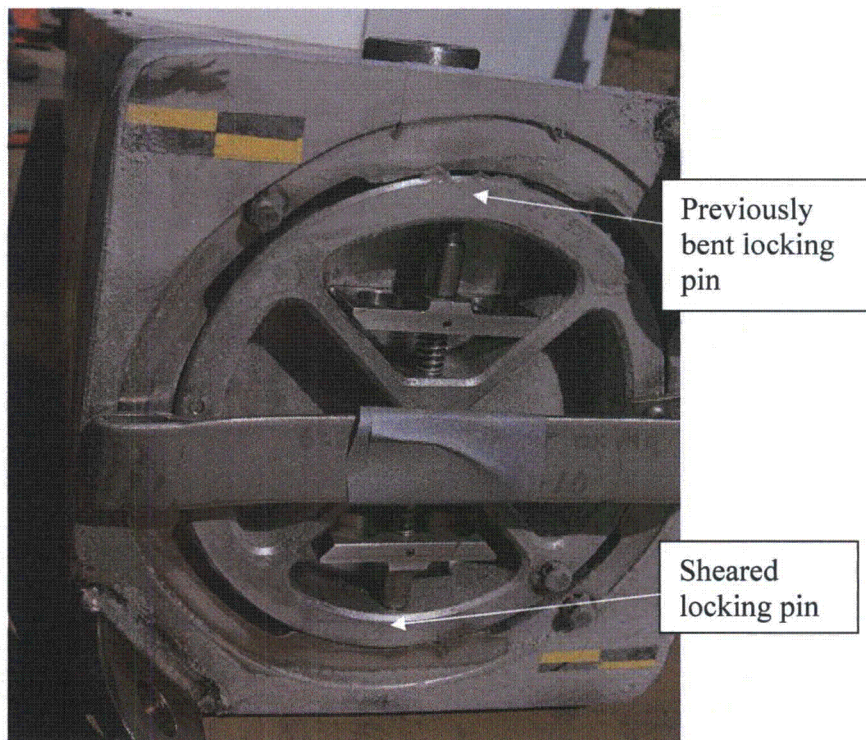


Figure 2.12.1-25 - View of Closure Following CD3-1

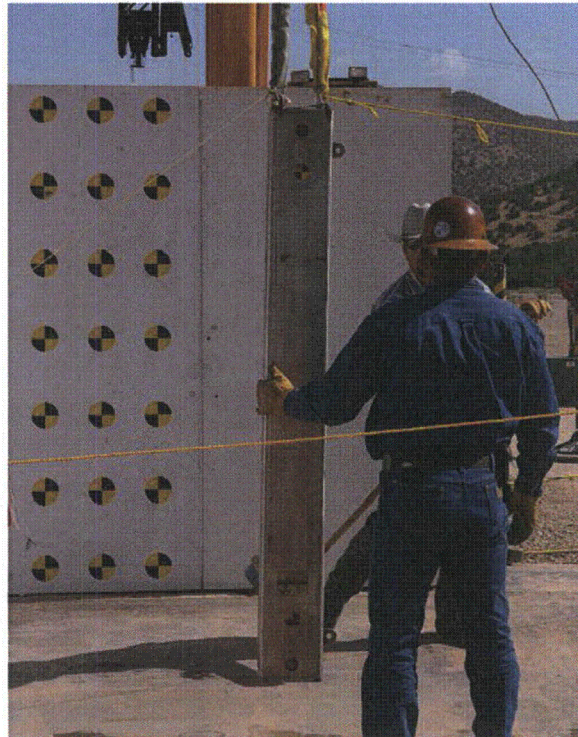


Figure 2.12.1-26 - CD4-1 Drop Orientation

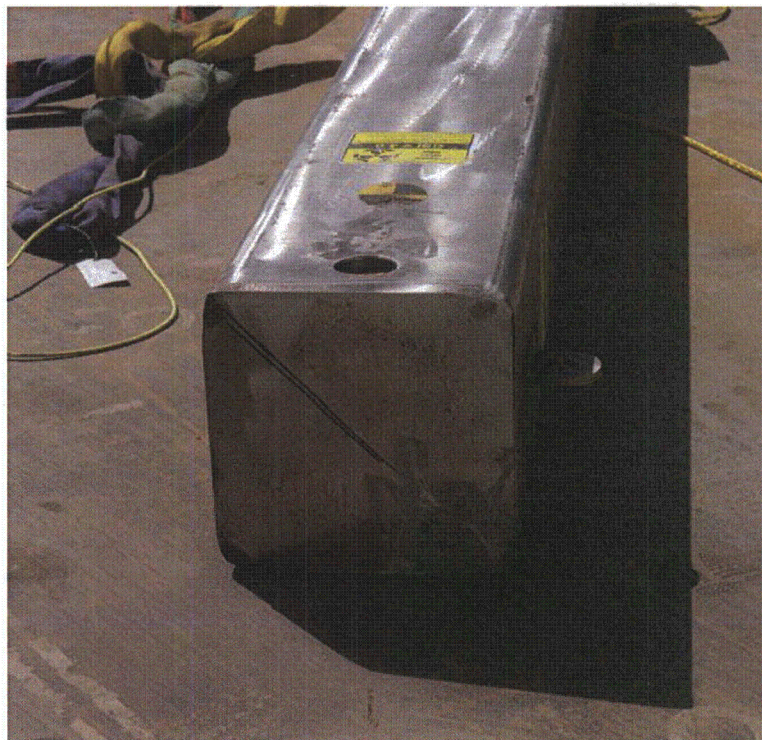


Figure 2.12.1-27 - View of Impact End Following CD4-1

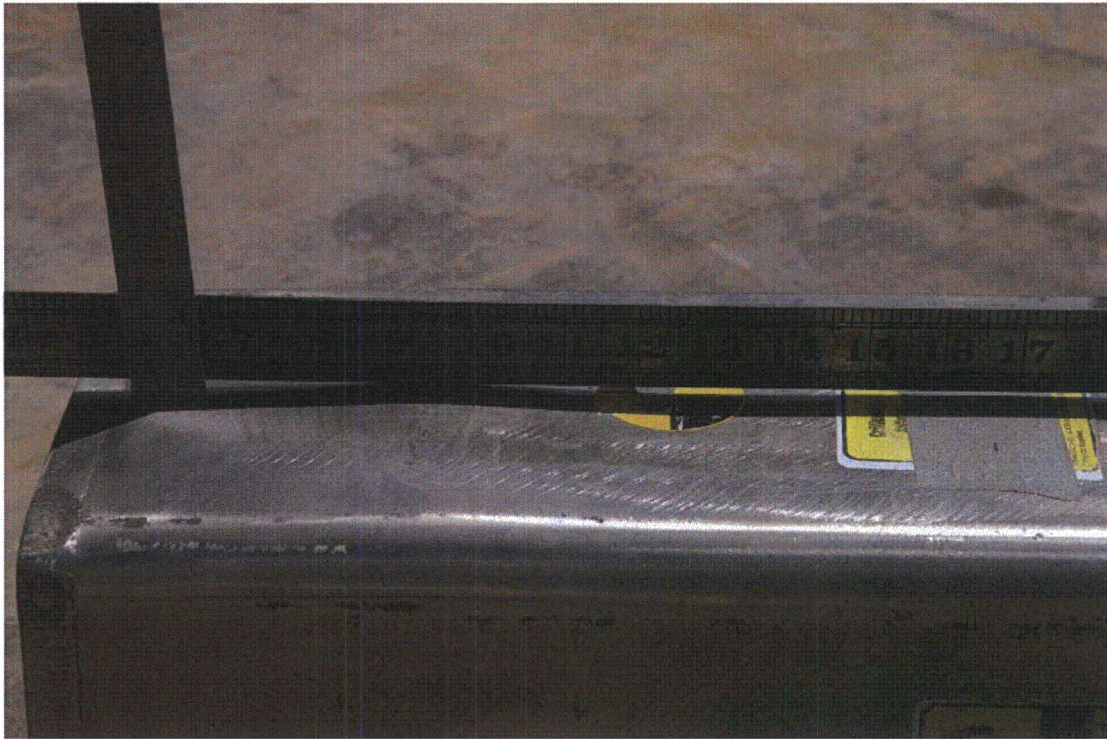


Figure 2.12.1-28 - View of Side Bowing Following CD4-1



Figure 2.12.1-29 - CP3-1 Drop Orientation – Front

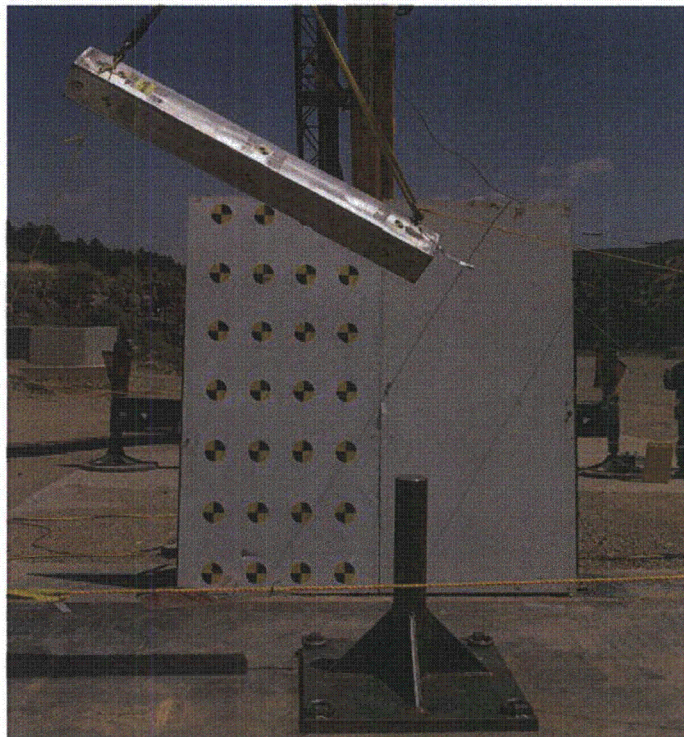


Figure 2.12.1-30 - CP3-1 Drop Orientation – Front



Figure 2.12.1-31 - CTU Following CP3-1 Impact

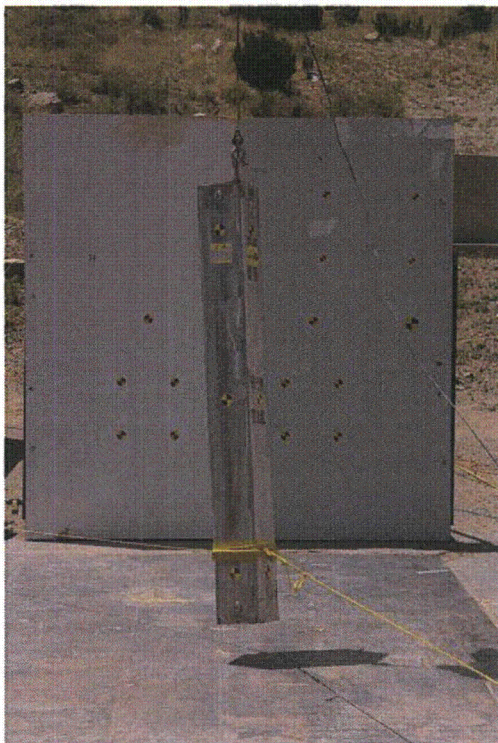


Figure 2.12.1-32 - CD5-1 Drop Orientation

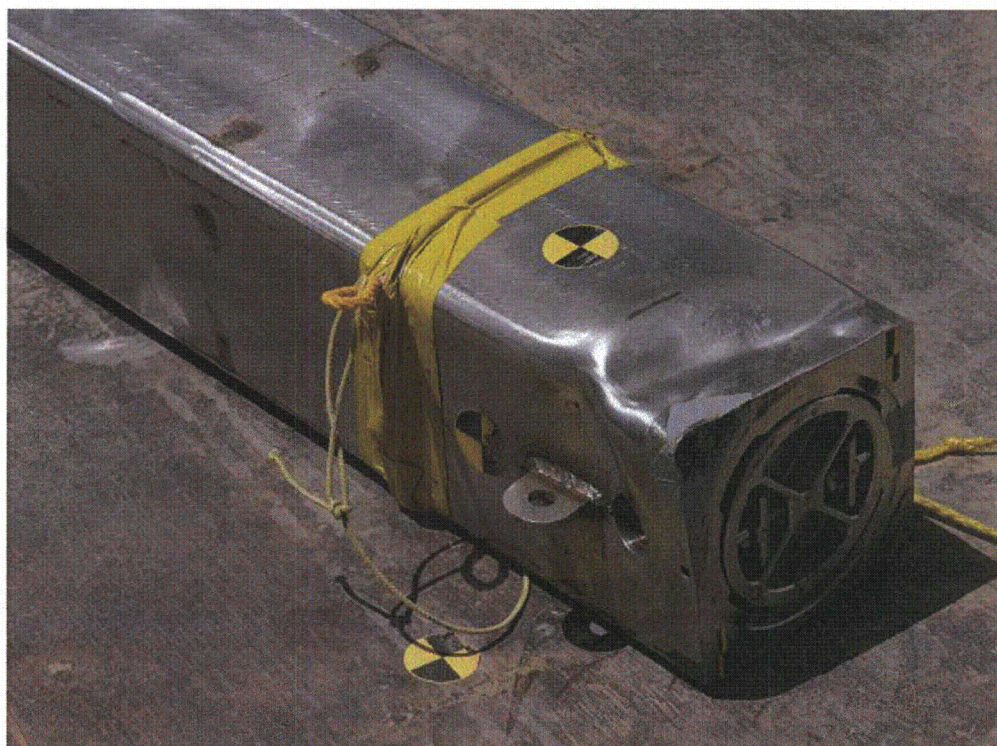


Figure 2.12.1-33 - CTU Following CD5-1 Impact

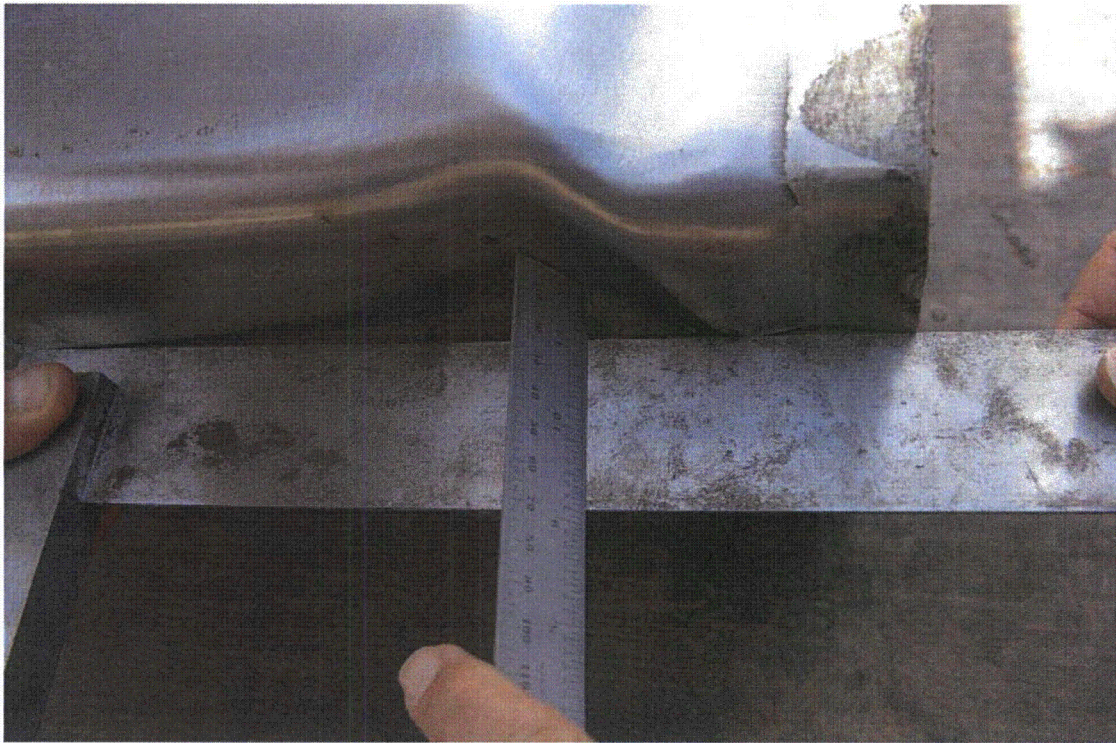


Figure 2.12.1-34 - CD5-1 Impact Damage on Bottom 180° Side



Figure 2.12.1-35 - CD5-1 Impact Damage on Closure End



Figure 2.12.1-36 - CD5-1 Impact Damage on Closure Area

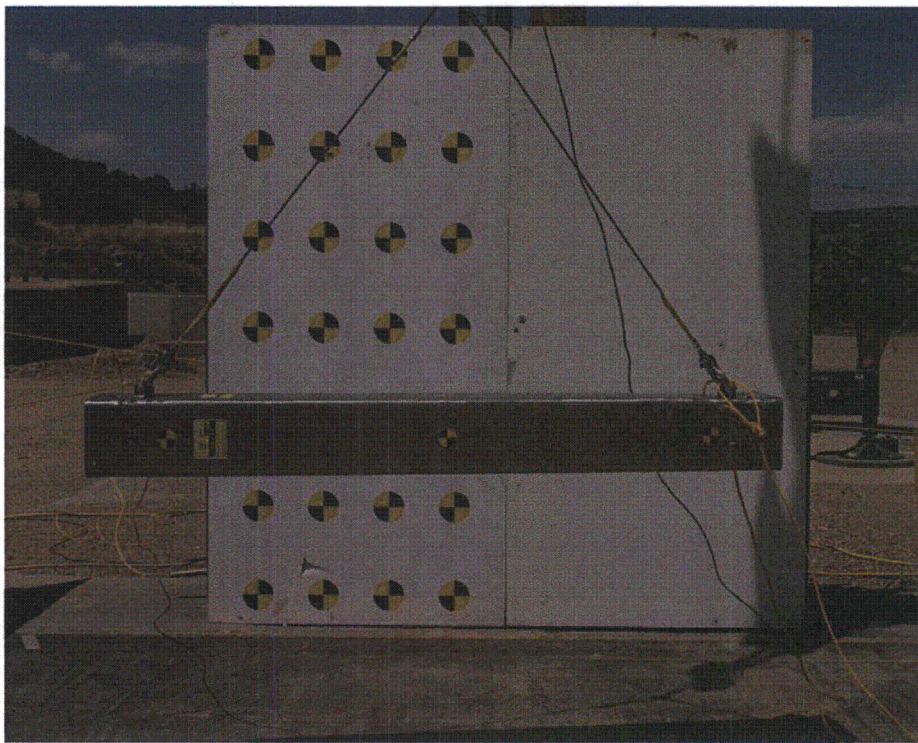


Figure 2.12.1-37 - CD2.C-1 Drop Orientation



Index lug
pressed flush

Figure 2.12.1-38 - Side View of CTU Following CD2.C-1 Drop



Figure 2.12.1-39 - Index Lug Near Closure End, CD2.C-1

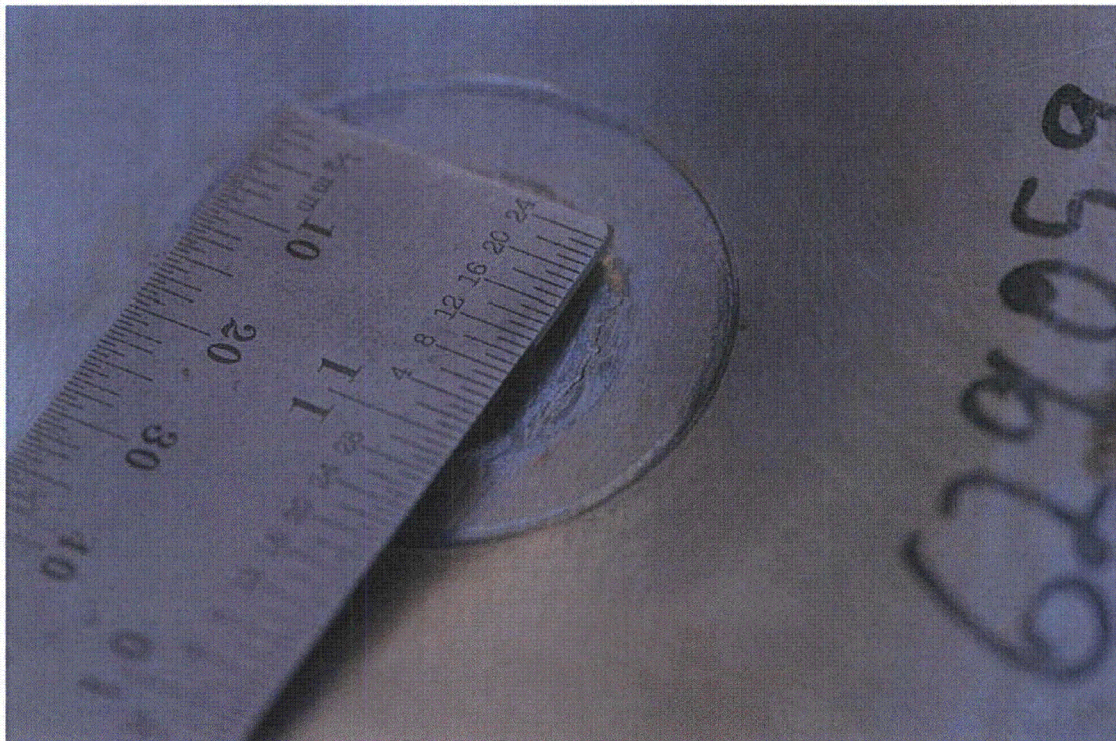


Figure 2.12.1-40 - Cracked Weld Under Index Lug, CD2.C-1

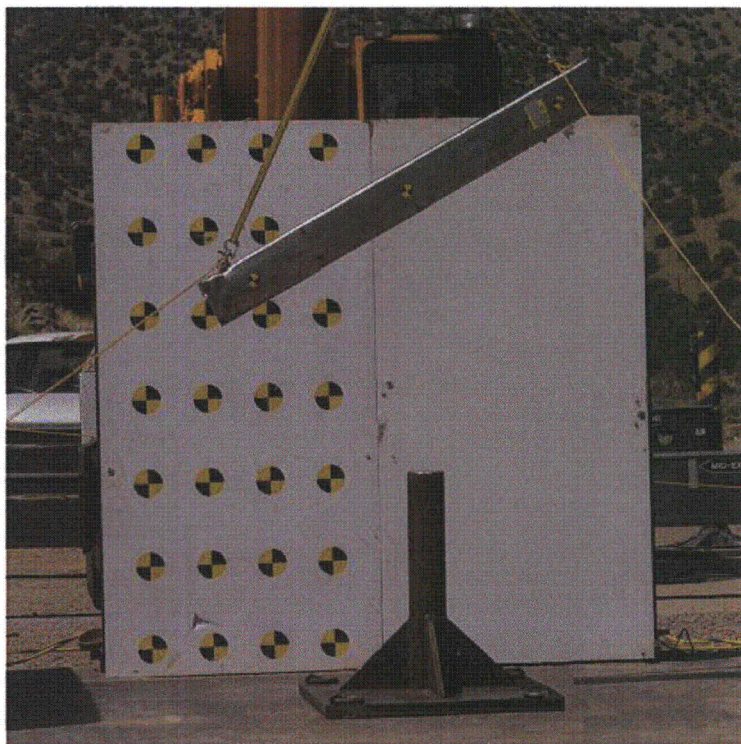


Figure 2.12.1-41 - CP2-1 Drop Orientation

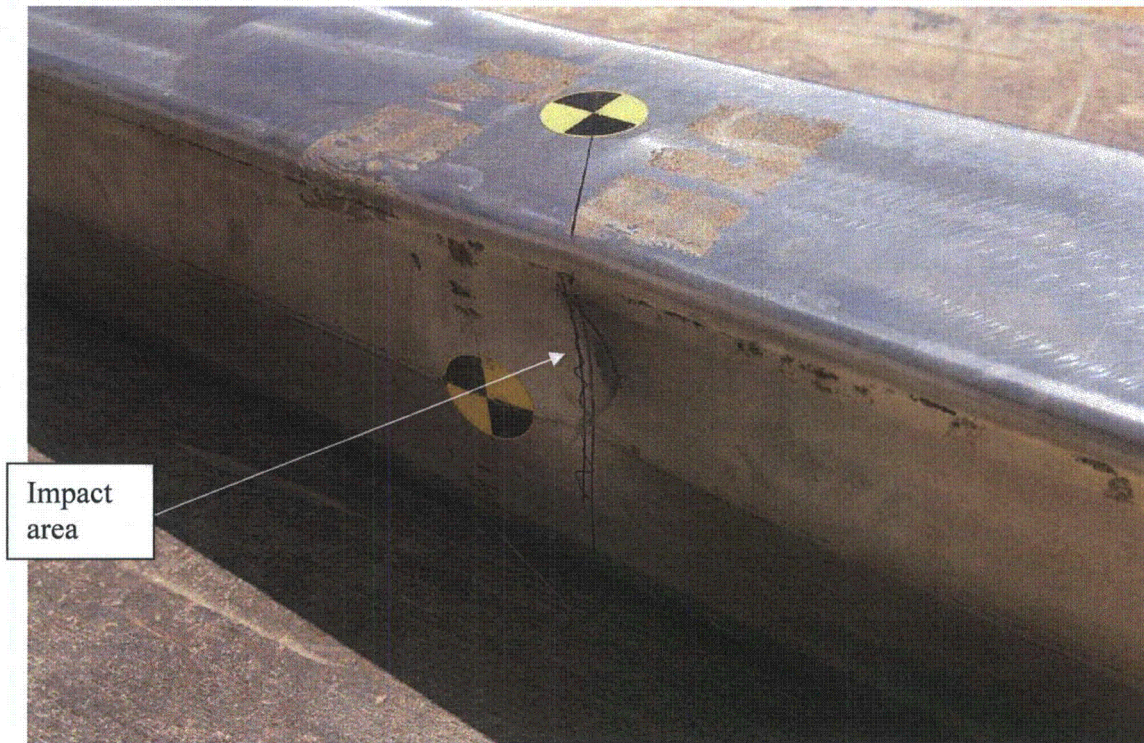


Figure 2.12.1-42 - CTU Following CP2-1 Impact

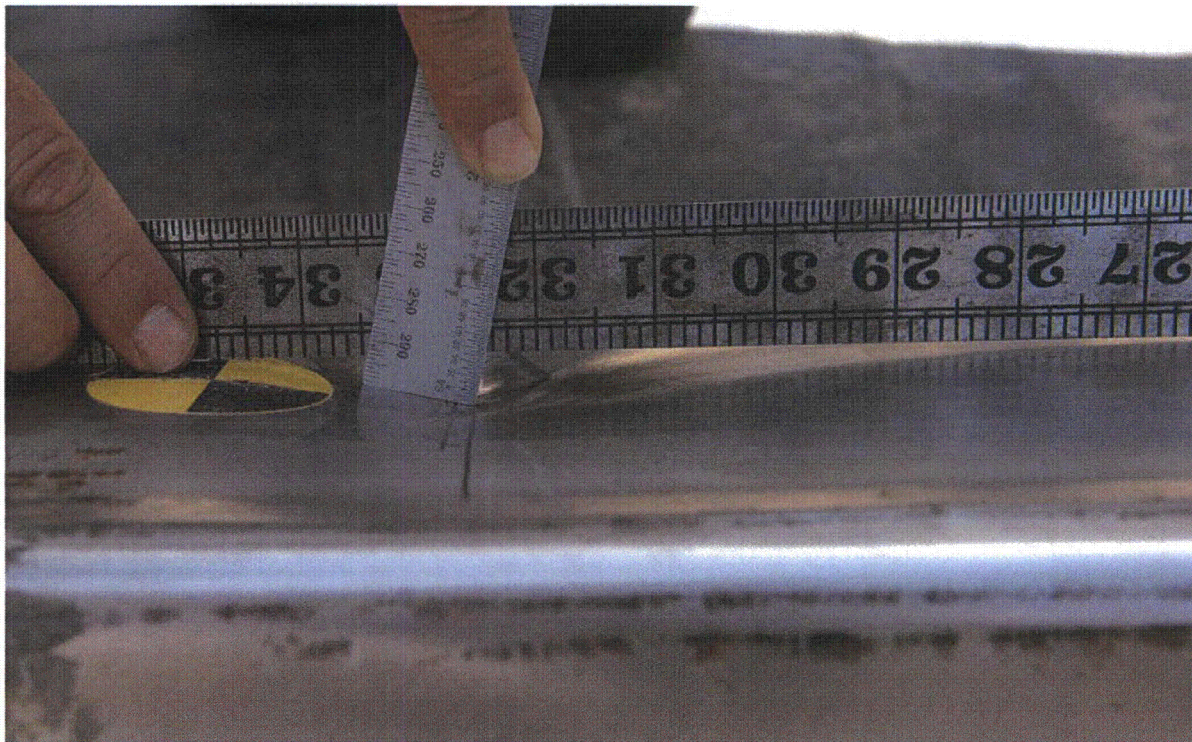


Figure 2.12.1-43 - CP2-1 Impact Damage

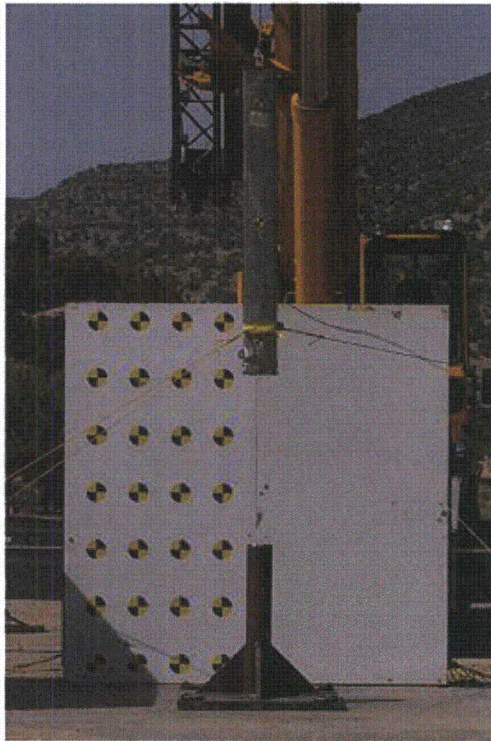


Figure 2.12.1-44 - CP1-1 Drop Orientation

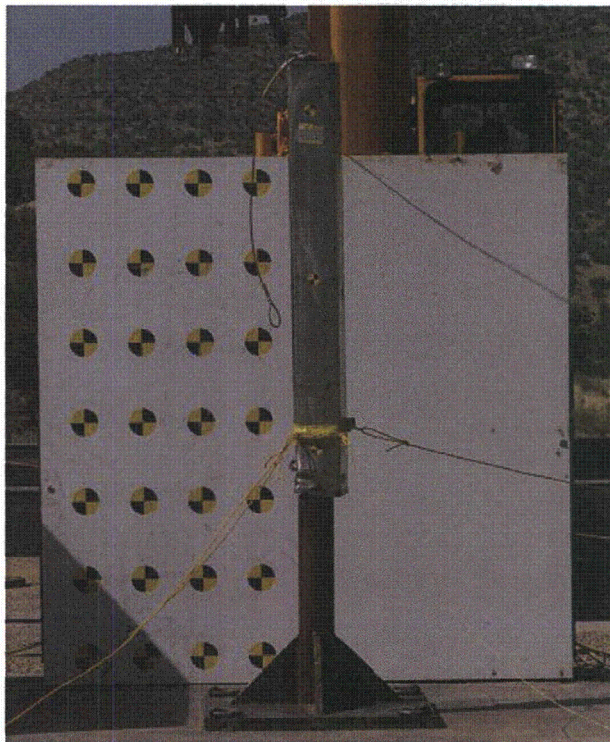


Figure 2.12.1-45 - CTU Following CP1-1 Impact



Figure 2.12.1-46 - CP1-1 Impact Damage (Shown Index Lugs Down)



Figure 2.12.1-47 - Attempted Closure Removal



Figure 2.12.1-48 - Exposure of Thermal Shield

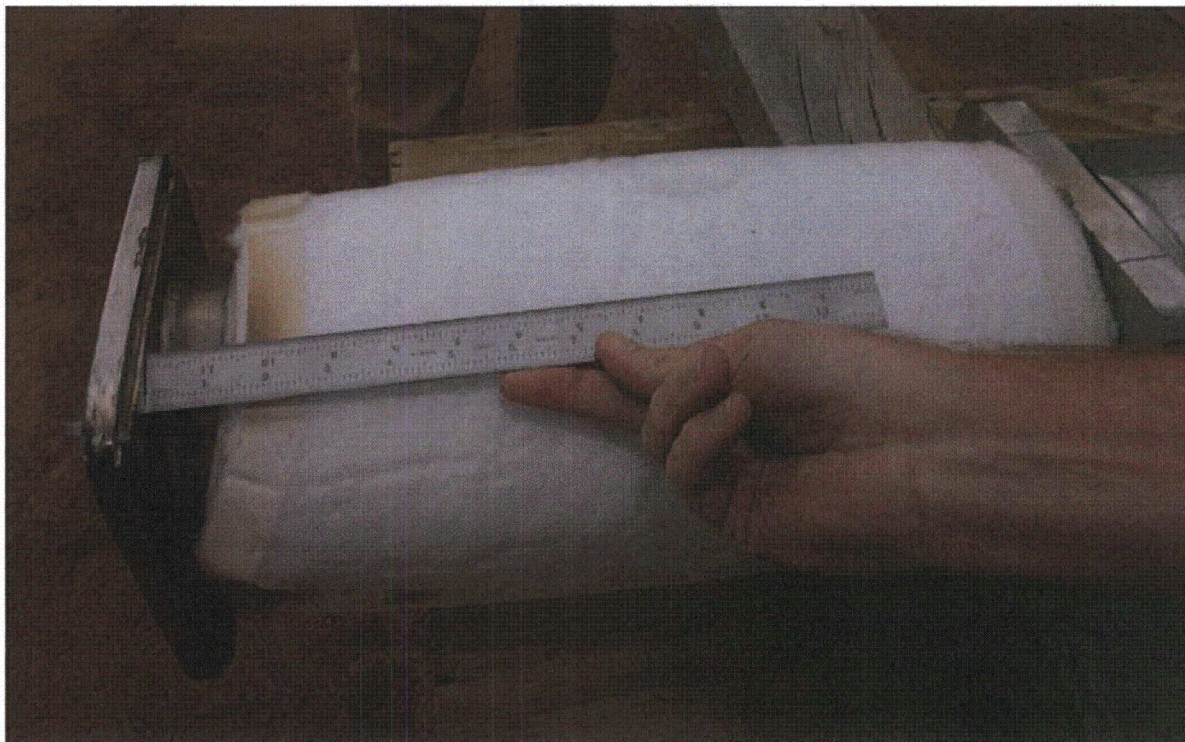


Figure 2.12.1-49 - Insulation After Removal of Thermal Shield



Figure 2.12.1-50 - Middle Insulation After Removal of Thermal Shield

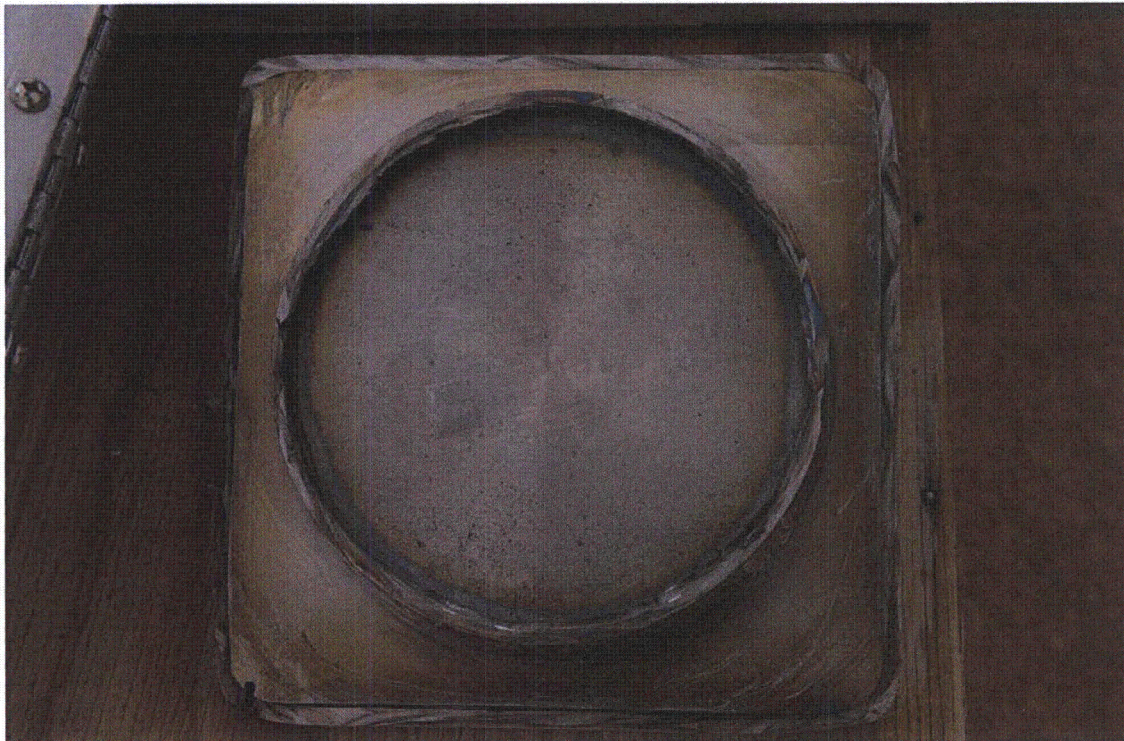


Figure 2.12.1-51 - Bottom End Plate Condition

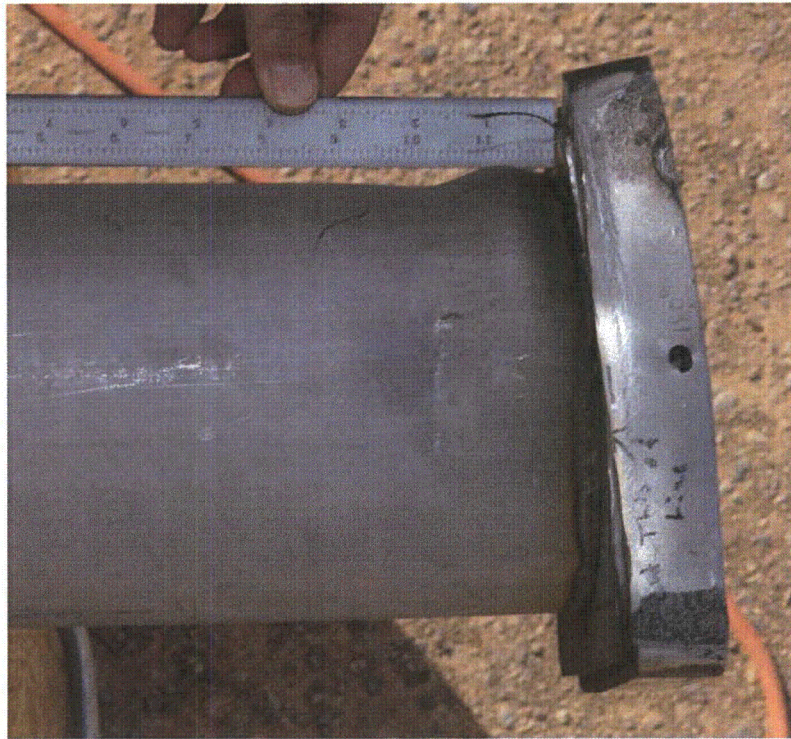


Figure 2.12.1-52 - View of Inner Tube at Closure End

Flattening of
FHE endplate

Inward
deformation of
inner pipe



Figure 2.12.1-53 - Inner Tube Deformation at Closure End

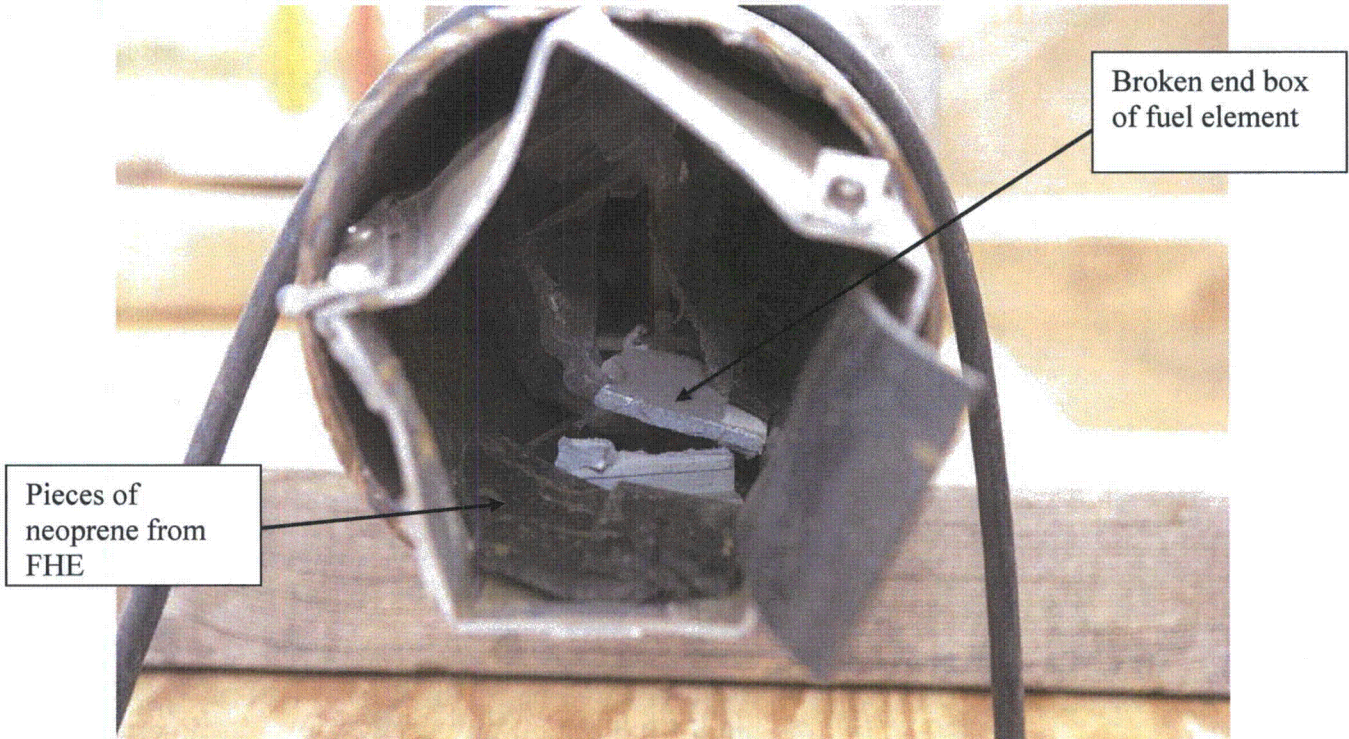


Figure 2.12.1-54 - End View (Bottom) of Opened CTU



Figure 2.12.1-55 - Removal of ATR Fuel Element

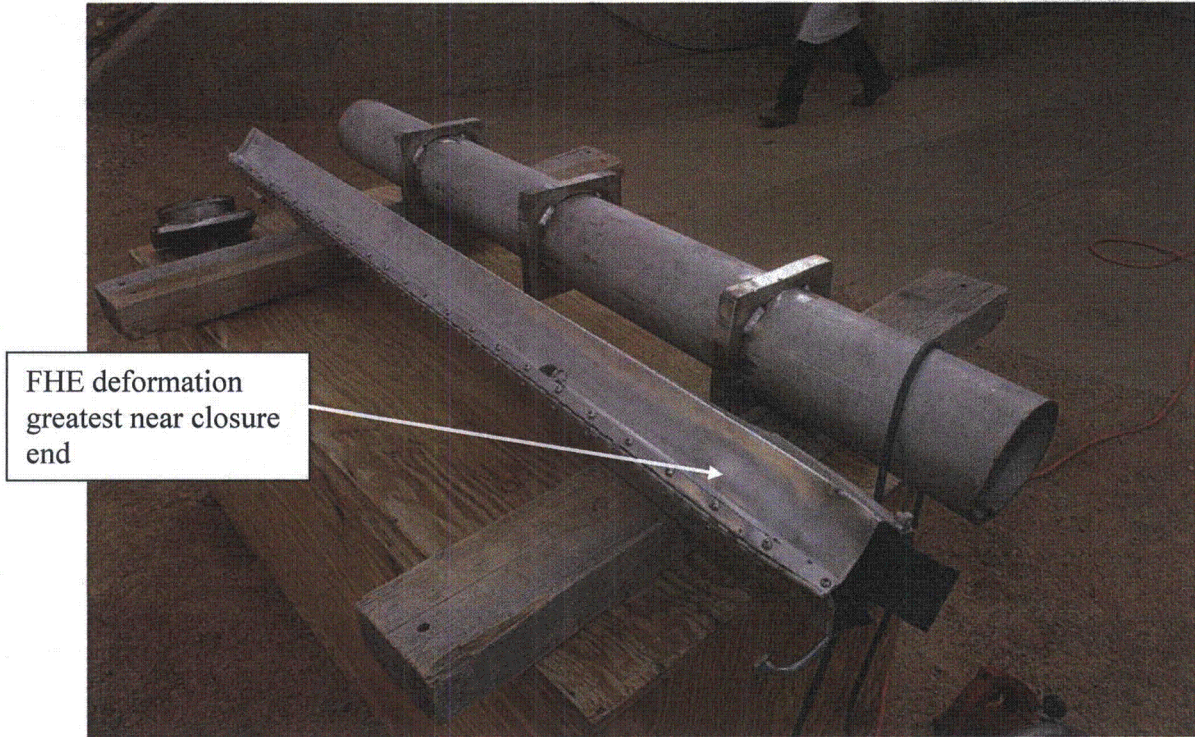


Figure 2.12.1-56 - Fuel Handling Enclosure Deformation



Figure 2.12.1-57 - ATR Fuel Element Inspection

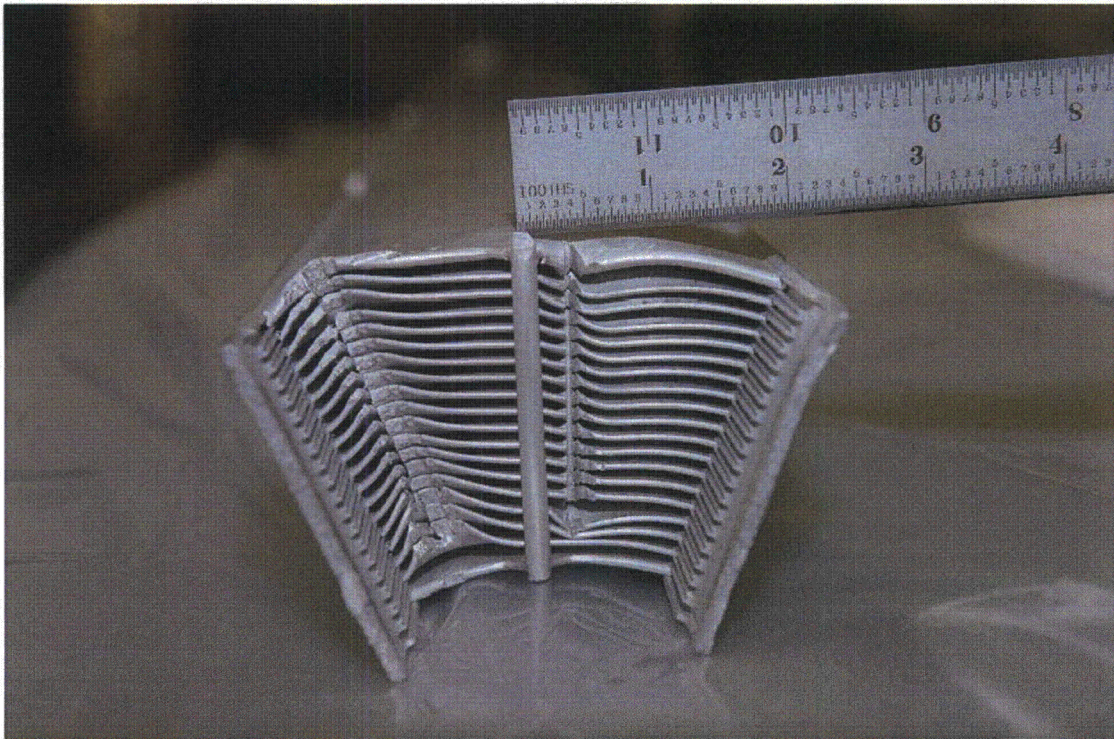


Figure 2.12.1-58 - ATR Fuel Element at Head End

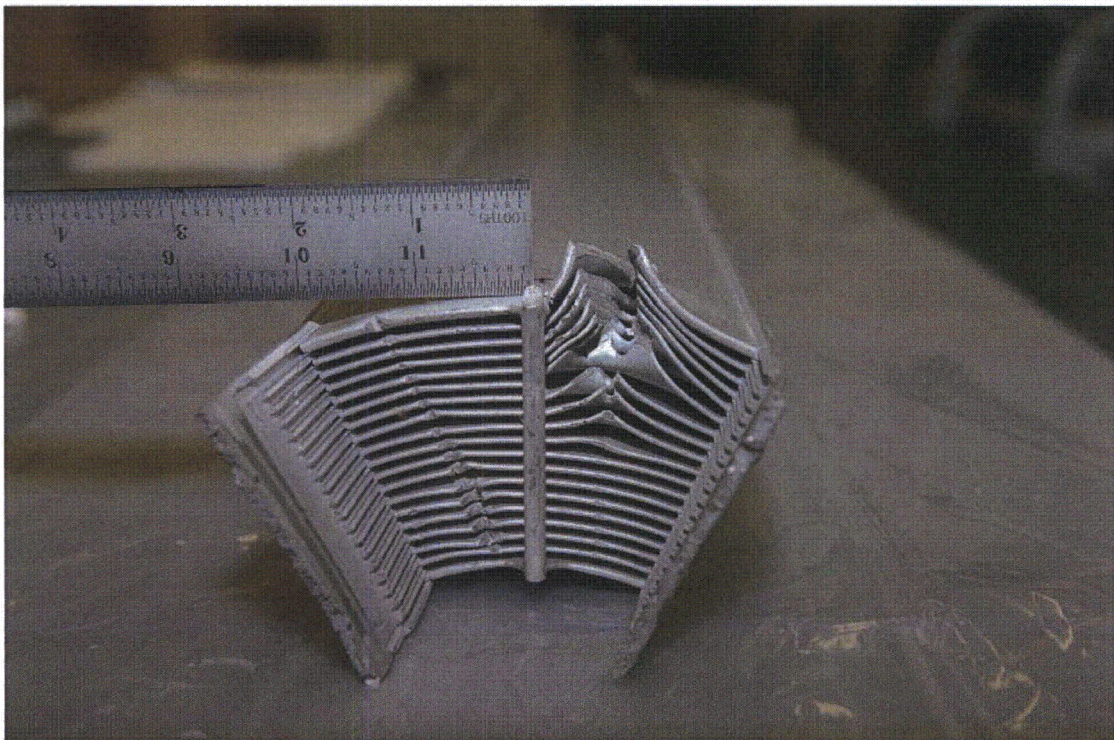


Figure 2.12.1-59 - ATR Fuel Element Damage at Bottom End



Figure 2.12.1-60 - Top View ATR Fuel Element at Bottom End

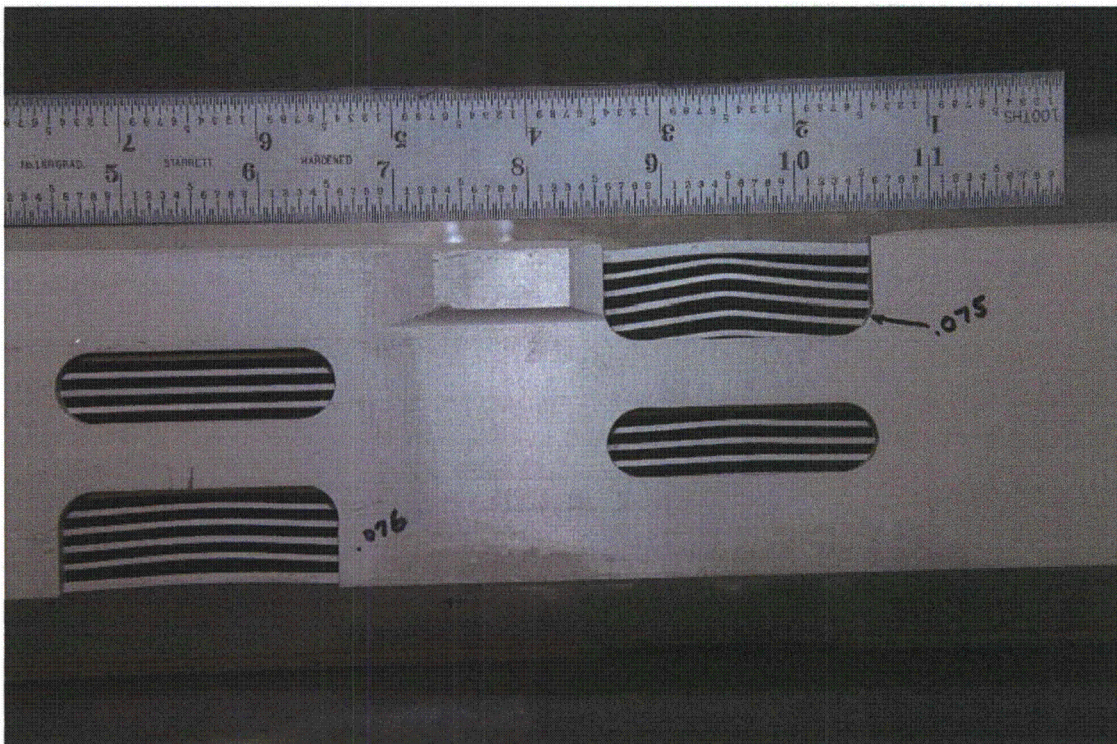


Figure 2.12.1-61 - ATR Fuel Element Fuel Plates Left Side

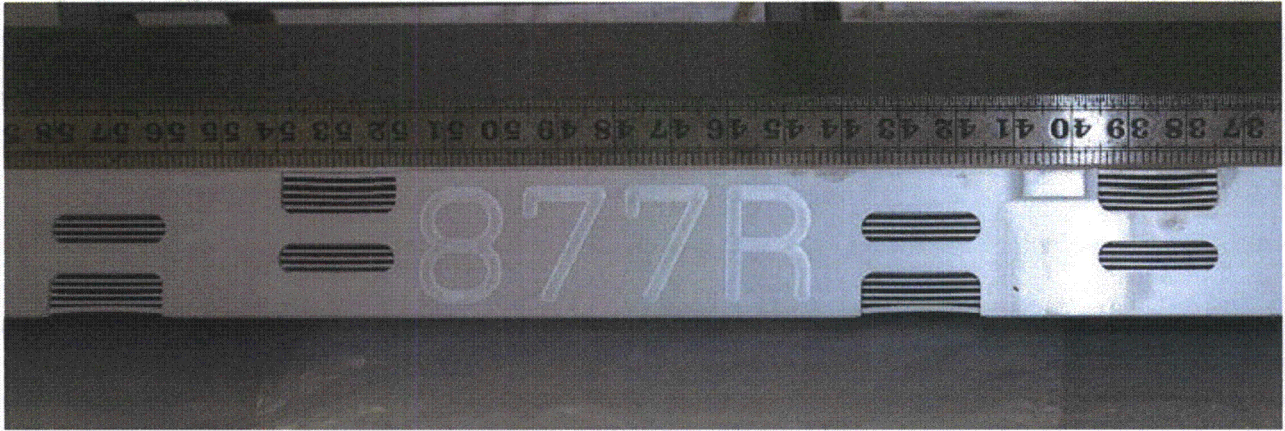


Figure 2.12.1-62 - ATR Fuel Element Fuel Plates Right Side

2.12.2 Certification Tests on CTU-2

This report describes the methods and results of a series of tests performed on the Advanced Test Reactor (ATR) Fresh Fuel Shipping Container (FFSC) transportation package, shown in Figure 2.12.2-1. The objective of testing was to conduct drop tests in accordance with the requirements of 10 CFR 71, §71.71 Normal Conditions of Transport (NCT), and §71.73 Hypothetical Accident Conditions (HAC). This test was primarily directed at verification of the loose fuel plate basket structural integrity and the performance of the package insulation. The package and ATR fuel element payload performance are supported by the tests described in Section 2.12.1, *Certification Tests on CTU-1*.

Testing was performed at HiLine Engineering in Richland, Washington on May 17, 2007. Color photographs and videos were taken to document the test events and results.

2.12.2.1 Overview

There are three primary objectives for the certification test program:

1. To demonstrate that, after a worst-case series of HAC free drops, the package maintains containment of radioactive contents.
2. To demonstrate that, after a worst-case series of HAC free drops, geometry of both the fuel and package are controlled as necessary to maintain subcriticality.
3. To demonstrate that, after the free drops, the package retains the thermal protection necessary to maintain the fuel below its melting point during the thermal evaluation.

Several orientations were tested to ensure that the worst-case series of free and puncture drop events had been considered. Post-impact examination demonstrated that the package sufficiently met the design objectives. The specific objectives of this test were to demonstrate:

- Any displacement of package insulation and/or thermal shields are bounded in the thermal analysis,
- Reconfiguration of the loose fuel plate basket and/or loose fuel plate payload is bounded in the criticality analysis.

2.12.2.2 Pretest Measurements and Inspections

The ATR FFSC packaging (serial number CTU1), loose fuel plate basket (serial number 1), and simulated ATR loose fuel plates were received at HiLine. The packaging and payload are identified as ATR FFSC Certification Test Unit CTU-2. The components arrived fully constructed and ready for testing.

The ATR loose fuel plates were simulated. The payload was comprised of a combination of 2- and 4-inch wide, .06-inch thick, 5052H32 aluminum flat plates. All plates were 49.5-inches long. There were 15, 2-inch wide plates and 10, 4-inch wide plates making up a total payload weight of 20.7 lbs.

The CTU was dimensionally inspected to the drawings at the fabricator and the fabrication records forwarded to PacTec. A Certificate of Compliance was issued by the fabricator of the CTUs documenting compliance with the fabrication drawings. Minor discrepancies

between the drawings and CTUs were identified and independently evaluated. The evaluations concluded that the discrepancies were minor and would not significantly affect the CTU during testing.

There were five fabrication deviations associated with the S/N CTU1 package fabrication:

- The 3/8-16 UNC index lug screws were obtained without specified ASTM F-879 certifications.
- The #10-24 UNC closure handle screws were obtained without specified ASTM F-879 certifications.
- Chemical overtesting of the package body closure plate material identified a manganese content 0.02% above the ASTM A479 maximum allowable.
- The tap failed when tapping one of the four #10-24 tapped holes for the closure handle screws. As a result, one of the four tapped holes had full threads to a depth of .44-inches rather than the specified .5-inches.
- The handle width is specified to be $7.5 \pm .3$ -inches. When measured in the free state (not secured to the closure), the handle width was undersized by approximately 0.1-inches.

Other deviations relative to the CTU are the absence of the stainless nameplate and the use of temporary rigging attachments. These items are also insignificant relative to the weight of the CTU and their impact upon the drop tests.

2.12.2.2.1 Component Weights

Component weights were measured and recorded as shown in Table 2.12.2-1.

2.12.2.2.2 Drop Test Pad Measurement and Description

The drop pad consists of a 7-foot square x 5-foot thick concrete block covered with a 6-foot square x 2.5-inch thick steel plate. The estimated weight of the pad is greater than 44,000 lbs. Thus the test pad was qualified as an essentially unyielding surface for the approximately 300 lb CTU.

2.12.2.2.3 Equipment and Instruments

Instrumentation used for the component weights and drop tests is given in Table 2.12.2-2. Calibrated test and measurement equipment used were the weight scale and temperature meter. Those two instruments were calibrated in accordance with HiLine procedures. It is noted that the HiLine calibration procedures require National Institute of Standards and Technology (NIST) traceability and that the HiLine records adequately demonstrated that the calibrations were NIST traceable.

A plumb bob with a stretch resistant string was used to determine the appropriate drop height. HiLine project personnel under the supervision of PacTec personnel measured the plumb bob and string using steel tape measures. The angle of the CTU prior to each drop was measured using a mechanical inclinometer.

One low speed digital video camera was used to record the drop events. In addition, color photographs were taken to document the testing.

2.12.2.3 Summary of Tests and Results

2.12.2.3.1 Initial Conditions

All three HAC drops, CD1-2, CD3-2, and CD4-2, were performed at ambient temperature. Ambient temperature and the package surface temperature was recorded before and after each drop. After each drop the closure was removed and the basket inspected. The basket was reassembled (the basket screws tightened to the "finger tight" condition) and the package re-closed for the following test. One tie wrap (securing the loose fuel plate payload) failed in the CD1-2 test and the second tie wrap failed in the CD3-2 test. Neither of the two tie wraps were replaced between tests.

2.12.2.3.2 Summary of Testing

Table 2.12.2-3 identifies the testing performed on the ATR FFSC CTU.

2.12.2.4 Certification Tests

2.12.2.4.1 Drop Tests

The three CTU-2 HAC drop tests were performed to augment the CTU-1 tests for the package, and to demonstrate acceptable performance of the loose fuel plate basket payload. In CTU-1, the package was subjected to end drops on both the closure and the bottom ends of the package. CTU-2 restricted the end drop test to just the bottom end to properly assess axial insulation displacement.

There were no NCT or puncture bar tests performed on the package, since CTU-1 adequately demonstrates acceptable package performance under those conditions. The two side drops subjected the loose fuel plate basket and simulated fuel to worst case impact conditions with the basket oriented perpendicular and parallel to the target surface.

The test identification numbering reflects the same drop orientation as performed in CTU-1. For example, CD3-2 is the same orientation as the third HAC drop in CTU-1, test CD3-1. The "-2" identifies this drop as a CTU-2 test.

2.12.2.4.1.1 CD1-2 –Flat (pocket side down) Side HAC Drop

The CTU was fitted with swivel lift eyes, and the lift eyes were threaded into the package lift points. This configuration oriented the package such that the package pocket side impacted the target surface. Slings were used to rig the CTU from the swivel lift eyes to the crane remote release hook. Figure 2.12.2-5 illustrates the drop orientation. Initial conditions were as follows:

- Ambient temperature: 73 °F
- Avg. surface temperature: 78 °F
- Time: 10:04 a.m. 5/17/2007
- Drop height: 30 ft

Following impact, the CTU bounced slightly and landed on the impact side. There was minor visible exterior damage, principally scuff marks, resulting from the drop. Close examination of

the package, on the impacted surface side, reveals minor distortion of the outer shell localized at the stiffening ribs. Figures 2.12.2-6 and 2.12.2-7 show the CTU prior to and following the drop. There was no bowing or other significant visible deformation. There was no visible deformation or rotation of the closure, and the locking pins condition and function were unaffected by the drop.

The basket was not affected by the drop, however the finger operated screws securing the two basket halves were loosened approximately one turn. One fuel tie wrap was broken but the simulated loose fuel plates were not damaged. The simulated fuel plates were replaced in the basket without installing new tie wraps, and the basket closure screws again tightened to the finger tight condition.

2.12.2.4.1.2 CD3-2 – Flat Side HAC Drop (90° from CD1-2)

Following the CD1-2 drop, lift points were welded to the package to enable a side drop rotated 90° from CD1-2 (Figure 2.12.2-8):

- Ambient temperature: 78 °F
- Avg. surface temperature: 85 °F
- Time: 10:50 a.m. 5/17/2007
- Drop height: 30 ft

The CTU rebounded from the drop pad approximately 1 ft following the 30 ft drop and came to rest on its side (rotated 90° from the drop orientation). As with the CD1-2 event, the outer shell exhibited minor deformation at the stiffening rib locations (reference Figure 2.12.2-9). There was no visible deformation or rotation of the closure, and the locking pins were undamaged and in good working order.

The closure was opened and the basket removed following the drop. The basket exhibited no signs of any deformation but the finger tightened basket screws were loosened approximately 1 turn by the drop.

The basket was opened and it was discovered that the second plastic tie wrap was broken (Figure 2.12.2-10). The simulated fuel plates were found to exhibit no significant damage. The simulated fuel plates were replaced in the basket without installing new tie wraps, and the basket closure screws again tightened to the finger tight condition.

2.12.2.4.1.3 CD4-2 – CG over Bottom End (Vertical)

Following CD3-2, the temporary rigging attachments were removed and the CTU rigged for CD4-2 by lifting the package from the closure handle (Figure 2.12.2-11). Initial conditions were recorded as follows:

- Ambient temperature: 88 °F
- Avg. surface temperature: 90 °F
- Time: 11:20 a.m. 5/17/2007
- Drop height: 30 ft

The CTU appeared to impact slightly off of true vertical; impacting near one corner of the package. This impact dented the lift point feature inward approximately ½-inch, and on one adjacent side, bulged out the square outer tube surface by approximately ½-inch. Following impact, the CTU rebounded vertically approximately 2-feet, tipped over, and landed on the CD3-2 impact side. There was no overall bowing or of the package or other significant visible deformation. There was no visible deformation or rotation of the closure. Figure 2.12.2-12 shows the bottom end of the CTU following the drop.

There was no visible damage to the closure or the locking pins. The closure was removed and the basket extracted following CD4-2. Damaged to the basket was limited to a small dent at the end of the basket that was situated closest to the package bottom. Upon destructive examination of the package, it was discovered that the weld between the package inner shell and the component at the bottom of the payload cavity had intruded into the payload cavity in a localized area (Figure 2.12.2-13). When the package impacted in CD4-2, the basket was partially supported by that weld bead. The end plate of the basket was slightly deformed (Figure 2.12.2-14) as the basket seated on the bottom of the package payload cavity. The damage was minor and did not impair the ability of the basket to retain the fuel plates.

The simulated fuel plates experienced localized deformation at the end of the basket closest to the package bottom (Figure 2.12.2-15 and Figure 2.12.2-16). Above this area the simulated fuel plates were not deformed.

2.12.2.5 Post-test Disassembly and Inspection

The final acceptance criteria for the ATR FFSC package lies with the criticality evaluation. Any increase in reactivity of the contents resulting from the certification tests must not exceed the allowable as defined in the criticality evaluation. The inspections required to support determination of compliance with the acceptance criteria are identified as follows:

- Inspect the outer shell to verify the thermal performance of the package is unimpaired by the free drop events. The thermal analysis assumes that the outer shell is intact such that there is no significant communication between the environment and the outer/inner shell annular space during the thermal event.
- Inspect the insulation to verify compliance with the assumptions of the thermal analysis.

- Inspect the overall package to verify that the package geometry remains within the criticality analyses assumptions.
- Inspect the simulated fuel plate payload to verify that the fuel geometry remains within the assumptions of the criticality analyses.

Any deviation of the test results from these acceptance criteria must be reconciled with the criticality evaluation.

2.12.2.5.1 CTU Inspection

The CTU-2 was disassembled and inspected on May 17, 2007. Prior to disassembly the exterior dimensions were recorded for comparison to the pre-test condition. Table 2.12.2-4 lists the measured dimensions and Figure 2.12.2-17 identifies the location of the identified measurements.

The closure handle was unaffected by the first two drops. In the CD4-2 drop, the handle was dented when it was struck by the rigging shackle. During the CD4-2 CG over bottom (vertical) HAC drop, the outer wall bulged out at the bottom end of the package and caused the width of the package to increase from 8 inches to approximately 8 5/8 inches in that area.

The CTU was disassembled systematically by cutting away the outer layers of the packaging using an abrasive saw. The destructive examination was necessary due to the required inspection of the interior insulation. The package was cut lengthwise along two opposite corners and at the ends to expose the thermal shield.

The stainless steel thermal shields were all intact (Figure 2.12.2-18 through Figure 2.12.2-20). There was minor deformation of the thermal shields at the interface to the stiffening rib. This deformation resulted from the CD4-2 drop and caused the thermal shields to buckle one end and pull away from the stiffening rib at the other end. Figure 2.12.2-21 is typical of this condition. The gap between the thermal shield and the stiffening rib, where the shield pulls away from the rib, is less than 1/16-inch.

Following documentation of the thermal shields the shields were removed to enable examination of the insulation. For reference purposes the ribs are labeled 1 through 3 (Figure 2.12.2-22). The number 1 rib is closest to the bottom end of the package.

As can be seen in Figure 2.12.2-23 through Figure 2.12.2-26 the largest gap occurred at the closure end of the package. The gap ranges from 1-inch to 1 3/4 inches at that location. At the rib 3 and rib 2 locations the gap ranged from 1- to 1 1/2-inches. At the rib 3 location the gap ranged from 1/2- to 1-inch. All gaps are within the 1.85-inch gap assumed in the thermal analysis.

Following thermal shield and insulation removal an abrasive saw was used to separate the bottom end plate from the inner tube. Figure 2.12.2-13 illustrates the condition of the end plate. The endplate showed no drop related deformation and there were no visual indications of broken welds or other damage near the end plate. Using a lathe, the bottom end plate was cut from the insulation pocket to determine the extent of possible insulation compression in the insulation pocket (Figure 2.12.2-27). There was no indication of compression in that region and it was determined that there was no need to open the closure insulation pocket.

The inner tube was inspected and, in general, showed no signs of buckling or large deformations. A minor deformation occurred near the bottom end of the package (Figure 2.12.2-28 and Figure 2.12.2-29) corresponding to the same area of deformation as the outer shell. The tube was bent in that area yielding a slight outward bulge of about 1/16-inch and, closer to the weld between the inner shell and the package bottom, an inward deformation of approximately 1/4-inch. These deformations were localized and did not impair free movement of the basket in the payload cavity. There were no weld failures.

The closure assembly remained fully functional throughout the test series. The only damage to the closure was the handle deformation caused by the rigging shackle. The locking pins and the engagement lugs showed no signs of any deformation. The closure could be freely removed and installed through the tests.

In conclusion, CTU-2 satisfied the acceptance criteria of preventing loss or dispersal of the contents, the outer shell remained intact, the insulation remained within the assumptions of the thermal analysis, and the package and fuel geometry remained greatly unchanged. The deformations of the package and condition of the ATR loose fuel plates were evaluated, against both the criticality evaluation and thermal analysis, and determined to be within the bounds of the assumptions and conditions used to ensure safety.

Table 2.12.2-1 - Component Weights

Component	Weight (lbs)
Body Assembly	224.1
Closure Assembly	8.9
Loose Plate Fuel Basket	29.9
Simulated Fuel Plate Weight	20.7
Package (fully loaded)	283.6

Table 2.12.2-2 - Instrumentation for Drop Tests

Item Description	Model	Serial Number	Calibration Due Date	Comments
Drop Height Indicators	N/A	N/A	N/A	String plumb bobs made specifically for this testing. The length was established using a metal tape measure.
Tape Measure	N/A	N/A	N/A	35-ft. steel tape
Mechanical inclinometer	N/A	N/A	N/A	Used to identify CTU orientation
Weight Scale	Ohaus, Model CD11	0042508-6BD	7/19/2007	Used to measure weights of CTU components. The scale calibration documents included NIST traceable records.
Temperature meter	Carson, Model 4085	41372269	3/1/2008	Handheld temperature reader for measuring ambient temperature and CTU surface temperature. Meter calibration documents included NIST traceable records.

Table 2.12.2.3 - Summary of Testing

Test No.	Test Description	Comments
CD1-2	Flat side drop, pocket side down. Fuel plates oriented perpendicular to target (see Figure 2.12.2-3).	Flat side drop from 30-feet. No visible damage to package. Both closure locking pins remained in the locked position. Closure could be freely opened and payload extracted. The eight hand tightened screws securing the basket halves together were loose (approximately one turn). No visible damage to basket or simulated fuel plates.
CD3-2	Flat side drop, pockets and index lugs on side. Fuel plates oriented parallel to target (see Figure 2.12.2-4).	Flat side drop from 30-feet. No visible damage to package. Both closure locking pins remained in the locked position. Closure could be freely opened and payload extracted. The eight hand tightened screws securing the basket were loose (approximately one turn). The plastic wire ties securing the fuel bundle failed as shown in Figure 2.12.2-10. No significant deformation was observed in the fuel plates.
CD4-2	CG over bottom end (vertical)	<p>Vertical end drop from 30-feet; bottom end of package impacting the target. Both closure locking pins remained in the locked position. Closure could be freely opened and payload extracted. The eight hand tightened screws securing the basket were loose (approximately one turn).</p> <p>The bottom end of the package was deformed on two surfaces (Figure 2.12.2-12). The surface with the threaded hole was dented inward and the adjacent surface 90° apart was bulged outward.</p> <p>The surface of the basket end plate contacting the bottom of the package was slightly dented.</p> <p>The simulated fuel plates were deformed at the bottom end of the basket (Figure 2.12.2-15 and Figure 2.12.2-16).</p>

Table 2.12.2.4 - Package Length Measurements

Test ID	1	2	3	4	5	6	7	8
Pre-Test (in.)	72 7/16	72 1/2	72 7/16	72 1/2	72 7/16	72 7/16	72 7/16	72 1/2
CD1-2 (in.)	72 7/16	72 1/2	72 7/16	72 1/2	72 7/16	72 7/16	72 7/16	72 7/16
CD3-2 (in.)	72 7/16	72 1/2	72 7/16	72 1/2	72 7/16	72 7/16	72 7/16	72 7/16
CD4-2 (in.)	72 7/16	72 1/2	72 3/8	72 7/16	72 5/16	72 5/16	72 3/16	72 3/8

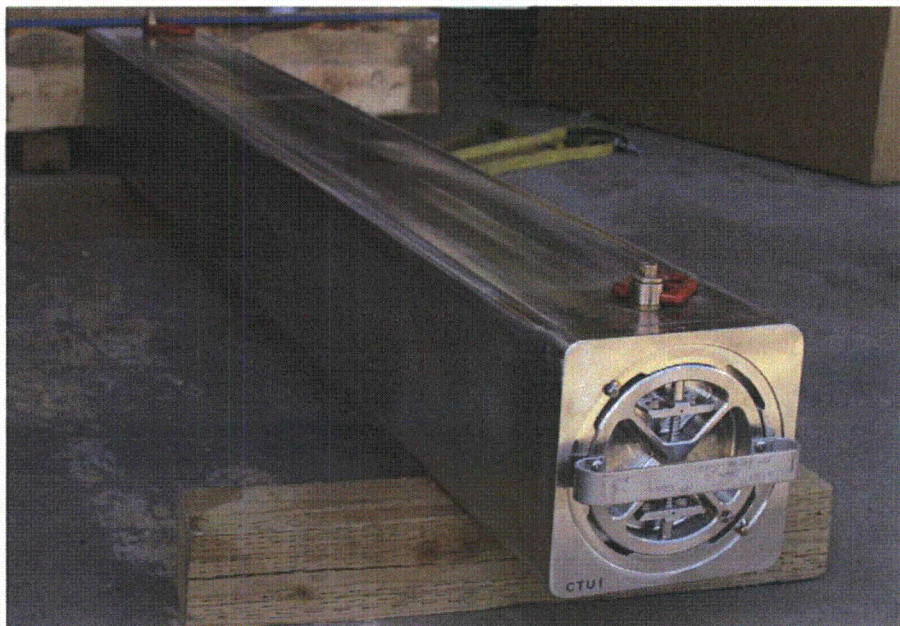


Figure 2.12.2-1 - ATR FFSC CTU-2
(CTU-2 uses package S/N CTU1)



Figure 2.12.2-2 - Loose Fuel Plate Basket and Simulated Fuel Plates



Figure 2.12.2-3 - Basket Orientation in CD1-2



Figure 2.12.2-4 - Basket Orientation in CD3-2



Figure 2.12.2-5 - CD1-2 Drop Orientation

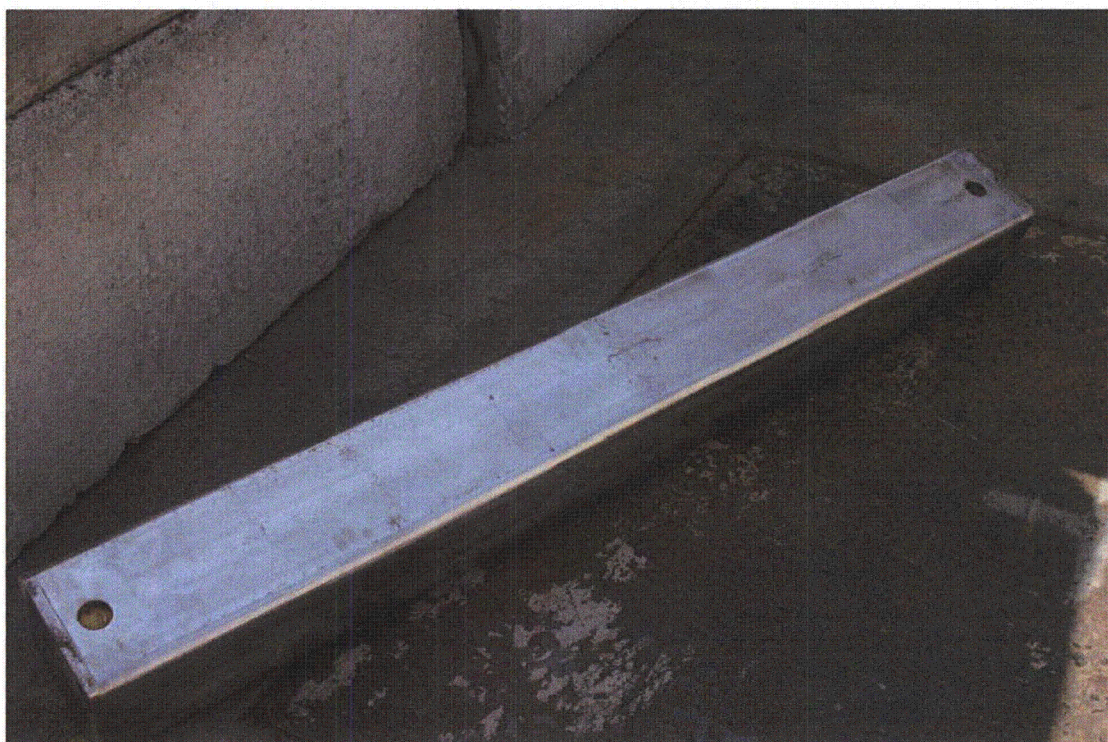


Figure 2.12.2-6 - CTU Following CD1-2 Impact
(impact side facing up)

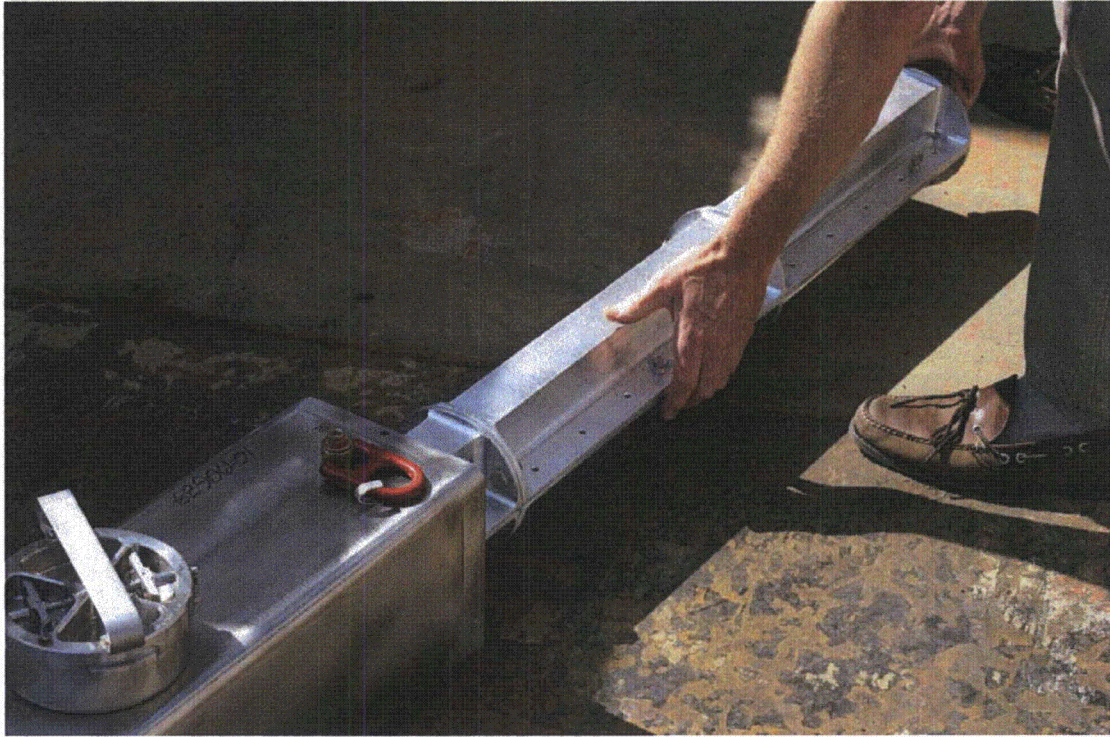


Figure 2.12.2-7 - CD1-2, Extracting Basket Following Drop

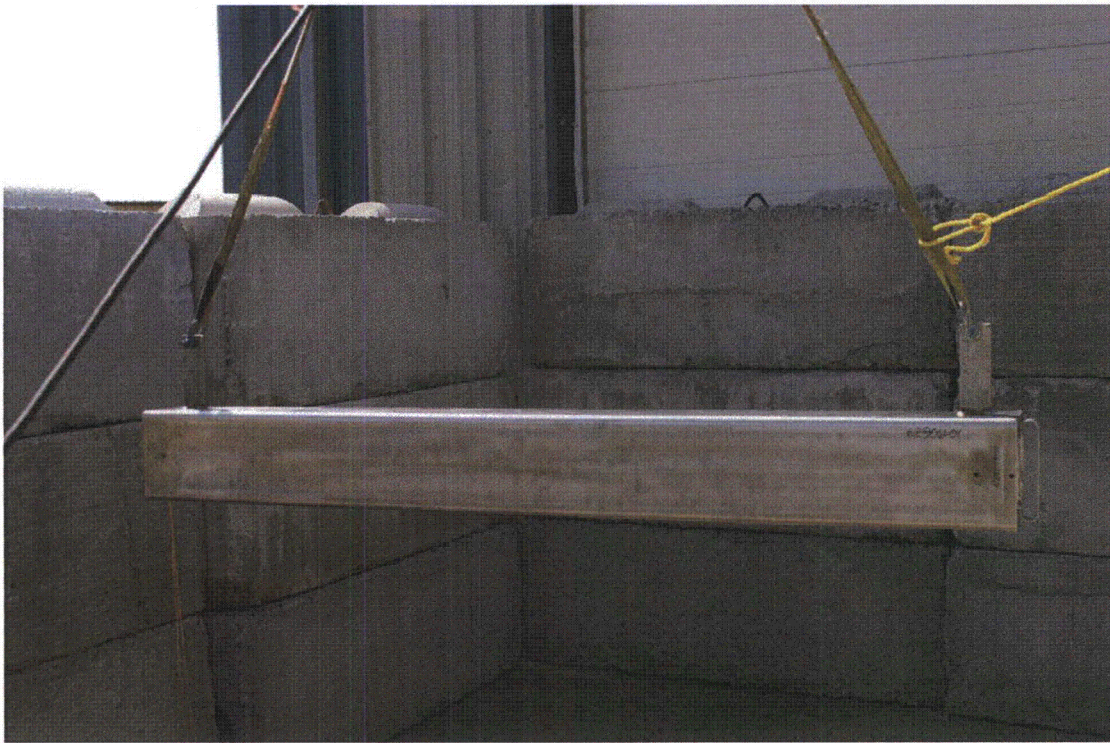


Figure 2.12.2-8 - CD3-2 Drop Orientation

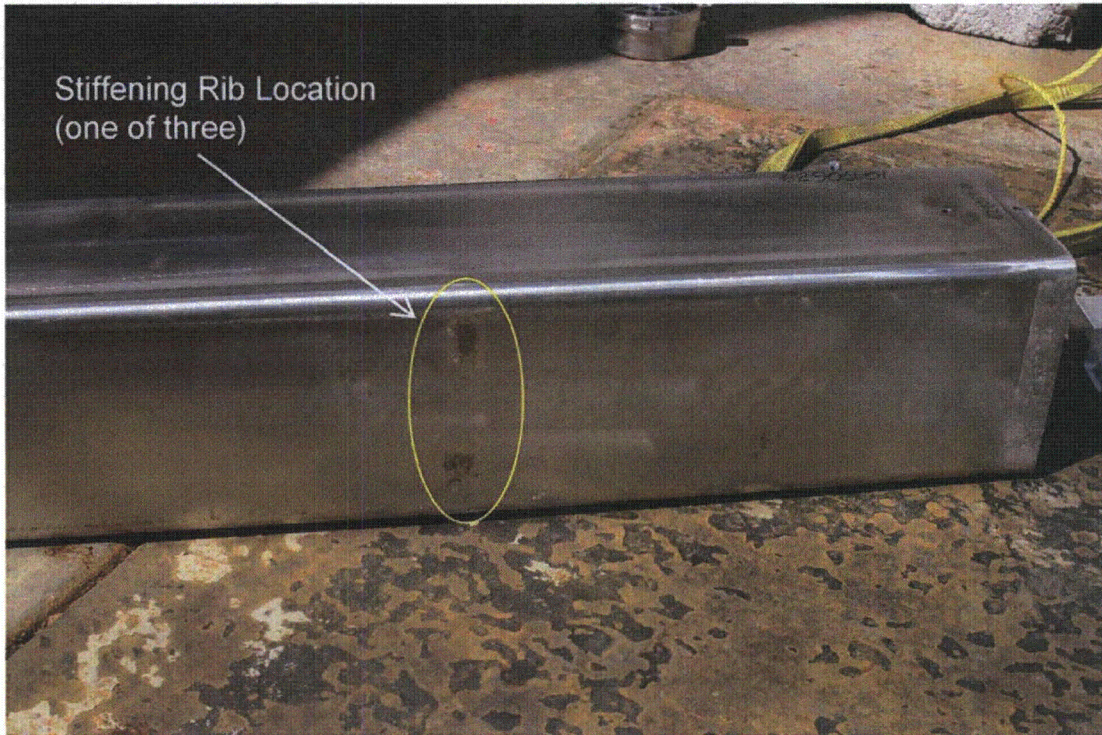


Figure 2.12.2-9 - CD3-2 Deformation at Stiffening Rib Location

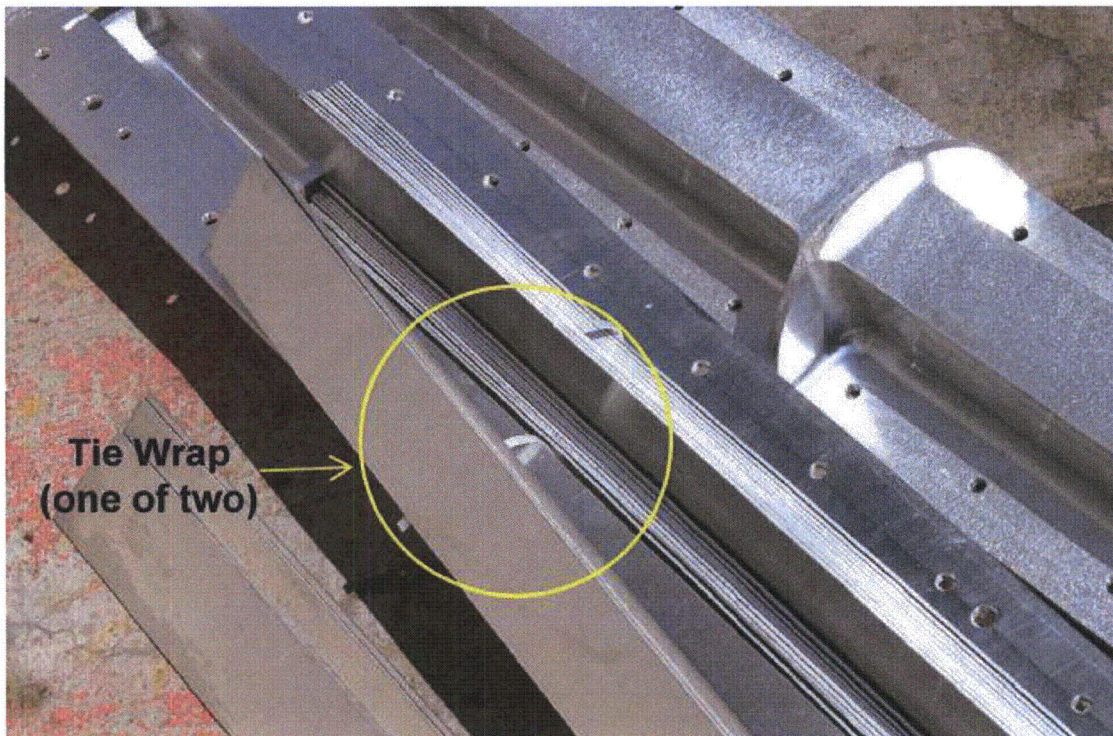


Figure 2.12.2-10 - CD3-2 – Failed tie wraps



Figure 2.12.2-11 - CD4-2 – Drop Orientation

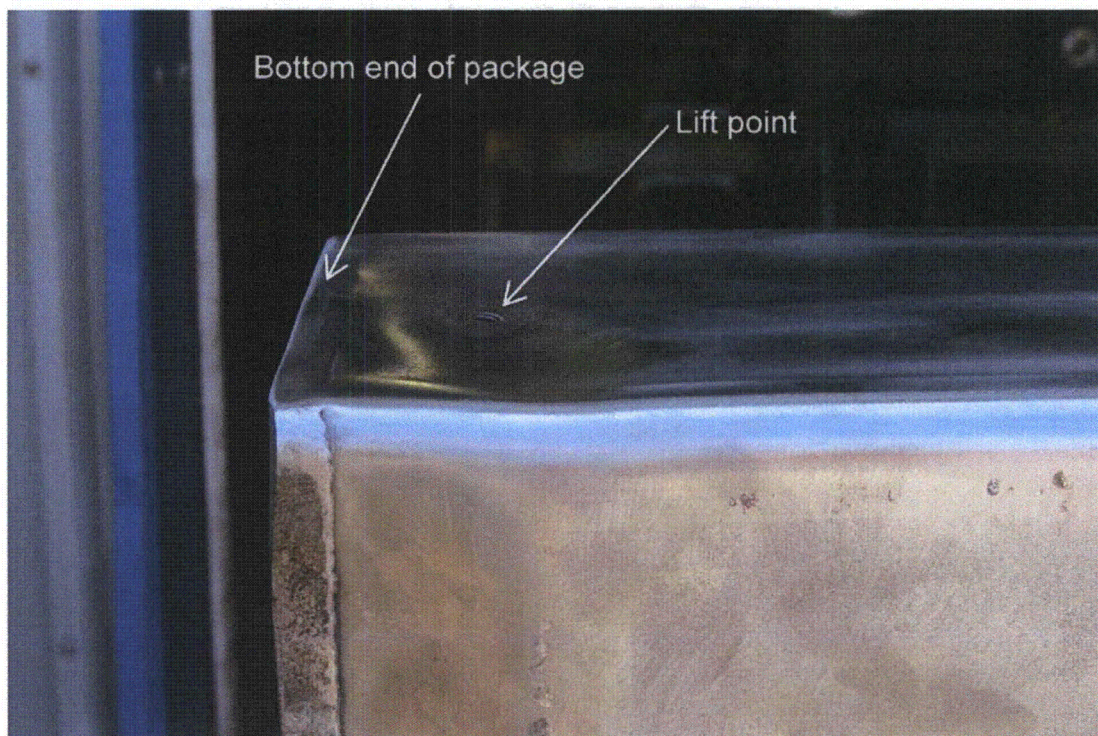


Figure 2.12.2-12 - CD4-2 Impact Damage to Package

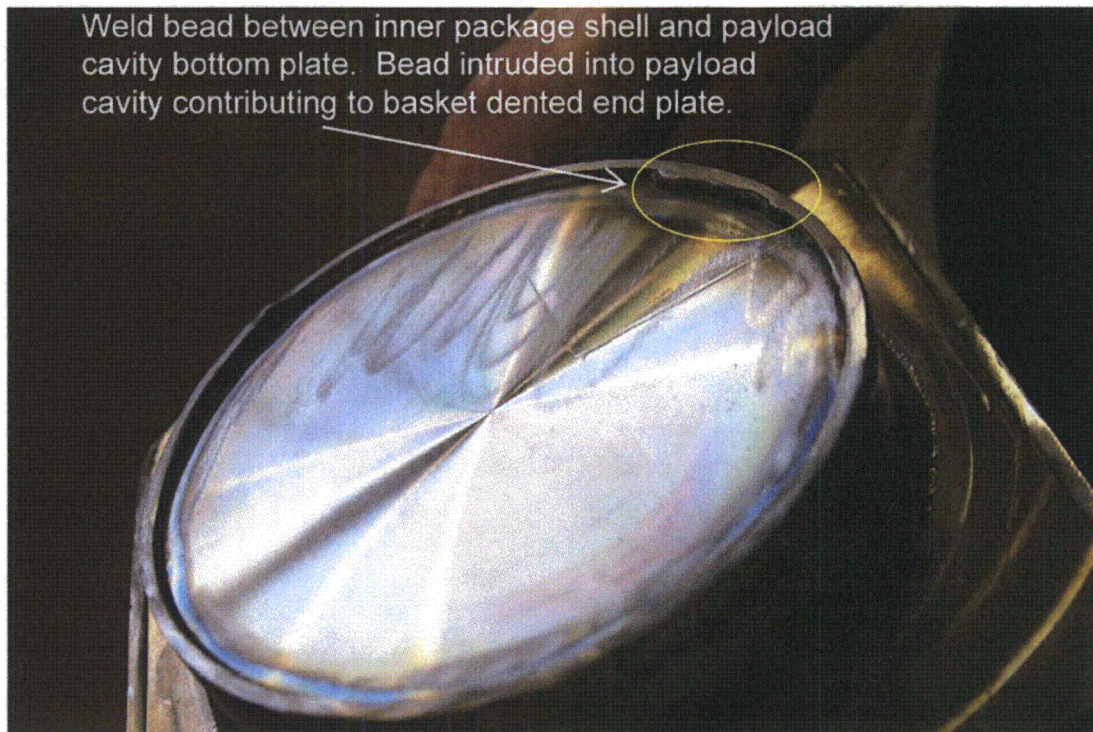


Figure 2.12.2-13 - Weld bead protruding into package payload cavity (inner shell has been removed in this photo)

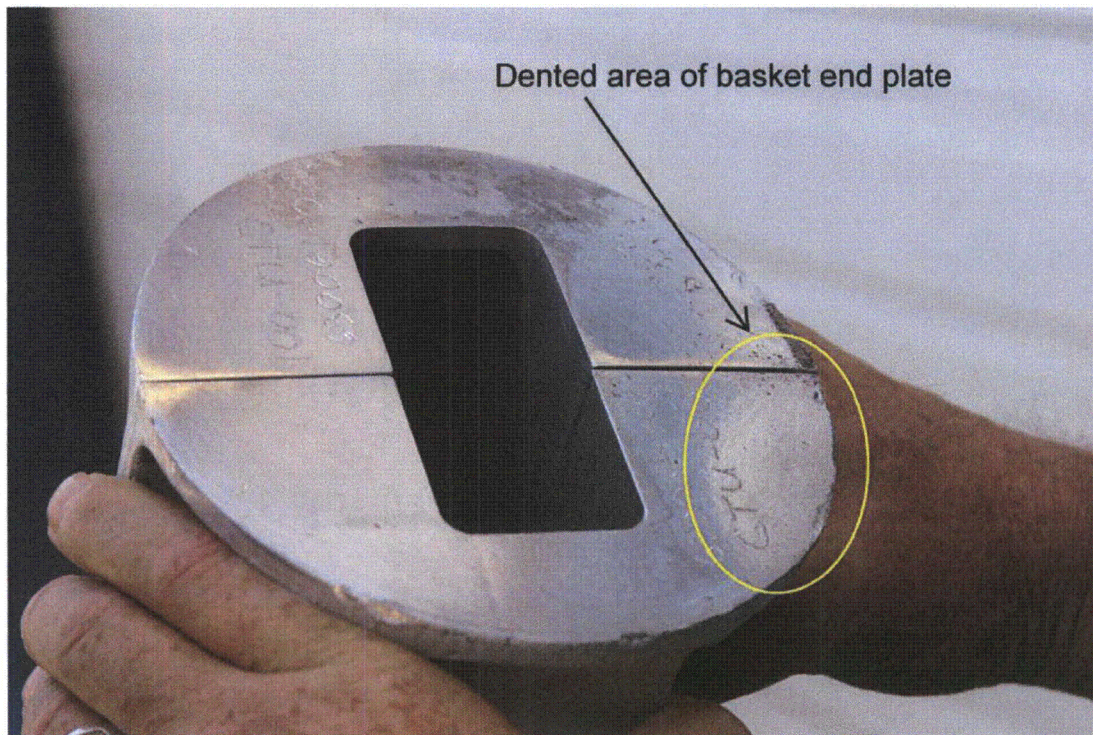


Figure 2.12.2-14 - Dented area – basket end plate

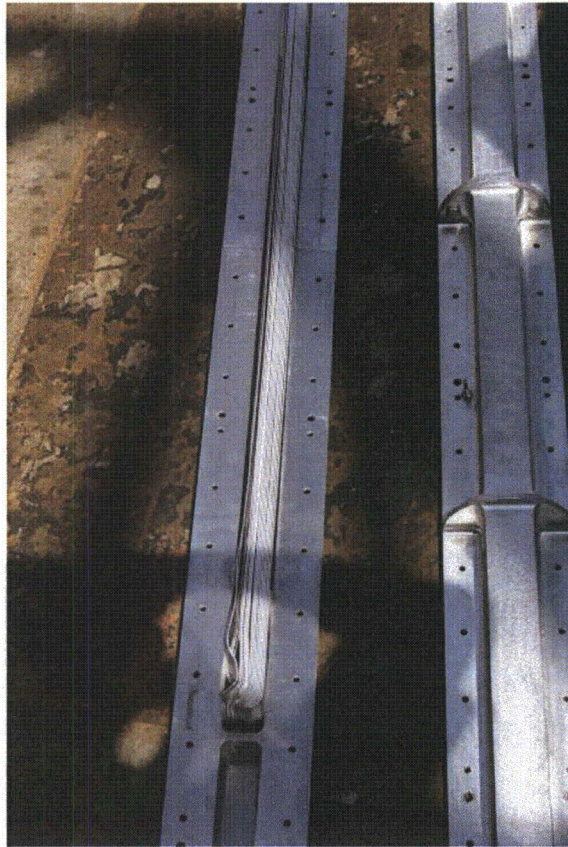


Figure 2.12.2-15 - CD4-2 Impact Damage to Simulated Fuel Plates

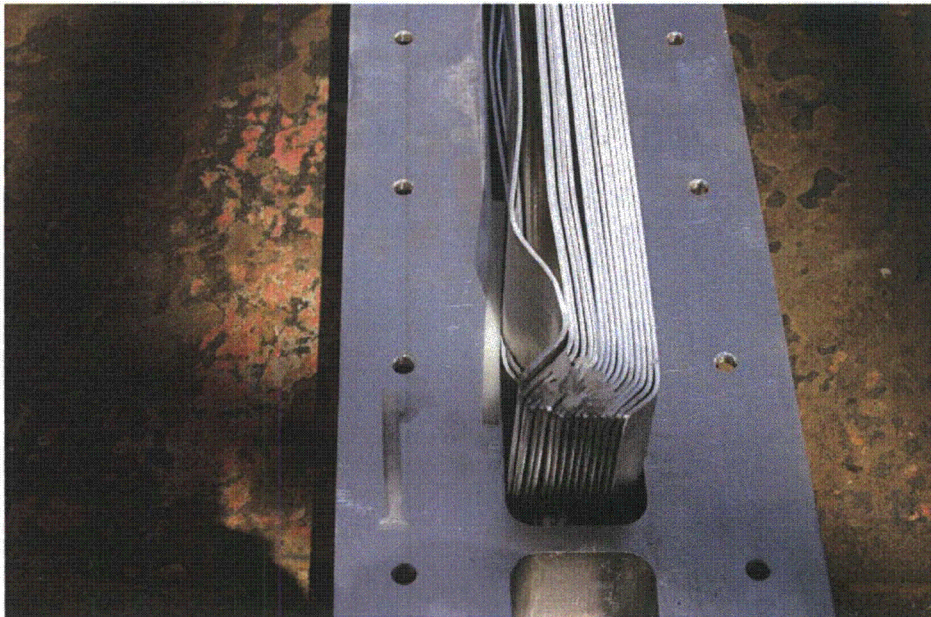


Figure 2.12.2-16 - CD4-2 Impact Damage to Simulated Fuel Plates (close up view)

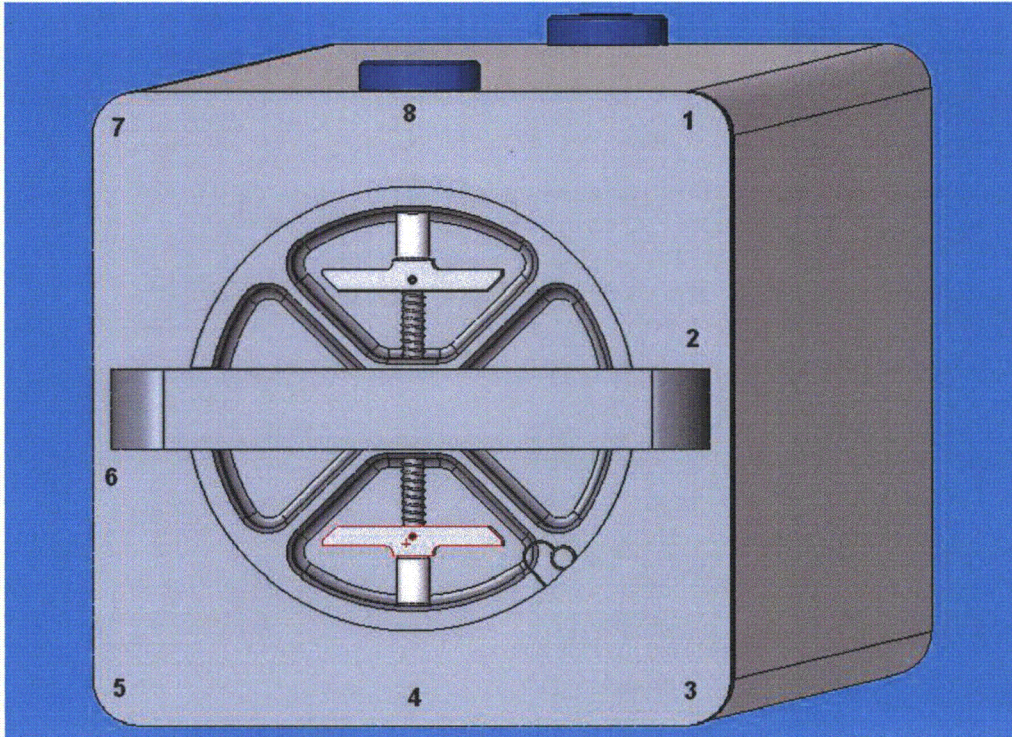


Figure 2.12.2-17 - CTU Measurement Locations



Figure 2.12.2-18 - Thermal Shield Condition, View 1

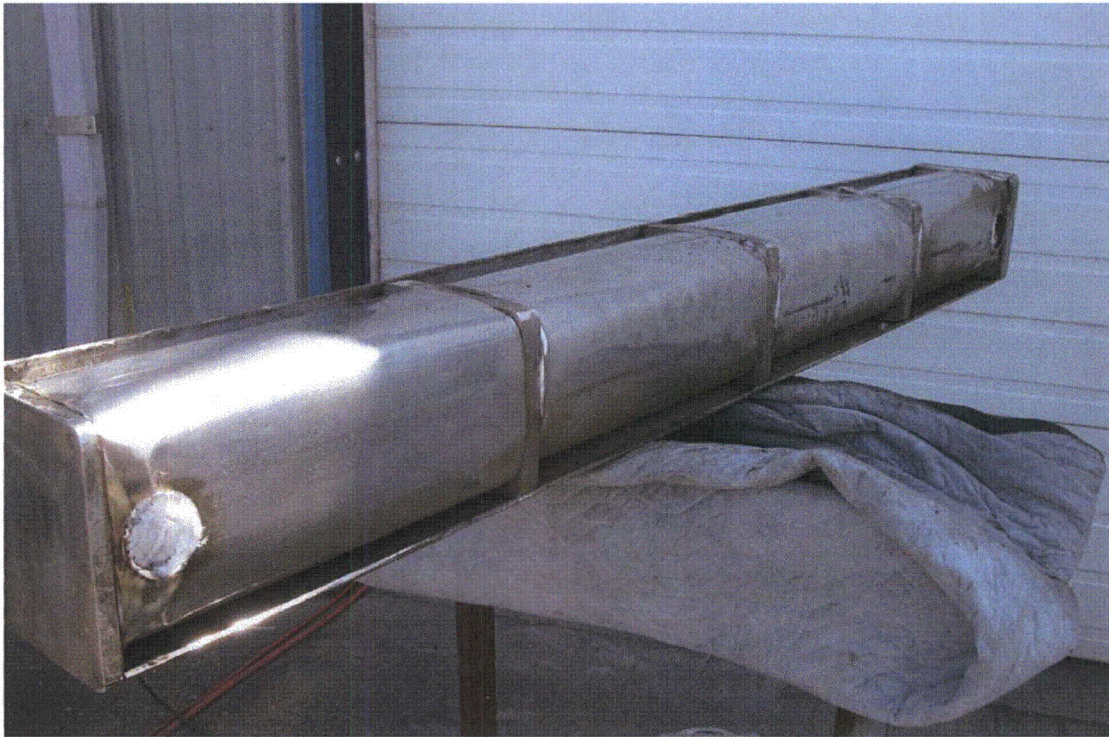


Figure 2.12.2-19 - Thermal Shield Condition, View 2



Figure 2.12.2-20 - Thermal Shield Condition, View 3



Figure 2.12.2-21 - Thermal Shields at Interface to Stiffening Rib

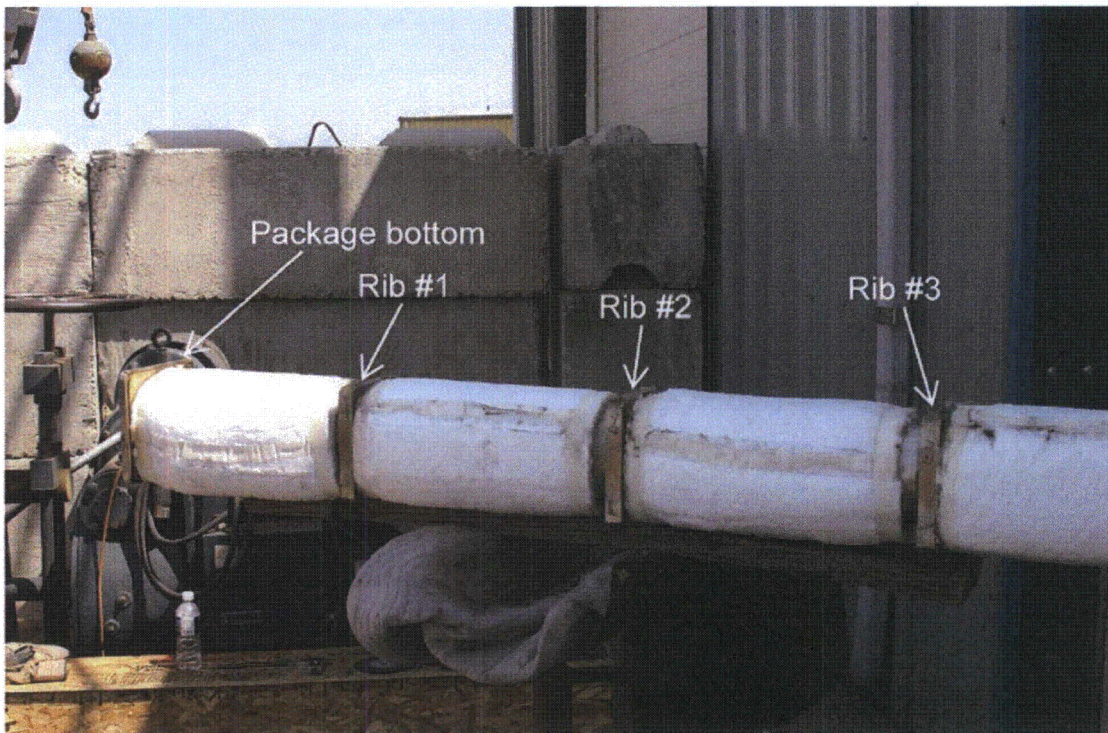


Figure 2.12.2-22 - Exposed Insulation - Overview



Figure 2.12.2-23 - Insulation Gap at Package Closure End

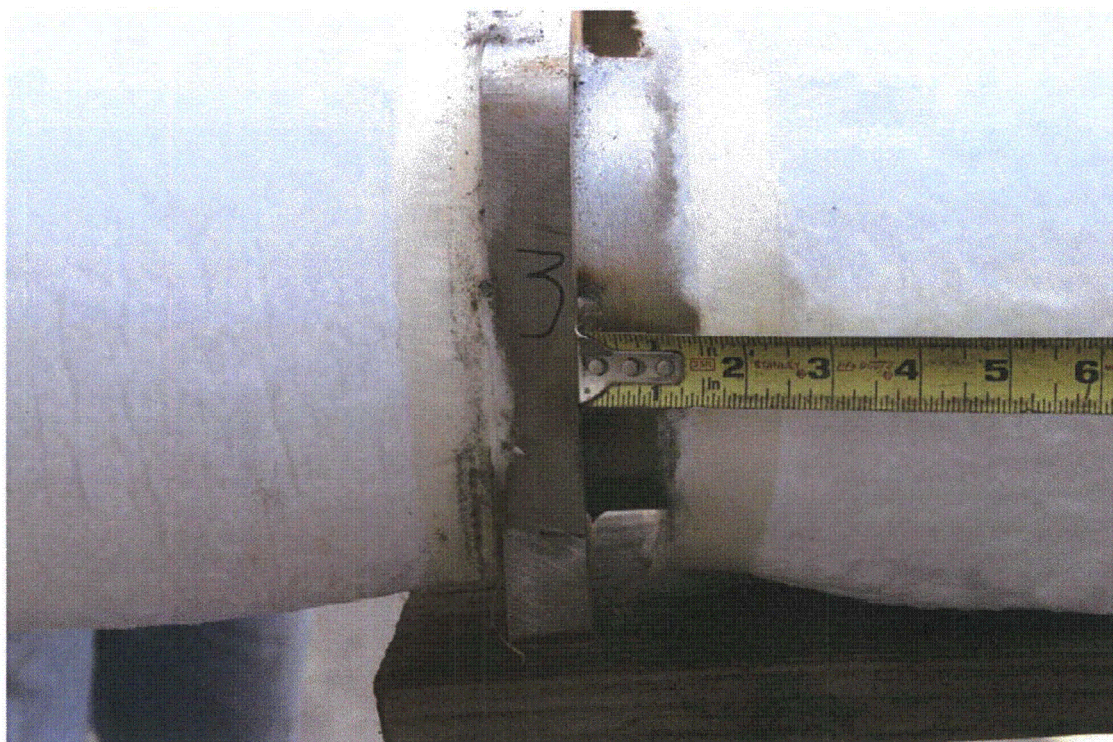


Figure 2.12.2-24 - Insulation Gap at Rib #3

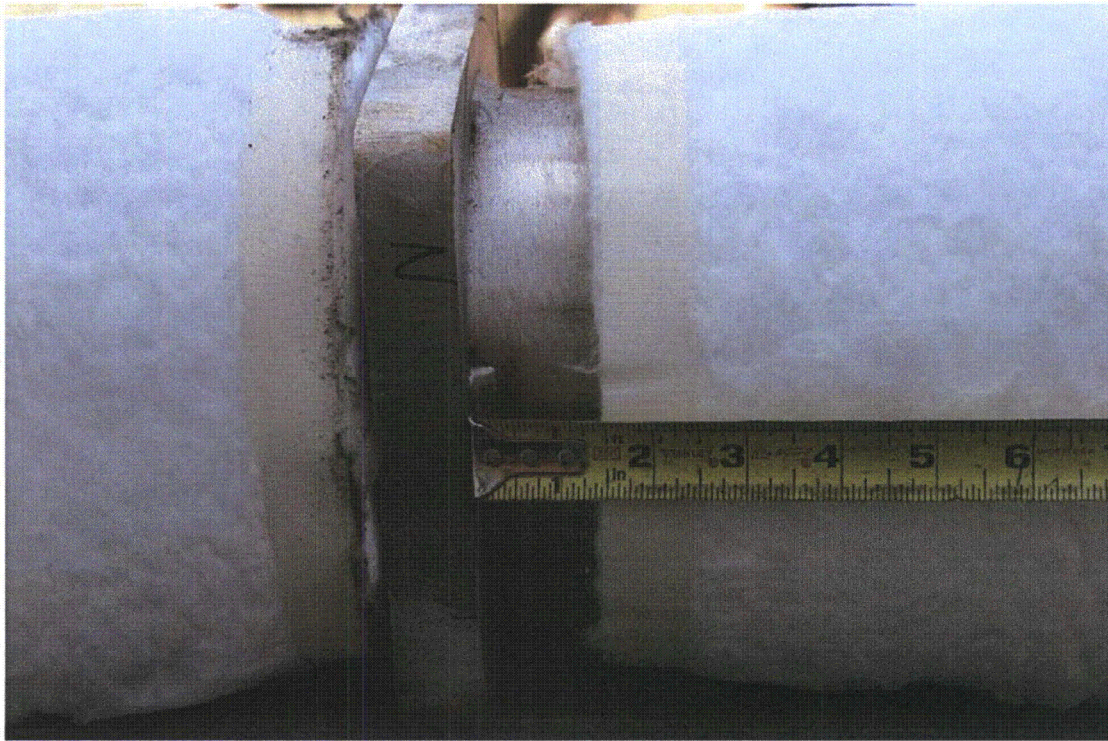


Figure 2.12.2-25 - Insulation Gap at Rib #2

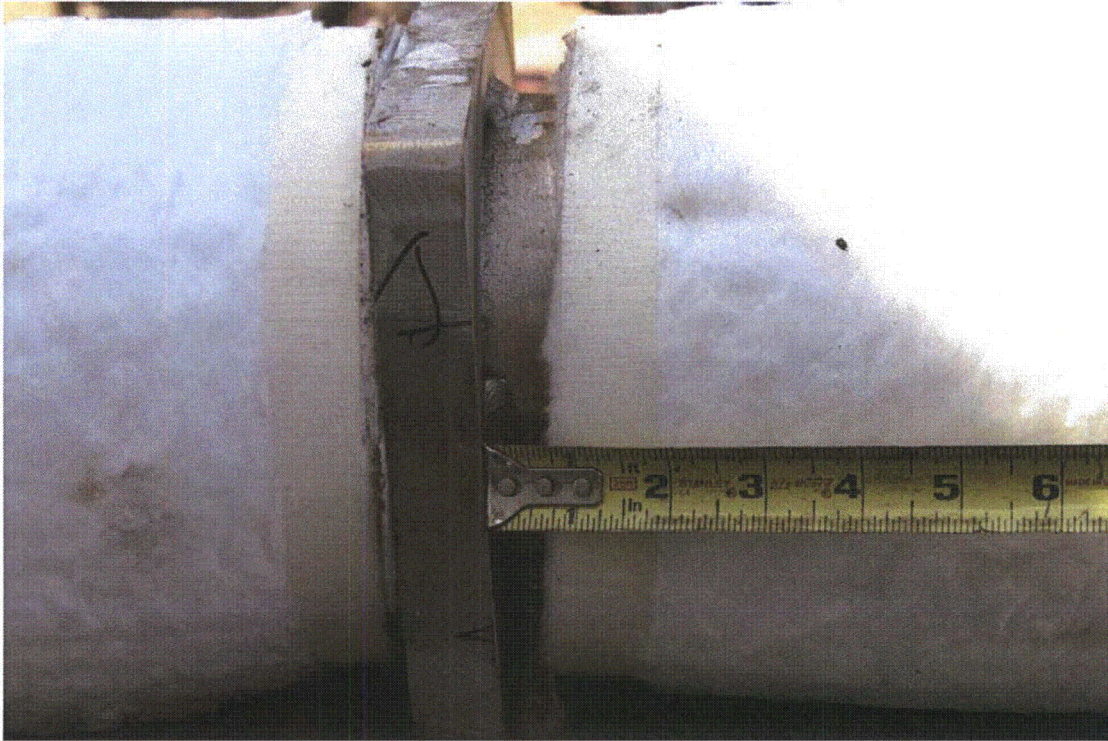


Figure 2.12.2-26 - Insulation Gap at Rib #1 (nearest impact)



Figure 2.12.2-27 - End Plate Insulation Condition

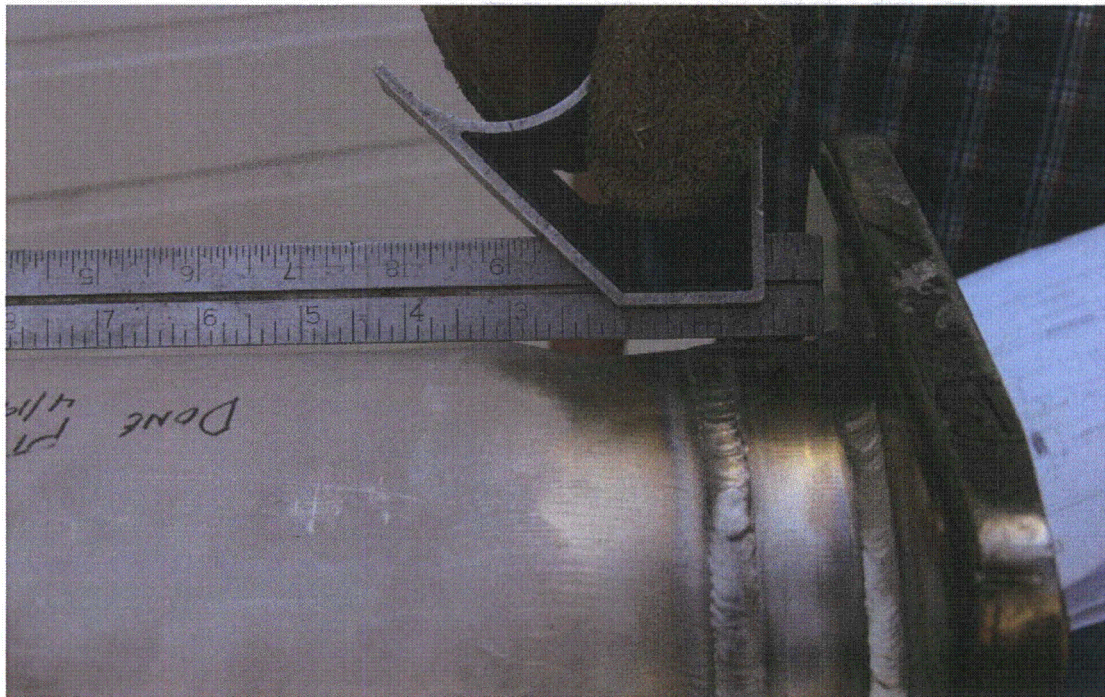


Figure 2.12.2-28 - Tube to Bottom End Plate – View 1



Figure 2.12.2-29 - Tube to Bottom End Plate – View 2

2.12.3 Structural Evaluation for MIT and MURR Fuel

The ATR FFSC may be utilized to transport a MIT fuel assembly or a MURR fuel assembly. Both of these fuels are high-enriched aluminum-clad uranium aluminide plate type fuel elements similar to the ATR fuel evaluated in this chapter. Since no MIT or MURR fuel elements were included in the drop tests, the following evaluation conservatively estimates a degree of failure and movement of the MIT and MURR Fuel Handling Enclosures (FHE) to develop a worst case pitch expansion of the corresponding fuel elements for evaluation in Section 6.10, *Appendix B: Criticality Analysis for MIT and MURR Fuel*. By conservatively bounding potential damage and evaluating the exceptional worst case pitch expansion of the MIT and MURR fuel elements the ATR FFSC complies with the performance requirements of 10 CFR §71.

2.12.3.1 Structural Design Discussion

A comparison is provided to highlight the similarities and differences between the MIT and MURR designs and the physically tested ATR design. Through this comparison, it is expected that both NCT and HAC testing would result in similar results for the MIT and MURR fuel elements. Similar to the ATR LFPB, the MIT and MURR FHEs are designed to restrict postulated fuel element pitch expansion under the HAC conditions.

The results of NCT conditions on the MIT and MURR payload are assumed to be equivalent to the ATR payload; i.e. there is no damage to the FHE or fuel element under NCT.

For conservatism in evaluating the HAC conditions, the MIT and MURR FHE damage postulated exceeds the results obtained during testing of the ATR payloads. The MIT and MURR FHEs are assumed to separate (fail) and spread apart to permit a worst case reactivity configuration of the fuel elements. The individual fuel plates of the fuel elements are assumed to spread apart uniformly to fill the resulting space.

2.12.3.1.1 Fuel Elements

The ATR FFSC packaging is not modified for the use of the MIT and MURR fuel elements. The MIT and MURR FHE are used in place of the ATR FHE or the LFPB within the ATR FFSC packaging. Similar to the ATR FHE and LFPB, the MIT and MURR FHEs are principally fabricated of aluminum construction and secured with stainless steel locking pins.

The MIT and MURR fuel elements are very similar to the ATR fuel element in design, materials, and fabrication. The weight of the fuel elements are 10 lb, 15 lb, and 25 lb, for the MIT, MURR, and ATR fuel elements respectively. All three fuel elements are fabricated of the same fuel type, aluminum-clad uranium aluminide fuel plates, with all fuel plates swaged into the side plates, and include cast or wrought aluminum end boxes. As such, the structural performance of the MIT and MURR fuel types are anticipated to behave very similarly to the ATR fuel element. Table 2.12.3-1 compares the three fuel element design dimensions. Figure 2.12.3-1 compares the three fuel elements in their overall length and fuel plate length in inches. In this figure, the inside dimension identifies the fuel plate length.

For comparative purposes, an approximate moment of inertia is calculated for all three fuel elements using AutoCAD[®]. The results are presented in Figure 2.12.3-2. The values were

determined by taking a cross section of the fuel plate region and selecting the solid boundaries to compute the moments of inertia about the identified axes.

The comparison of the moments of inertia demonstrates that the three fuel elements are similar in stiffness and expected to perform in a similar fashion during NCT and HAC drop events. The length and weight of the fuel elements is clearly bounded by the ATR fuel element. The materials of construction and fabrication techniques are the same for each fuel type. The relatively minor dimensional changes of the ATR fuel element plates as a consequence of the testing identified in Section 2.6, *Normal Conditions of Transport*, and Section 2.7, *Hypothetical Accident Conditions*, further justifies the similar performance of the MIT and MURR fuel elements.

Table 2.12.3-1 –Fuel Element Design

Component	MIT	MURR	ATR
Approximate Weight, lbs	10	15	25
Number of Fuel Plates	15	24	19
Nominal Plate Spacing, in.	.08	.08	.08
Fuel Plate Length, in.	23.00	25.50	49.50
Fuel Plate Thickness, in.	.08	.05	.05, .08, .10
Approximate Fuel Plate Width, in.	2.5	2.0 - 4.3	2.0 – 3.9

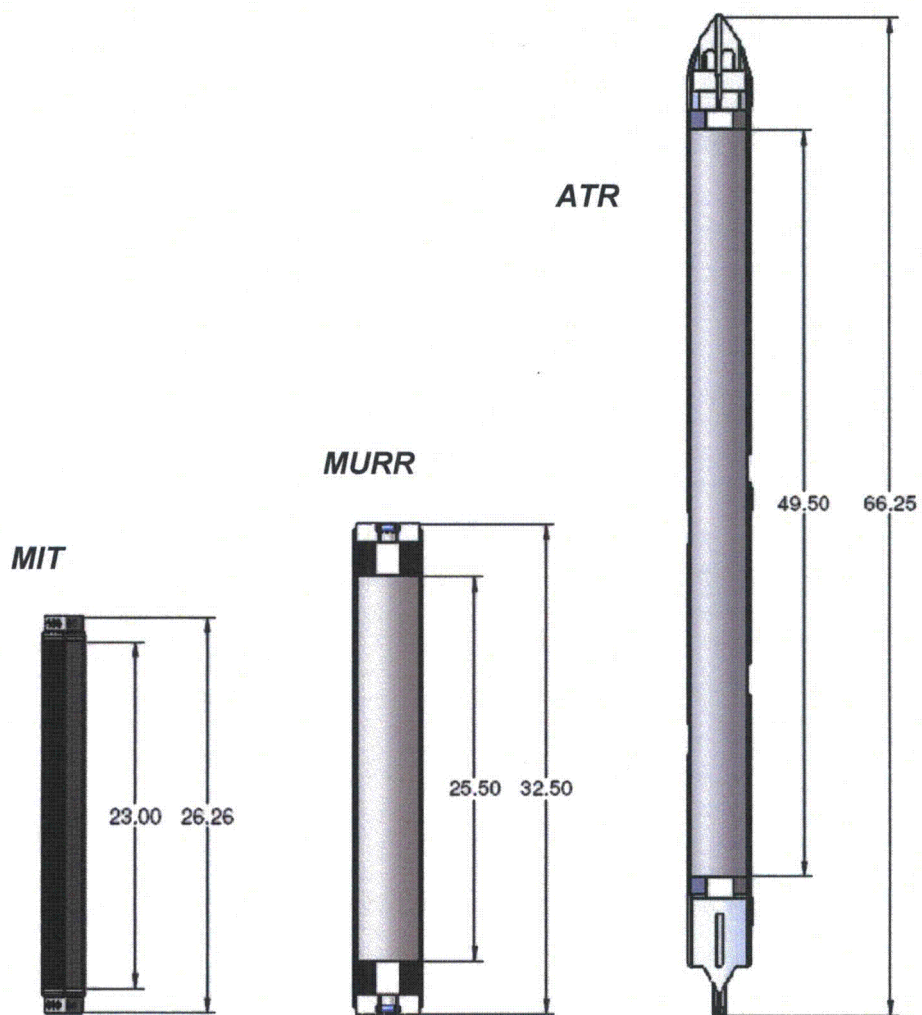


Figure 2.12.3-1 – MIT, MURR, and ATR Fuel Elements

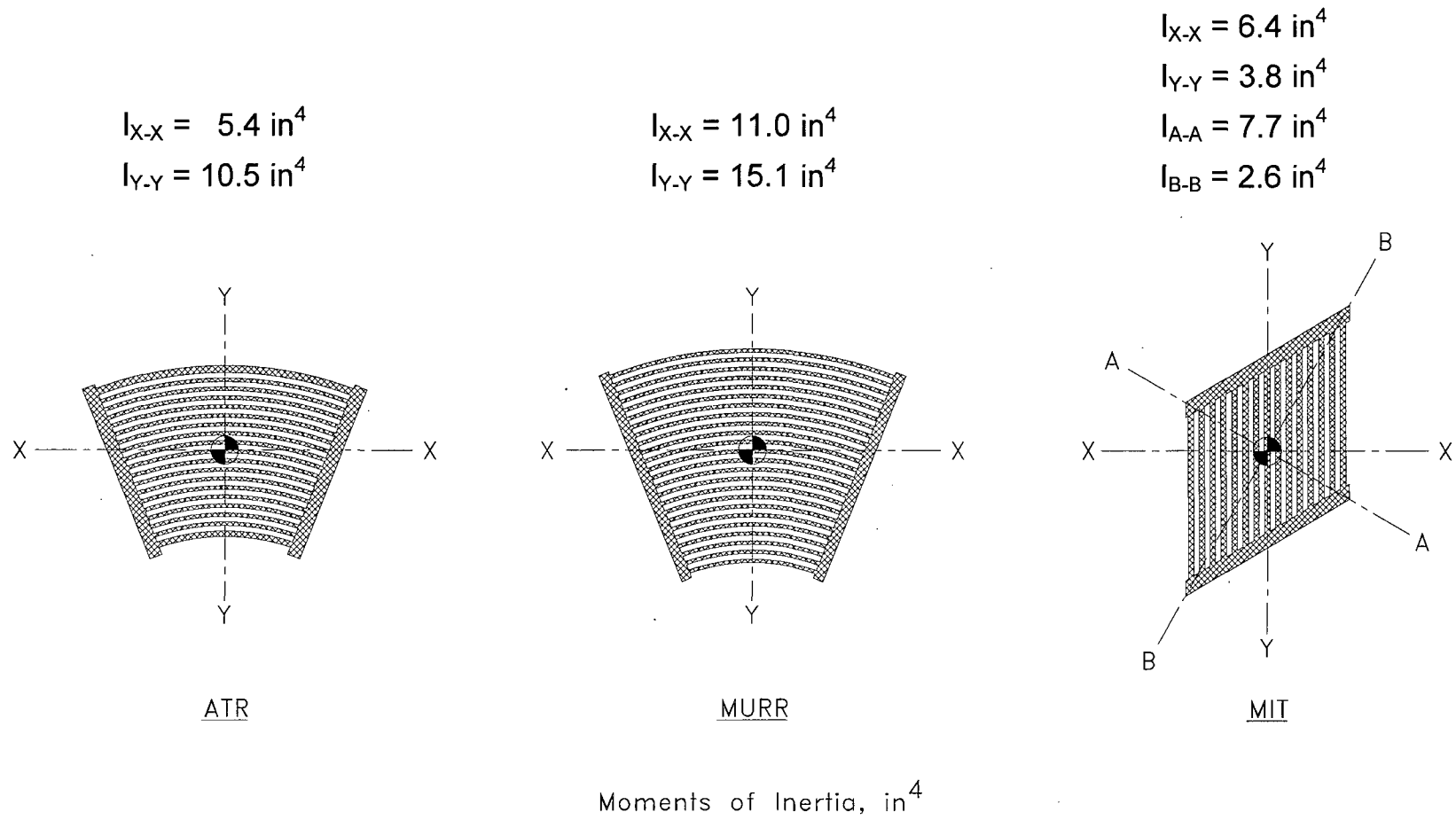


Figure 2.12.3-2 – Fuel Element Moments of Inertia

2.12.3.1.2 Fuel Handling Enclosures

The MIT FHE incorporates two end spacers and a two-piece machined aluminum enclosure to protect the MIT fuel element from damage during loading and unloading operations. The enclosure halves are identical segments machined from 6061 aluminum plate. Neoprene rub strips are used to cushion the contact points between the fuel element and enclosure. The end spacers are also fabricated of 6061 aluminum. The end spacers lock the enclosure halves together and are secured using stainless steel ball lock pins. The end spacers also prevent axial movement since the MIT fuel element is much shorter than the package cavity. The weight of the MIT FHE is 25 lb. Figure 2.1-3 illustrates the assembly view of the MIT FHE.

The MURR FHE is designed in the same manner as the MIT FHE. The weight of the MURR FHE is 30 lb. Figure 2.1-4 illustrates the assembly view of the MIT FHE.

The MIT and MURR FHE design is similar to the 30-lb LFPB in that it utilizes machined enclosure halve segments to encase the payload. The use of the enclosure halves makes the MIT and MURR FHEs more robust than the ATR FHE, which weighs 15 lb. The wall thickness of the enclosure halves is 0.19 in compared to the 0.09 in thick sheet used in the ATR FHE. For comparison, the typical machined wall thickness of the LFPB is also 0.19 in thick. The weight of the enclosures and fuel elements are 35 lb, 45 lb, 40 lb, and 50 lb for the MIT payload, MURR payload, ATR payload, and LFPB payload respectively.

Based on the similarity in design and function, the structural and thermal performance of the MIT and MURR FHEs is anticipated to be similar to the physical testing performed using the ATR FHE and LFPB.

2.12.3.1.3 Loose Fuel Plates

MIT and MURR loose fuel plates are not evaluated for use within the LFPB.

2.12.3.2 Allowable Damage

For HAC tests the MIT and MURR fuel elements are anticipated to perform in a similar manner to the ATR fuel element based on the comparable designs and assembly techniques. To conservatively encompass potential damage, the FHE halves are considered to separate while each half is sized at the extreme tolerances to encourage the maximum space around each fuel element. Based on the maximum space developed by the separated FHE, the fuel element plates separate to create a more reactive configuration for the fuel. The proposed pitch expansion greatly exceeds the results of the physical testing performed on the ATR fuel element.

Axial movement of the fuel element within the package inner tube, which occurs by hypothetical neglect of the FHE end spacers, has no adverse effect on the performance of the ATR FFSC. Energy dissipated by failure of the spacers would result in lowering the HAC loads to the MIT and MURR elements. However, the structural tests identified that the ATR fuel element survives the impact loads with damage that has no impact on reactivity. The MURR and MIT fuel elements are of similar materials and of similar construction to the ATR fuel elements. Assuming the spacers to fail with no energy absorption, the impact velocities of the MURR and MIT FHEs on the end fitting of the package would be nearly identical. It is therefore concluded

that the damage to MURR and MIT fuel elements is bounded by the damage sustained by the ATR fuel element in the structural tests. However, for conservatism, the fuel plate pitch of the MURR and MIT elements is set to the condition that results in the worst case reactivity under the volumetric constraints presented by the FHEs.

The HAC criticality array model is a 5x5x1 array of packages and all fuel elements are positioned at the same axial location. The FHE end spacers are conservatively neglected and modeled as water. Axial shifting of fuel elements from the modeled configuration would result in a less reactive condition; therefore, failure of the FHE end spacers is not a criticality concern. For the thermal evaluation, the position of the MIT or MURR fuel element is naturally bounded by the ATR fuel element since its length extends to each end of the package.

The modeled separation of the FHE halves inside the inner tube of the package is determined by using the maximum inner diameter of the package's inner tube and the minimum outer radius of each FHE half as illustrated in Figures 2.12.3-3 and 2.12.3-4. The FHE cavity dimensions are expanded using the maximum tolerance of the parts. Note that this is only hypothetically possible, since this causes the corners of the FHE for both the MIT and MURR to exceed the point of interference with the inner tube wall.

The dimensions for the criticality model of the MIT FHE are determined in the following manner:

- Package inner tube maximum inside diameter: Diameter is specified as 6.0 in. OD X 0.12 in. wall thickness ± 0.030 in. OD and $\pm 10\%$ thickness (per drawing 60501-10 and ASTM A269). Resulting maximum ID is 5.814 in.
- Minimum outside radius of the FHE half: Radius is specified as 2.8 in ± 0.2 (per drawing 60501-40). Resulting minimum radius is 2.6 in.
- Minimum wall thickness of the FHE half: Wall is specified as 0.19 in ± 0.06 (per drawing 60501-40). Resulting minimum thickness is 0.13 in.
- Maximum cavity height of the FHE half: Wall height specified as 2.82 in ± 0.06 (per drawing 60501-40). Resulting maximum height is 2.88 in. (which is greater than the 2.6 maximum radius).
- Maximum cavity width of the FHE half: Wall width specified as 1.62 in ± 0.06 (per drawing 60501-40). Resulting maximum width is 1.68 in.

The dimensions for the criticality model of the MURR FHE are determined in the following manner:

- Package inner tube maximum inside diameter: Diameter is specified as 6.0 in. OD X 0.12 in. wall thickness ± 0.030 in. OD and $\pm 10\%$ thickness (per drawing 60501-10 and ASTM A269). Resulting maximum ID is 5.814 in.
- Minimum outside radius of the FHE half: Radius is specified as 2.8 in ± 0.2 (per drawing 60501-50). Resulting minimum radius is 2.6 in.
- Minimum wall thickness of the FHE half: Wall is specified as 0.19 in ± 0.06 (per drawing 60501-50). Resulting minimum thickness is 0.13 in.
- Maximum cavity height of the FHE half: Wall height specified as 2.00 in ± 0.06 (per drawing 60501-50). Resulting maximum height is 2.06 in.

- Maximum cavity width of the FHE half: Wall width specified as 1.85 in \pm .06 (per drawing 60501-50). Resulting maximum width is 1.91 in.

The thermal evaluation in Section 3.6, *Thermal Evaluation for MIT, MURR, and RINSC Fuel*, makes the following conservative assumptions to bound damage to the fuel elements and FHEs as a result of NCT and HAC events.

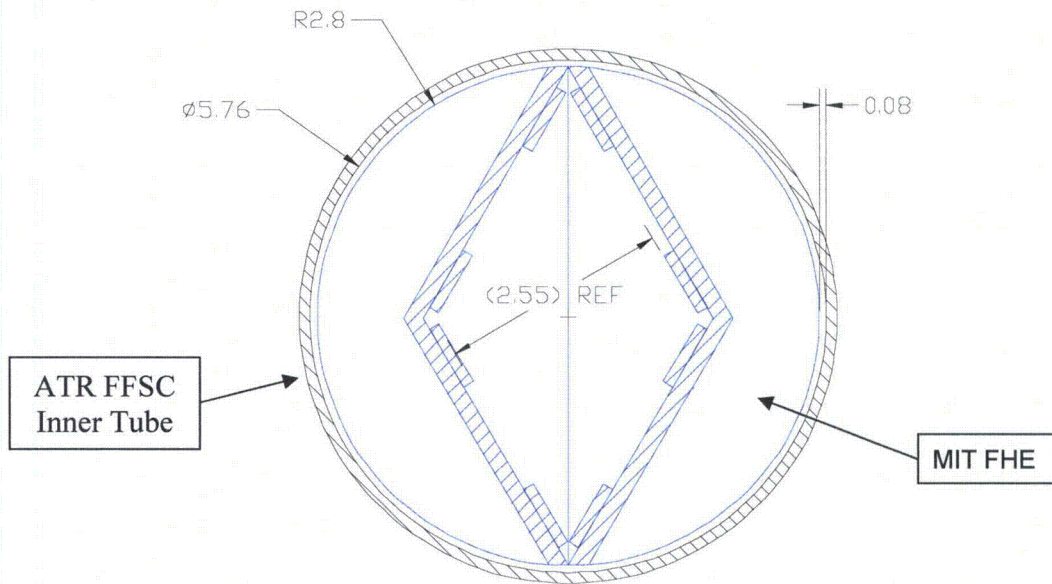
- Idealized contact between the FHE and the package inner tube. The majority of the heat input to the fuel element comes from the radial direction rather than the axial direction. By maximizing the contact, the greatest heat is transferred. Deformation of the payload would have the effect of reducing the contact area, and therefore reducing the conductive heat input.
- Axial movement of the fuel element, as a result of deformation of the FHE end spacers has a negligible effect. The majority of the heat input to the fuel element comes from the radial direction rather than the axial direction (ends). As the fuel element moves closer to the ends of the package the heat input rises. However, the heat input from either end of the package is negligible compared to the heat input received axially from the sides. Furthermore, any credible axial distance of the MIT and MURR fuel elements to the end of the package is bounded by the ATR fuel element.

The criticality evaluation in Section 6.10, *Appendix B: Criticality Analysis for MIT and MURR Fuel*, makes the following conservative assumptions to bound damage to the fuel element as a result of HAC events.

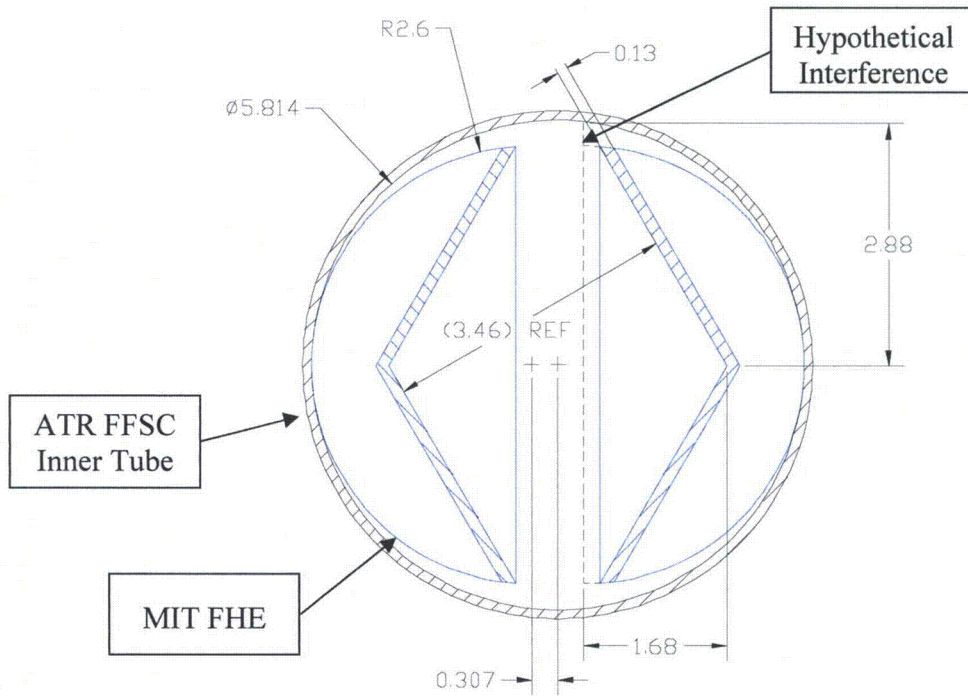
- Neglecting the function of the end spacers, the two halves are pushed apart to the maximum extent to maximize the available space for pitch expansion.
- Although it is not feasible in actual practice to push the FHEs to the center of the array if the two FHE halves are already pushed apart, both the MIT and MURR models are shifted by 0.307-in towards the center of the array.
- Fuel element end boxes are not modeled. For criticality purposes, any amount of damage to the end boxes is acceptable.
- Note that the MIT and MURR FHEs are “sliced off” in the corners because such a translation is not possible without interference.

Due to the conservative assumptions utilized for the thermal and criticality evaluations, the allowable damage to the FHEs is considered severe and therefore far exceeding the physical testing results performed using the ATR fuel element and LFPB payloads covered in Section 2.12.1, *Certification Tests on CTU-1*, and Section 2.12.2, *Certification Tests on CTU-2*.

For containment purposes, the MIT and MURR fuel element plates must remain intact to prevent the fuel meat from within the fuel plate from exiting the package. The MIT and MURR fuel elements are fully supported over the length of the fuel plates by the FHE enclosure halves. The enclosure halves are specifically designed to fully support each fuel element and minimize any deformation or change in the fuel plate geometry. By design the MIT and MURR FHEs are more robust (thicker side walls) than the ATR FHE and therefore provide better support compared to the testing performed using the ATR fuel element and ATR FHE.

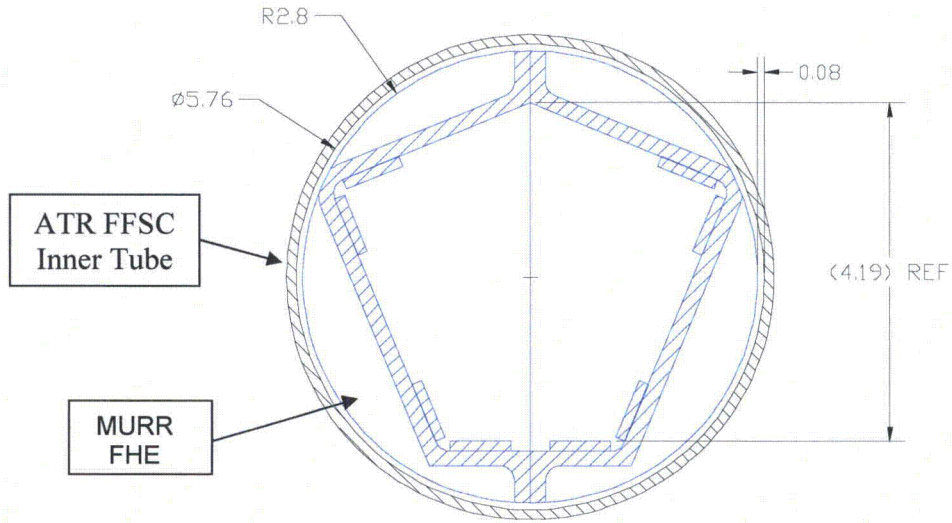


Nominal MIT FHE Dimensions

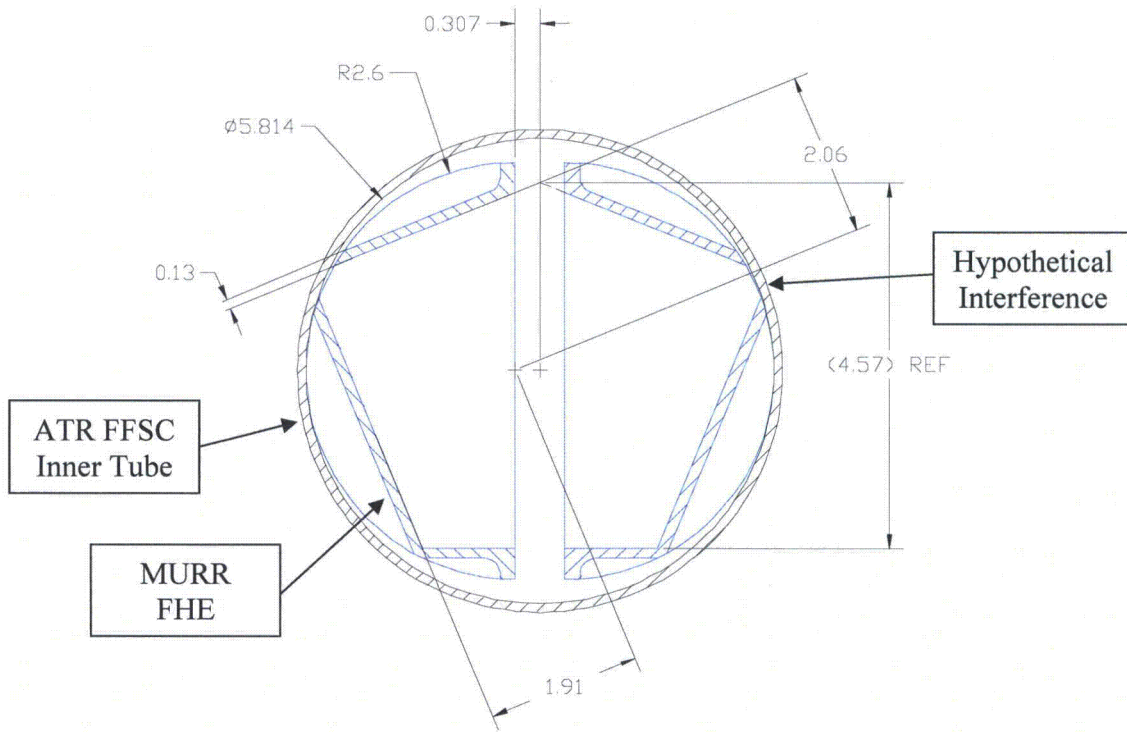


Maximum Tolerances Incorporated to Separate FHE Halves

Figure 2.12.3-3 – MIT FHE Damage



Nominal MURR FHE Dimensions



Maximum Tolerances Incorporated to Separate FHE Halves

Figure 2.12.3-4 – MURR FHE Damage